https://doi.org/10.59761/RCR5194

Hybrid molecularly imprinted nanomaterials for therapy and diagnostics

Anastasia Yu. Sedelnikova, Dmitrii V. Pyshnyi, Elena V. Dmitrienko

Institute of Chemical Biology and Fundamental Medicine, Siberian Branch, Russian Academy of Sciences 630090 Novosibirsk, Russian Federation

Hybrid molecularly imprinted polymers combine features of molecularly imprinted polymers (MIPs) and other functional components such as inorganic materials (*e.g.*, nanoparticles), which provides enhanced selectivity, stability, and reactivity. This combination makes it possible to integrate benefits of MIPs (specific binding of a molecular template) with those of other materials such as high surface area, stability, and catalytic activity. Recent advances in nanotechnology have improved the production of new hybrid molecularly imprinted polymers, which resulted in rapid growth of the use of hybrid MIPs in biomedicine. Lately, the number of publications (including reviews) devoted to both classic and hybrid MIPs has been constantly increasing; however, none of the publications focuses on the preparation and use of hybrid MIPs for medicine and their possible contribution to this field. This review presents a detailed description of the latest research advances in molecular imprinting technology with the use of nanomaterials in diagnostics, therapeutics, and theranostics. The goal of the review is to provide a comprehensive picture of the diversity of currently available hybrid systems for molecular recognition and their applications in biomedicine.

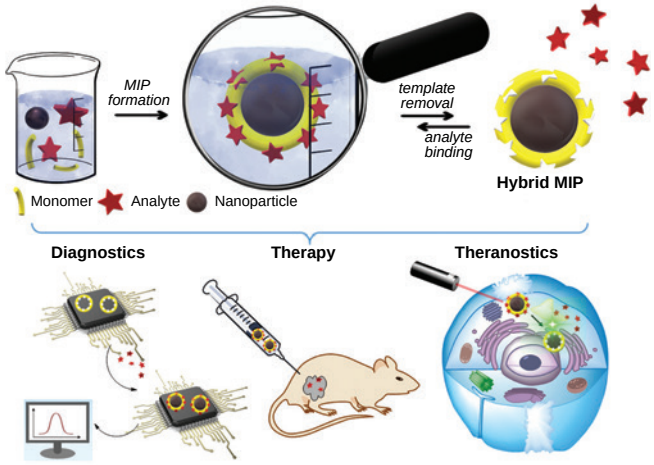

The bibliography includes 252 references.

Keywords: molecular imprinting, hybrid molecularly imprinted polymers, nanocomposite materials, inorganic nanoparticles, therapeutics, diagnostics, MIP, theranostics.

Contents

A.Yu.Sedelnikova. Master degree from Novosibirsk State University, Laboratory Assistant at the Laboratory of Biomedical Chemistry, Institute of Chemical Biology and Fundamental Medicine SB RAS.
E-mail: sedelnikovanastasia@gmail.com
D.V.Pyshnyi. Doctor of Chemical Sciences, Professor, Corresponding Member of RAS, Chief Researcher of the Institute of Chemical Biology and Fundamental Medicine.
E-mail: pyshnyi@niboch.nsc.ru
E.V.Dmitrienko. Candidate of Chemical Sciences, Head of the Laboratory of Biomedical Chemistry, Institute of Chemical Biology and Fundamental Medicine SB RAS.
E-mail: elenad@niboch.nsc.ru
Current research interests of the authors: biomedical chemistry.

Translation: Z.P.Svitanko

1. Introduction

Molecular recognition is in the focus of many researchers, since it is fundamentally important for biological processes.[1] This unique feature is inherent in molecularly imprinted polymers (MIPs), synthetic analogues of natural antibodies that can selectively bind various compounds such as metal ions,[2–8] organic molecules,[9–14] and biological macromolecules.[15–21] Therefore, these materials are widely used in various fields of biomedicine. Fast development of the molecular imprinting technology began in the 1990s, and since then, the interest of researchers in this subject has not declined.

Among recent scientific reviews, there are numerous works that comprehensively consider the capabilities of molecular imprinting. First of all, quite a few reviews describe the history of discovery and development milestones of this subject and the

Received 12 August 2025

position of MIPs among other types of macromolecular compounds. In particular, these publications describe in detail the principles of molecular imprinting, the mechanisms of specific binding of target molecules, and methods for the synthesis and characterization of imprinted polymers; they also briefly highlight the properties and various application fields of these materials, including biomedicine, ecology, and biotechnology.[22–24] Our paper considering the potential of these materials in the context of biomedical applications was already published in *Russian Chemical Reviews*;[25] however, the current progress of nanotechnology has brought about a new wave of development of molecularly imprinted polymers, which provides for improving the technology and increasing the potential for practical application, namely, the possibility of functionalization with various nanomaterials. In view of the high promise of hybrid MIPs, publications addressing these materials have already appeared in the scientific literature. Fresco-Cala *et al*.[26] focused attention on the main methods for the production and structural properties of imprinted nanocomposite materials and demonstrated various analytical applications of these materials. In addition, there are studies describing a particular type of hybrid MIPs and its possible applications. For example, Ramin *et al*.[27] reported magnetic molecularly imprinted polymers, with the key idea being to describe an environmentally friendly green approach to the production of nanoparticles (NPs) using various living systems as well as fundamentals of this concept and application of magnetic MIPs for analysis of natural, food, and biological samples. The existing reviews follow a general trend towards exhaustive description of various classic approaches to the design of imprinted nanocomposites, while consideration of the practical applications of these materials receives less attention. This prevents readers from fully appreciating the capabilities and potential of hybrid MIPs, particularly in a scientific area such as biomedicine. Therefore, the goal of this review is to provide a detailed account of the latest achievements in the field of molecularly imprinted polymers functionalized with nanomaterials meant for the development of modern specific and effective diagnostic, therapeutic, and theranostic methods, revealing the potential of currently existing hybrid systems for molecular recognition.

2. Molecular imprinting concept

The technique of production of synthetic polymers containing imprints of analyte molecules and capable of specific binding to these molecules is called molecular imprinting. The foundations of this concept were laid in 1931 by M.V.Polyakov,[28] who observed the ‘molecular memory’ effect for benzene in a synthetic silica matrix. Over the next few decades, this field developed and extended to include a wide range of polymer materials.[29] In 1973, Wulff *et al*.[30] described polymer structures acting as enzyme analogues. The term ‘imprinted polymer’ was first mentioned in the publications by K.Mosbach and co-workers[31] and G.Wulff *et al*.,[32] which appeared in 1984 and 1985, respectively. These researchers became the founders of the molecular imprinting concept and the authors of its covalent (G.Wulff) and non-covalent (K.Mosbach) approaches. Subsequently, K.Mosbach’s studies made it possible to convert molecular imprinting from a theoretical concept into a practical tool used in various fields such as purification and isolation of components from complex mixtures, detection of specific analytes, selective catalysis of chemical reactions, and drug delivery. In addition, Mosbach’s group was the first to demonstrate that MIPs can indeed be used in immunoassays instead of antibodies, which significantly expanded the potential of this field.

Since the 1980s, the molecular imprinting technology has rapidly developed. Over the past 40 years, MIPs have progressed from a basic idea to a practically applied area, being developed from laboratory production and use to a wide range of biomedical, environmental, and chemical applications, including the design of highly selective sorbents, drug delivery carriers, and sensors. The elaboration of the molecular imprinting technique can be conventionally divided into three stages.

1. From concept inception to technology shaping up (1980s and 1990s). This period comprised an increasing number of studies dealing with the preparation of MIPs for a wide range of molecular templates using various functional monomers and cross-linking agents. The obtained MIPs were mainly used as effective tools for separation and purification of complex samples.

2. Development of synthesis methods and improvement of characteristics of MIPs (2000s). This period was marked by the development of new approaches to polymerization, which enabled the production of MIPs with a more controlled structure and enhanced selectivity.[33] In addition, the range of used functional monomers has been expanded, which made it possible to vary the physicochemical properties of the formed polymers and to obtain MIPs for the solution of particular problems, *e.g*., biocompatible MIPs for biomedical applications.

3. Expansion of the scope of applications and entry into the market (from the 2010s up to now). In recent years, there has been rapid development of MIPs for biomedical applications such as controlled drug delivery and development of biosensors. The improvement of the methods of synthesis of imprinted materials resulted in the fabrication of responsive MIPs capable of changing their properties in response to external stimuli, which opens up new prospects for the use in medicine.

Currently, the number of publications describing the design, development, and use of molecularly imprinted polymers has sharply increased, which reflects the maturity of this research area and considerable interest of the scientific community.[29]

The idea of molecular imprinting is to prepare organic or inorganic macromolecular compounds and polymer matrices capable of recognizing molecules that were used as molecular templates during the formation of the polymer backbone. The structures of these polymers have binding sites capable of specific interactions with target molecules or structurally similar molecules. The recognition can be based on the shape or size of the imprinted molecule or on reactions between functional groups of the template and the polymer matrix.

The main characteristic of a molecularly imprinted polymer, like that of natural recognition systems, is the selectivity of binding to the analyte molecule. In various publications, the selectivity of MIPs is evaluated by the imprinting factor or the selectivity coefficient. It is noteworthy that the former value is the ratio of binding efficiencies of the template to MIP and the template to a reference non-imprinted polymer (NIP) in isolated systems, while the latter is the ratio between the efficiencies of MIP binding to the molecular template and to a structural analogue (reference molecule). Either of these values can be used to characterize molecular recognition using an imprinted polymer.

The classic synthetic route to MIPs consists of three main stages. In the first stage, called pre-polymerization, functional monomers react with the molecular template to form a complex (Fig. 1 *a*). After that, a cross-linking agent and/or polymerization

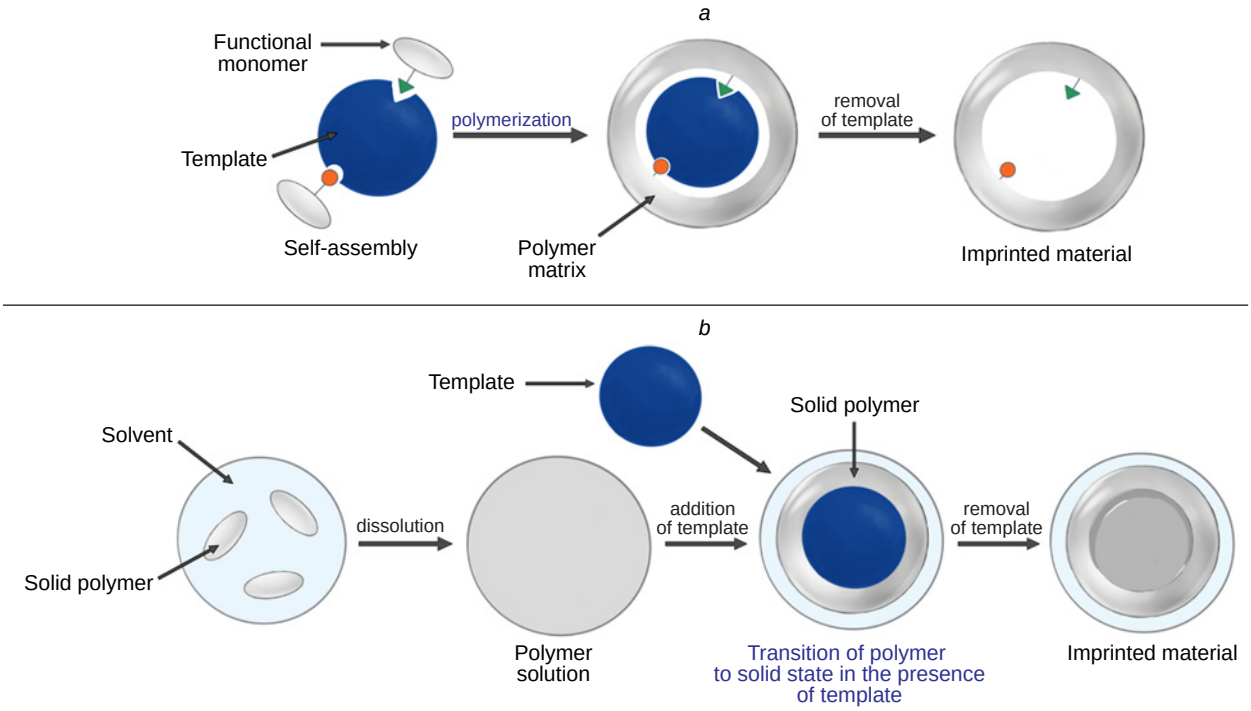

Figure 1. Classic (*a*) and alternative (*b*) synthetic routes to MIPs.

initiator is added to form a polymer with cavities defined by the molecular template. In the final stage, the template molecule is removed, resulting in a polymer material with imprinted cavities that have a high affinity for the target compound.[1,23,34] According to the type of interactions between the molecular template and functional monomers during the MIP preparation and secondary template recognition, imprinting can be covalent or non-covalent (involving covalent or non-covalent bonds, respectively). In addition, there is also semi-covalent imprinting in which the imprint is formed through the formation of covalent bonds between functional monomers and the molecular template, while the secondary binding is achieved through non-covalent interactions.

Depending on the goals set, characteristics of the imprinted polymer such as binding strength, selectivity, rigidity, porosity, molecular weight, stability in the medium, and stimulus sensitivity can be modulated using various approaches (Table 1).[35]

While choosing a molecular imprinting approach in each particular case, it is necessary to consider quite a few parameters ranging from the size, structure, and properties of the template to the intended subsequent application of the resulting material. The covalent imprinting is preferred in the case where high binding selectivity is required; however, this approach often restricts the reusability of the material. If it is necessary to ensure several cycles of reversible binding, it is better to use non-covalent imprinting. Combining covalent binding for the stage of imprinting and non-covalent recognition during the operation is implemented in the semi-covalent imprinting technique, which provides enhanced specificity of binding of target molecules and improves the kinetic parameters of template binding during recognition.

Table 1. Classification of methods for MIP synthesis.

Classification principle	Nature of interactions	Ref.
Nature of interactions	Covalent	1, 30, 32, 36–38
	Noncovalent	1, 31, 39–44
	Semi-covalent	1, 29, 45, 46
Position of template imprints in a polymer	Bulk imprinting	47–50
	Surface imprinting	47, 51–56
	Epitope imprinting	47, 57–63

The choice of bulk, surface, or epitope imprinting usually determines the size and properties of the molecular template: bulk imprinting is more preferable for low-molecular-weight templates, while surface imprinting is better for macromolecular templates, including biomolecules such as proteins or even whole cells. The epitope imprinting is implemented in the case of high variability of the imprinted template or impossibility of forming an imprint for the whole object.

Molecular imprinted polymers are prepared using a variety of polymerization or polycondensation techniques. The most widely used classic method is free radical polymerization of functional monomers, the activation of which requires initiation of the chain reaction by generating free radicals using initiators that form free radicals upon action of heat or light.[1,64] Radical polymerization can be carried out under both homogeneous or heterogeneous conditions. Molecular imprinted polymers can also be obtained by copolymerization in which two or more monomers are involved in the polymer formation. Alternatively, it is possible to use controlled radical polymerization, class of methods for polymer synthesis in which the radical polymerization is carried out in such a way as to obtain polymers with specified properties: controlled molecular weight, low dispersity, and specific architecture (linear, block, star-shaped, *etc*.). Unlike conventional radical polymerization, in which the process is terminated randomly, in the case of controlled radical polymerization, the active chain propagation centres are deactivated, resulting in more regular polymers with a narrow molecular weight distribution (low dispersity) and a clearly defined structure, which is impossible with the classic free radical mechanism.[64,65] In addition, MIPs can be formed by

electropolymerization, in which polymers are synthesized under the action of an electric current on the surface of an electrode. The key features of electropolymerization include the possibility of preparing polymers in thin films, with the structure and properties of the polymer layer being controlled during the synthesis by variation of electrolysis parameters, and the preparation of metal–polymer composites by conducting the process in the presence of metal salts, which increases the conductivity and improves the electroanalytical properties of the materials.

Methods that are now used most often to prepare MIPs are based on heterogeneous radical polymerization such as precipitation polymerization,[35,66–68] emulsion (miniemulsion, microemulsion) polymerization,[35,67,69–71] and heterogeneous seed polymerization methods to give core–shell structures.[35,67,72–74]

In addition to the classic methods of MIP synthesis, an alternative two-stage approach has been described (see Fig. 1 *b*). According to this approach, the polymer is first dissolved in an organic solvent and incubated together with the molecular template to generate a specific interaction between them. After drying of the solvent or polymer precipitation, the imprinted compound is removed. In this case, MIP is formed *via* a change in the polymer structure on going from the dissolved state to the solid state.[25,75,76] The cavities formed in the polymer material are capable of specific interaction with the template molecules to form a high-affinity complex with them. The benefits of this approach include the absence of additional components such as polymerization initiators or cross-linking agents, which substantially reduces the probability of toxic effects, and that the synthesis is cost-effective, technologically rational, and facile.

The diversity of approaches to the preparation of MIPs makes it possible to select an optimal composition of the system depending on the particular requirements. Owing to the molecular recognition behaviour, MIPs can be compared with natural structures that possess this feature.

2.1. MIPs as synthetic analogues of antibodies and aptamers

Systems with molecular recognition behaviour are widely used in fundamental and applied research owing to their ability to selectively bind to various compounds that have a pronounced biological significance. Natural recognition systems are antibodies, while the most well-known synthetic nature-inspired systems are aptamers, that is, synthetic nucleic acid molecules (DNA or RNA) or small peptides.[35,77] Being a highly diverse class as regards chemical composition, MIPs may possess the same key properties and can be quite competitive with natural biopolymers.

Despite the different nature of MIPs and antibodies, their comparison is appropriate, since the most important biomacromolecules such as DNA, RNA, and proteins are synthesized and programmed in biological systems in the presence of a molecular template. Accordingly, the 'synthetic antibodies' featuring a molecular fingerprint are prepared by a method similar to biosynthesis. Furthermore, functional groups in the 'synthetic antibody molecules' are spatially ordered; therefore, a sort of recognition of the target compound by an imprinted polymer takes place *via* dynamic change in the conformation, which is also observed in the case of natural antibody–antigen interactions.[78]

The need to find and use alternative molecular recognition techniques for various processes became most acute when certain limitations in the application of natural platforms were identified (Table 2).[35,44,79,80]

Table 2. Comparison of antibodies, MIPs, and aptamers.

Characteristics	Antibodies	MIPs	NA-based aptamers
Thermal stability	Low	High	High
pH stability	Low	High	Low
Chemical stability	Low	High	Low
Physical stability	Low	High	Low
Immunogenicity	High	–	Low
Production cost	High	Low	Medium
Production method	Immunization of animals	Chemical synthesis	Chemical synthesis
Batch variability	High	Low	Low
Number of target molecules	Medium	High	High
Possibility of functionalization	Low	High	High

Antibodies, most of all, monoclonal ones, have low stability; this decreases the shelf life of products based on them and requires continuous provision of storage and transportation conditions such as cold chain supply and protection from light, moisture, and temperature gradients.[67] Conversely, MIPs are stable over a broad range of conditions including pH, temperature, pressure, and action of organic solvents. The molecular imprinting technology is more versatile due to the possibility of choosing from a wide variety of functional monomers, providing recognition of a wider range of target substrates than in the case of monoclonal antibodies (Fig. 2). However, it should be notes that the use of MIPs *in vivo* may face problems related to toxicity, immunogenicity, and clearance that are not taken into account in the *in vitro* development and upgrading by combining several MIPs, in some cases, for the same analyte.

Comparison of MIPs with aptamers (mainly based on nucleic acids) shows opposite binding affinity. For example, development of MIPs targeting small molecules is currently a relevant trend, whereas the selection of aptamers for small molecules is a challenging task due to the absence of mass transfer (the size difference between bound and free nucleic acid molecules is insignificant) upon binding to a small molecule. Also, MIPs can demonstrate non-specific binding, as incomplete removal of the template after the synthesis is possible, and this gives rise to false-positive results.[80]

The affinity and specificity of natural and artificial recognition systems are difficult to compare directly. The affinity and specificity of MIPs may be comparable to those of antibodies and aptamers, but the properties of MIPs are more dependent on the properties of the molecular template and functional monomers and on the optimization of the imprinting process. The MIP affinity can vary from moderate to very high depending on how successfully the imprinting components were selected and formation of 3D structure of the polymer matrix mimicking the shape of the target molecule was optimized.

Table 2 gives a qualitative comparison of various recognition systems; however, it is noteworthy that direct comparison of MIPs and antibodies is rarely presented in a single study. Nevertheless, S.Piletsky's research group[81] reported a comparison of monoclonal antibodies for fumonisin B2 and L-thyroxine and

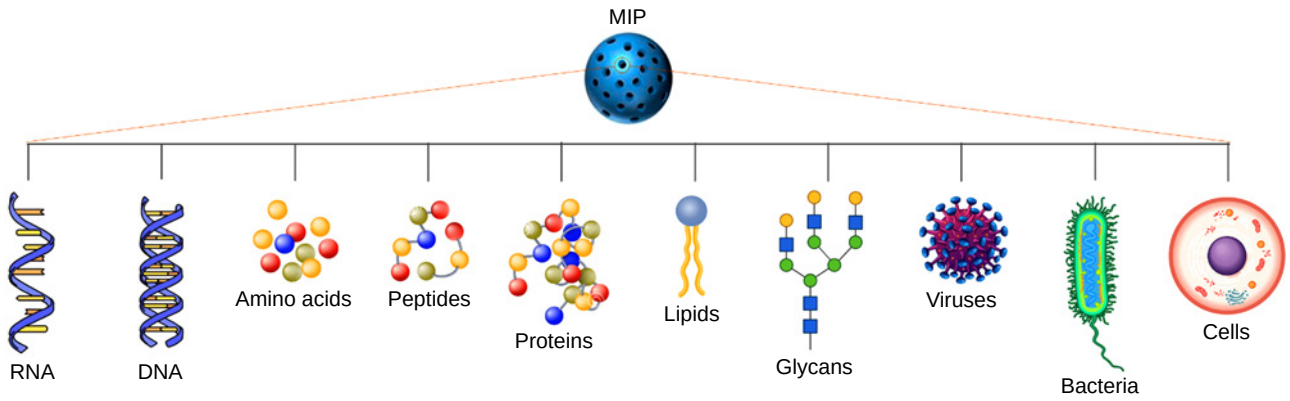

Figure 2. Diversity of the target compounds for MIPs.

polyclonal antibodies for glucosamine and biotin with analogues based on hybrid molecularly imprinted polymers. For the preparation of MIPs, molecular templates were immobilized on the surface of SiO_2 NPs functionalized with 3-aminopropyltriethoxysilane (APTES). This was done by binding glutaraldehyde to the amino groups of APTES and template to give Schiff base, which was then selectively reduced with sodium cyanoborohydride. Biotin was an exception, as it was directly immobilized on the surface of SiO_2 NPs after its carboxyl group was activated with water-soluble *N*-ethyl-*N*′-(3-dimethylaminopropyl)carbodiimide (EDC/NHS). The MIP synthesis was carried out in an aqueous medium using a monomer mixture comprising *N*-isopropylacrylamide (NIPAM), *N*,*N*′-methylenebis(acrylamide) (MBA), *N*-*tert*-butylacrylamide (TBAM), acrylamide (AA) (for all templates except for fumonisin B2), and *N*-(3-aminopropyl)methacrylamide (for fumonisin B2) in the presence of sodium persulfate initiator and *N*,*N*,*N*,*N*-tetramethylethylenediamine (TMED) catalyst (Fig. 3 *a*). The control polymer was prepared using the same monomer composition against an unrelated template, trypsin (the imprinting factor was 2.5).

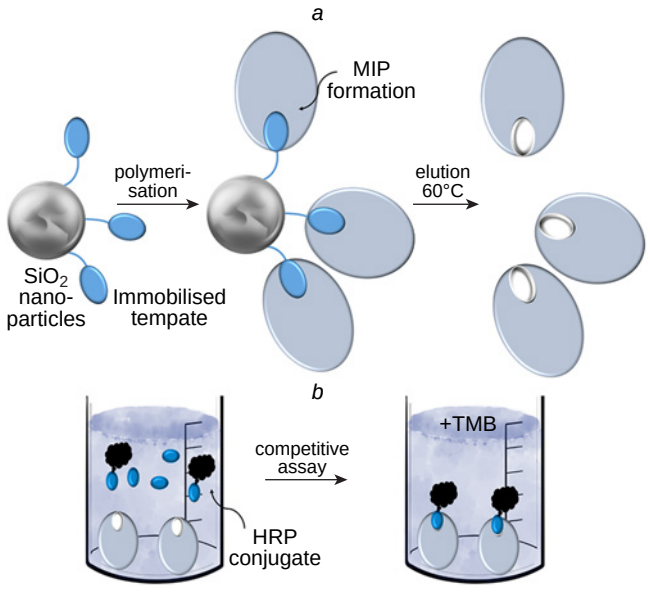

Figure 3. Schematic diagram of the synthesis of MIPs (*a*) and enzyme-linked competitive assay involving HRP conjugates of the analyte and TMB detection (*b*).[81]

An enzyme-linked competitive assay was used to compare the efficiency of MIPs and antibodies. For this purpose, conjugates of each target molecule with horseradish peroxidase (HRP) were prepared by means of EDC/NHS coupling, targeting the same functional group that was used for template immobilization on the NP surface. The assay was carried out in 96-well microplates using 3,3′,5,5′-tetramethylbenzidine (TMB) as the substrate for HRP (Fig. 3 *b*). The results are summarized in Table 3.

As can be seen from the presented data, in almost all cases, the performance of MIPs was not inferior, or even superior, to that of antibodies. These studies show that the hybrid MIPs can compete with antibodies in analysis of at least small-molecule templates.

Pang *et al*.[82] clearly demonstrated the competitiveness MIPs relative to natural molecular recognition systems for the diagnosis of cancer, due to determination of the relative expression level of the pathological form of α-fetoprotein. The authors paid attention to determination of the precise glycosylation status of protein biomarkers, which is of great importance for accurate and early diagnosis of cancer. In relation to α-fetoprotein as a glycoprotein biomarker, the authors proposed a new approach based on MIPs, which demonstrated a higher selectivity and affinity for the imprinted compound compared to the classic method involving the use of antibodies and lectins. The strategy was based on triple recognition of the used biomarker by different types of MIPs in a single detection system using plasmon-enhanced Raman scattering. In particular, the imprinted polymer for the N-terminal α-fetoprotein epitope was formed on glass coated with Au NP monolayer, whereas the MIP coating for the C-terminal epitope was deposited on silver NPs with Raman reporter 1. 3-Aminopropyltriethoxysilane, ureidopropyltriethoxysilane, isobutyltriethoxysilane, and tetraethoxysilane (TEOS) in 10 : 20 : 40 : 30 ratio were used as functional monomers. Furthermore, the α-fetoprotein form

Table 3. Comparison of antibodies and MIPs.[81]

Analyte	MIP-based assay		Antibody-based assay	
	limit of detection, pM	linear range, pM	limit of detection, pM	linear range, pM
Biotin	1.2	0.1 – 30	2.5	$0.1 – 10^3$
Fumonisin B2	6.1	$1 – 10^4$	25	$1 – 10^3$
Glycosamine	0.4	$0.1 – 10^3$	0.3	$0.1 – 10^4$
L-Thyroxine	8.1	$1 – 10^4$	17.5×10^3	$10^3 – 10^5$

expressed in hepatocellular carcinoma has one glycosylation site that mainly consists of fucosylated glycans. Therefore, using boronic acid-based oriented surface imprinting, the authors also prepared MIP for the fucose residue on the surface of silver NPs with Raman reporter 2, which has characteristic peaks different from those of reporter 1. The Raman signal from reporter 1 corresponding to the total α-fetoprotein level in the blood serum and the signal from reporter 2 characterizing the level of fucosylated glycans of α-fetoprotein were subject to plasmonic detection. The relative level of expression of fucosylated glycoforms in relation to the total level of α-fetoprotein served as a reliable marker of cancer in patients. A comparison of the proposed system with the classic method demonstrated that the approach based on natural recognition elements showed a high level of cross-reactivity towards other monosaccharides (not less than 35.7%), whereas in the case of MIPs, the cross-reactivity did not exceed 16% in all cases. In addition, the proposed synthetic platform demonstrated increased accuracy compared to classic immunofluorescence assay; this proves the potential of this system for early diagnosis of diseases.

Comparison of MIPs and natural molecular recognition techniques unambiguously indicates that the 'synthetic antibodies' proved to be efficient owing to their benefits such as reproducibility, high speed, and relative cost-effectiveness of the synthesis, high stability, and resistance to organic solvents. In addition, functionalization of MIPs with various nanomaterials bring about additional physicochemical properties (*e.g.*, magnetic or photochemical properties) and expands the scope of applicability of imprinted polymers for biomedical purposes.[9,11,13,14,19,52,54,63,83]

2.2. Nanosized MIPs and their functionalization with inorganic nanomaterials

Molecularly imprinted polymers can be manufactured in various forms such as films, membranes, hydrogels, microparticles, or nanoparticles. The decades of studies demonstrated high efficiency of nanosized MIPs compared with their macroscopic analogues. In the case of macroscopic materials, performance decreases due to poor accessibility of interior binding sites for the molecular template. For the same reason, complete removal of the template is also complicated in the case of bulk MIPs.[84] Conversely, nanosized materials have a number of advantages, including a high surface area-to-volume ratio, accessibility of the imprinted cavities and, as a result, easier removal of the molecular template, and improved recognition capability.[74]

The achievements in nanoparticle synthesis and in the production of hybrid MIPs have made it possible to overcome the drawbacks of the finely divided bulk MIPs used by Vlatakis *et al.*[40] The solid-phase approach using immobilized templates allows for the successful production of hybrid MIPs in both organic and aqueous media. Nanoparticles are chosen on the basis of their affinity for the template, and the synthesis can be scaled up and automated. Nanoparticles can be additionally modified by forming functional surface layers that alter the NP properties and improve characteristics and molecular recognition performance of the resulting hybrid MIPs.

By combining MIPs with various nanomaterials, it is possible to take advantage of the benefits of all components and obtain systems featuring enhanced performance and new functional capabilities. Despite the fact that the term 'nanomaterials' is broad and covers various types of structures,[85] we focus attention on inorganic NPs, which are used most often to functionalize MIPs. Among the most studied and widely used nanoparticles, one can distinguish gold (Au NPs), iron oxide, and silica nanoparticles as well as carbon (CQDs) and graphene quantum dots (Fig. 4).[83] The most important properties of these materials are summarized in Table 4.

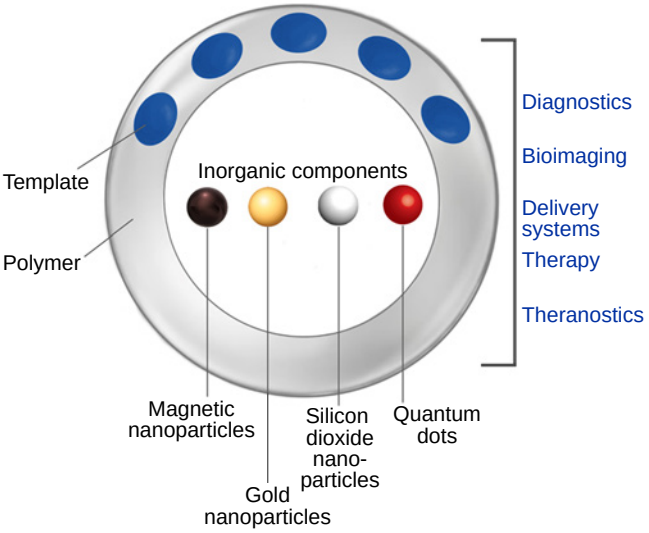

Figure 4. Various types of inorganic NPs in combination with nano-sized MIPs and their possible biomedical applications.

Table 4. Types and properties of the most common inorganic NPs used for MIP functionalization.

NPs	Main properties	Ref.
Au	Localized surface plasmon resonance	86–104
	Radioactivity (^{198}Au, ^{199}Au)	86, 105–112
	High X-ray absorption coefficient	86, 113–118
	Formation of stable chemical bonds with N- and S-containing groups	86, 119
	Catalytic activity	86, 120–124
	Biological activity	39, 86, 125–127
Fe_3O_4	Superparamagnetism	128–133
	High magnetic susceptibility	132, 134–136
SiO_2	Versatility with regard to various surface modification protocols	137–142
	Concentration of silanol groups	137, 143–146
Carbon and graphene quantum dot-based particles	Tunable photoluminescence	147–157
	Upconversion photoluminescence (multiphoton excitation)	151, 158–162
	Electrochemiluminescence	151, 163–165

It is noteworthy that the behaviour of particular inorganic NPs depends appreciably on their characteristics such as shape, size, morphology, and dispersity. The size of NPs can be responsible for some of their properties such as the plasmonic properties of Au NPs (1–100 nm), fluorescence properties of quantum dots (1–10 nm), magnetic properties of iron oxides (2–50 nm), and sedimentation stability (1–100 nm). The similarity of the size of nanomaterials to the size of biological systems such as ion channels (<1 nm in diameter), membranes (3–8 nm), lipid rafts (<50 nm), endocytic vesicles (60–120 nm in diameter), viruses (from nano- to microscale), and protein

microstructures (from nano- to microscale) provides the possibility of effective development and implementation of nanomaterials for medicine. The range of possible biomedical applications for NPs includes the following:

— detection of single biomolecules;
— bioimaging;
— penetration of nanomedicines through the cell membrane;
— prevention of lysosomal/endosomal degradation of nanomedicines.

However, the use of inorganic NPs in biomedicine requires particular attention to their characteristics, because additional requirements are imposed on the materials in this case, *e.g.*, biocompatibility, the lack of toxicity, chemical inertness, and colloidal stability.[166–169] The development of nanoparticles for biomedical applications includes

— chemical synthesis of NPs of various sizes;
— functionalization of the NP surface;
— investigation of the effect of NP size on biochemical and biophysical processes;
— the choice of optimal size for biomedical applications.

The combination of inorganic NPs and MIPs, that is, the formation of hybrid molecularly imprinted polymers can be accomplished using various approaches that include encapsulation of nanomaterials in a polymer matrix during or after polymerization and surface modification of NPs for better compatibility with MIPs. The formation of hybrid MIPs during the synthesis (*in situ*) is achieved by addition of NPs into a solution of functional monomers followed by polymerization to give MIPs. It is possible to use NPs with immobilized molecules as templates for the formation of pores in MIPs. The removal of NPs leaves structures in the polymer matrix that can subsequently adsorb target molecules, thus improving the MIP performance. The surface of inorganic NPs can also be modified towards the formation of bonds with MIP by treatment with a molecular template during imprinting or by conducting post-polymerization modification. Among the most widely used structures of hybrid materials, one can distinguish those with uniform distribution of NPs within the polymer and core–shell structures in which NPs serve as the core and MIP is the shell.

The use of inorganic NPs for the formation of hybrid MIPs dictates the need to ensure reliable attachment of the polymer. Depending on the chemical composition of inorganic materials, different approaches are required for functionalization of the polymer component. One approach includes modification of the surface of inorganic NPs with various bifunctional molecules capable of binding to both the inorganic surface and the polymer, *i.e.*, an additional organic layer is formed on the surface. An alternative approach implies the presence of functional groups in the inorganic component for chemical binding to the polymer surface.[84]

The possibility of using inorganic NPs to design composite materials based on MIPs opens up new opportunities for the use of these systems to solve various biomedical problems such as isolation of biomolecules, diagnosis, therapy, drug delivery, and theranostics. Knowledge of the properties of inorganic NPs helps to make a choice in favour of a definite type of NPs depending on the particular problem.

2.3. Biocompatibility and *in vivo* efficiency of hybrid MIPs

An important characteristic that should be taken into account for the use of any material *in vivo* is biocompatibility, that is, the absence of unfavourable effects on healthy cells and tissues. In the case of hybrid MIPs, this characteristic depends on the chemical composition of both the polymer matrix and the inorganic NPs, as the complexity of the system can increase the number of possible side effects.

New materials are typically tested for biocompatibility *in vitro* using various cell lines. The toxic effects are evaluated depending on whether or not the system under study induces cell death. The cytotoxicity concept is tightly connected to certain aspects such as inflammatory response, changes in the natural morphology and functions of cells, and the overall impact on cellular metabolism.[170]

In a recent study, Peng *et al.*[171] reported the development of a hybrid MIP capable of active tumour targeting and providing the possibility of simultaneous delivery of the photosensitizer chlorin e6 and the anticancer drug doxorubicin (Fig. 5). The resulting composite was a core–shell polymer nanomaterial, in which gadolinium-doped SiO_2 NPs and an added photosensitizer acted as the fluorescent core, while the imprinted polymer layer for molecular templates such as doxorubicin and the epitope of CD59 protein, which is overexpressed in many cancer cells, served as the outer shell. The functional monomers were NIPAM, TBAM, and AA; the imprinting factor was 5.46. Owing to the fluorescent core, the resulting hybrid MIPs were applicable for fluorescence imaging and MRI. The authors achieved a synergistic therapeutic effect owing to the fact that chlorin e6 is able to generate toxic singlet oxygen under the action of laser radiation at 655 nm to kill cancer cells. The possibility of doxorubicin release in the acidic microenvironment of a tumour was studied by placing hybrid MIPs in neutral (pH 7.4) and acidic (pH 5.5) solutions, which resulted in a total drug release of 4.6% and 27.4%, respectively. This demonstrates the potential of the obtained nanocomposite for targeted release of an anticancer drug. The internalization and targeting and therapeutic efficiency were evaluated using the MCF-7 cell lines (overexpression of CD59) and LoVo (low expression of CD59). It was shown that hybrid MIPs had high penetration efficiency and higher cytotoxicity and had a synergistic effect on cancer cells compared to the effect of monotherapy. The cytotoxicity was evaluated *in vitro* using two cell lines, while biosafety and histocompatibility were investigated *in vivo* using histopathological analysis. The testing showed that the developed hybrid MIPs have biocompatibility and minor side effects (the

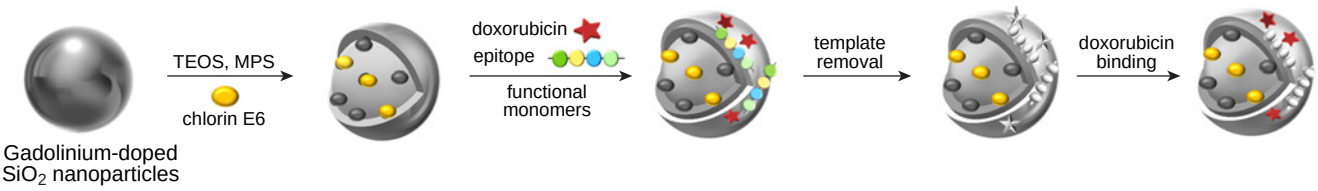

Figure 5. Schematic diagram of the synthesis of hybrid MIPs based on fluorescent NPs against doxorubicin and epitope of CD59 protein.[171]

cell viability in the presence of MIPs was markedly higher than 80% even at a high concentration of 1000 μg mL^{-1}).

In another study, Boitard *et al.*[172] addressed the influence of polymer coating of hybrid MIPs on the intracellular degradation of γ-Fe_2O_3 NPs, as this issue was directly related to the possible accumulation of this material in organs and tissues. As the molecular template, the authors used green fluorescent protein, which is absent in cells or in the culture medium; therefore, the observed effects could be attributed only to the presence of the imprinted polymer rather than to particle binding to any cellular structure. The biocompatibility and degradation experiments were conducted in a buffer solution simulating the internal medium of lysosomes using the PC3 prostate cancer cell line and a model of cartilage tissue formed by differentiated human mesenchymal stem cells. These cells serve as a biocompatibility standard, as they are highly sensitive to any toxic extracellular perturbations. According to the results, the hybrid material is biocompatible and the polymer coating does not markedly affect the degradation of maghemite NPs or cellular internalization; therefore, this material can be considered for clinical use.

For biomedical applications of hybrid MIPs, it is important to consider one more factor, that is, endocytosis by macrophages, as excess endocytosis reduces the number of circulating particles. Dong *et al.*[173] reported a hybrid MIP with fluorescein isothiocyanate-doped fluorescent SiO_2 NPs meant for blocking the signalling pathway of HER2, which is overexpressed in some types of breast cancer cells, *via* binding to HER2 glycans (Fig. 6). HER2 is a glycoprotein containing seven N-glycosylation sites in the extracellular domain. All N-glycans were obtained, purified, and used as templates for imprinting (Fig. 7).

The nanocomposites were obtained by oriented surface imprinting using boronic acid. The cytotoxicity of the obtained MIPs was evaluated using normal mammary epithelial cells (MCF-10A). The high biocompatibility of hybrid materials was

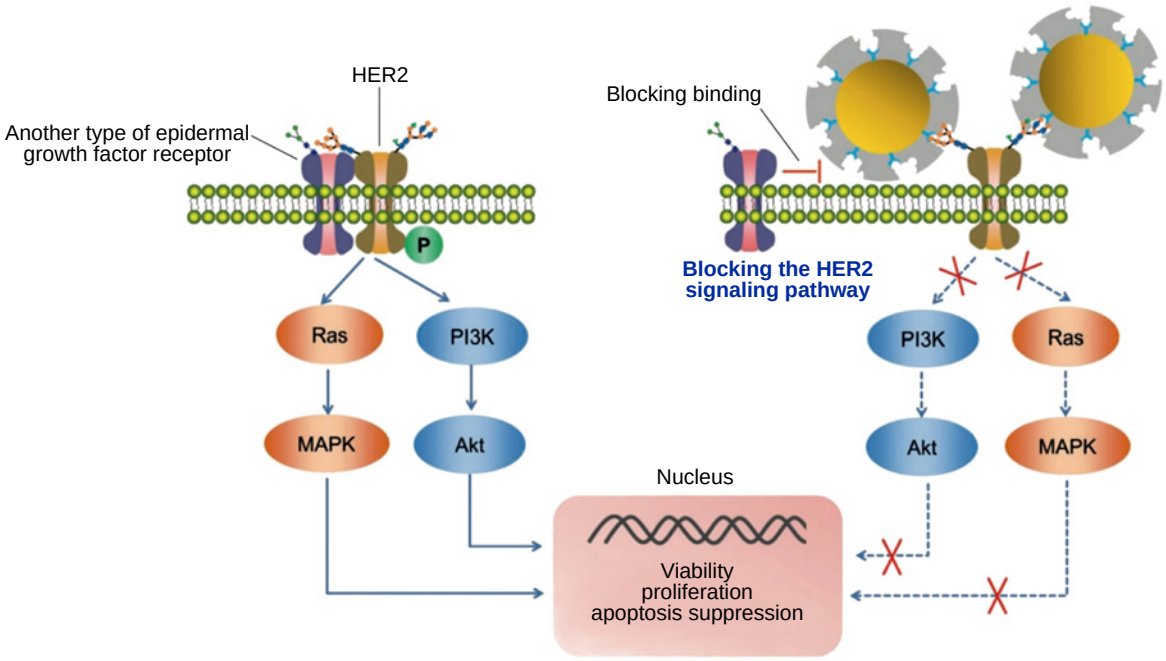

Figure 6. Schematic diagram of the blocking principle of the HER2 signalling pathway through receptor binding to MIPs.[173] Copyright 2019, Wiley.

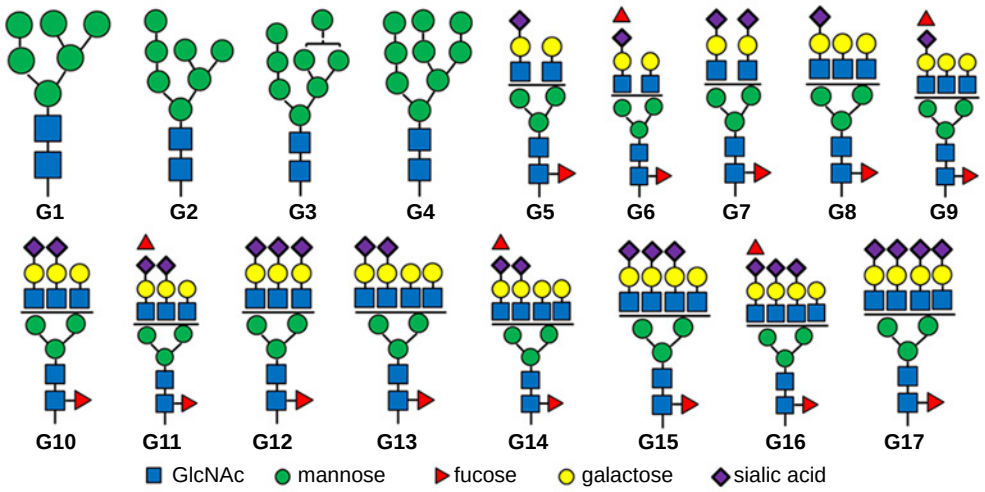

Figure 7. Structures of HER2 N-glycans used as templates for the synthesis of MIPs.[173] Copyright 2019, Wiley.

demonstrated. The *in vitro* experiments carried out with SKBR-3 (overexpression of HER2) and MCF-7 (low expression of HER2) cell lines showed that MIPs are selective to cells that overexpress the imprinted receptor and that they inhibit tumour cell proliferation by 30%. The nanocomposite uptake by macrophages was evaluated. The results attest to endocytosis of a minor amount of MIPs by immune system cells. According to *in vivo* tests in mice, the average tumour volume in the group of mice that received the hybrid material was only about half the tumour volume in the untreated group. The data presented in this study indicate that this hybrid system could serve as an effective strategy for combating breast cancer. Despite the fact that the issue of biocompatibility of MIPs and nanocomposites based on them has long remained poorly addressed, numerous studies along this line have been carried out in the last decade and the methods of synthesis were advanced and improved to provide the absence of toxicity of the imprinted material. These results attest to the possibility of the safe use of hybrid MIPs for the development of new biomedical tools.

3. Hybrid MIPs and their application in biomedicine

3.1. Diagnostics

The development of new diagnostic platforms is an actively developing trend of biomedicine, which opens up new prospects for highly sensitive and specific detection of a broad range of analytes and, as a consequence, for the fight against many socially important diseases.

Modern diagnostic systems are based on analytical methods of molecular biology and bioorganic chemistry such as chromatography, enzyme-linked immunoassay, hybridization analysis, enzymatic approaches, and various imaging methods, including radiology and ultrasound examination. Most often, specific interaction is provided in these systems by using biological molecules such as antibodies, enzymes, and receptors that possess molecular recognition properties, which accounts for the wide use of these molecules in biosensors. The use of these approaches ensures high reliability and sensitivity of the results. Although natural recognition elements possess high affinity for their targets, their practical use is markedly limited because of high sensitivity to the environmental conditions and low stability. Meanwhile, synthetic MIPs can act as alternative recognition elements free from these drawbacks (Section 2.1).[174] Therefore, there is now considerable interest in the development of inexpensive methods for accurate and fast diagnosis of target analytes, including devices with high selectivity. The development of highly stable synthetic platforms mimicking the capabilities of natural analogues is very relevant today.[175]

The advances in the study of hybrid polymer materials and their applications in nanotechnology induced the emergence of a research area focused on molecularly imprinted polymer sensors. The increasing interest in these materials is due to their benefits associated with specific action of the recognition element provided by the imprinted component and with the possibility of choosing the most appropriate method for signal detection owing to diversity of inorganic components and their properties. The affinity and selectivity of imprinted systems are comparable to those of natural receptors. MIP stability and resistance to environmental conditions are many times greater than those of natural biomolecules. Due to the ease of synthesis, preparation of the receptor for a particular analyte can be much faster than, for example, isolation of an antibody. Certainly, mention should be made of the versatility of this approach for virtually any molecular template and easy adaptation to practical applications such as various types of analysis and sensors (Fig. 8).[176]

The first attempts to use imprinted polymers in sensor applications were made in 1992. Since then, a huge number of papers on the use of MIPs in various detection systems have been published, indicating growing interest in this field and its high promise (see, for example, a review [176]).

In recent years, studies have mainly focused on the development of electrochemical and optical platforms based on hybrid imprinted materials.[177,178] A pronounced increase in the sensitivity of these diagnostic systems can be followed: the sensitivity reaches pico-, femto-, and even attomolar concentrations of the analyte.[179,180]

Recently, Majd and co-workers [180] succeeded in the development of a highly selective and sensitive hybrid diagnostic system, which included aptamer and molecularly imprinted components, with a limit of detection of 3.0 aM. The goal of the work was to fabricate a platform for early diagnosis of breast cancer based on the detection of the breast cancer susceptibility gene 1 (BRCA1) (Fig. 9). The synergistic effect was achieved

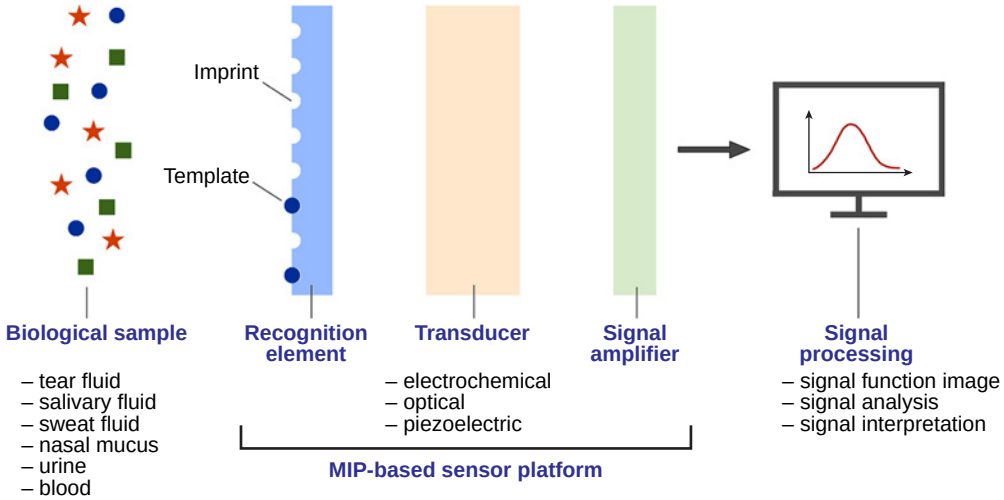

Figure 8. General schematic diagram of the diagnostic process using MIP-based sensor platforms.

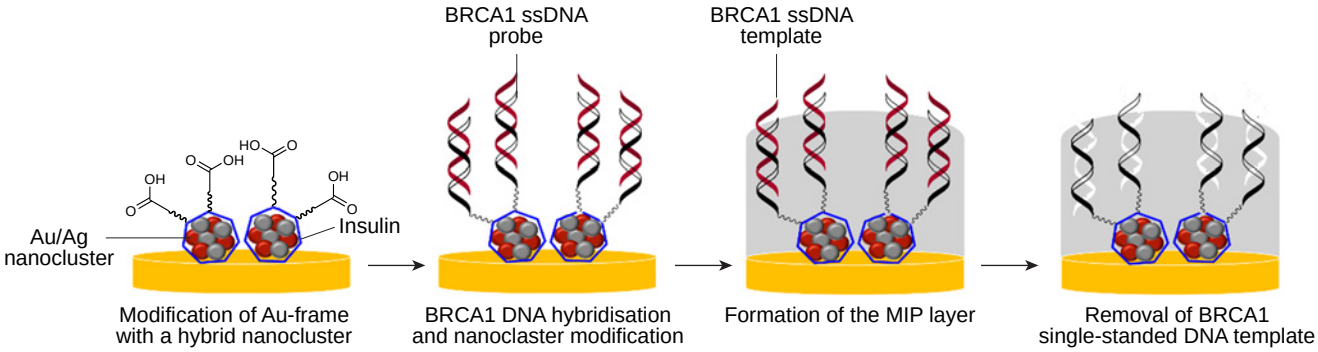

Figure 9. Schematic diagram of synthesis of the hybrid aptasensor with a molecular imprinted layer to detect BRCA1.[180]

by using insulin-stabilized Ag and Au NP-containing bimetallic nanocluster as the inorganic component, on which aptamer probes and a molecularly imprinted layer were immobilized. *o*-Phenylenediamine was used as a functional monomer, and BRCA1 single-stranded DNA target sequence acted as the template to form an aptamer–MIP hybrid detection system. The analytical characteristics of the produced sensor system were studied to determine the target complementary single-stranded DNA; the obtained results revealed the sensitivity of the hybrid material in the linear range from 10 aM to 1 nM. In this case, a combination of molecular imprinting technology with highly sensitive electrolyte-gated molybdenum disulfide field-effect transistor (FET) was demonstrated. Owing to the semiconductor nature, FET biosensors provide a high level of detection of biological objects, while combination of this sensor with the MIP- and aptamer-based hybrid sensing element provides selectivity of the proposed platform. The selectivity of the aptasensor to the template sequence was confirmed by conducting experiments with a single-stranded DNA fragment differing from the target sequence by one base; a very high selectivity of the hybrid material with a coefficient of 12.28 was demonstrated. The analytical applicability and accuracy of the proposed diagnostic platform was evaluated by detecting a complementary sequence in a real blood serum sample from a healthy person after addition of the target template. Under these conditions, the detection limit was calculated as 6.4 aM, which attests to correctness and accuracy of operation of the molecularly imprinted hybrid as well as to the possibility of using this hybrid for diagnostic purposes.

Moving beyond laboratory experiments to the practical use of MIP-based detection platforms on real samples occurs more and more often. Wang and co-workers[177] developed a simple and effective approach to the fabrication of test strips based on dual-emission fluorescent molecularly imprinted polymeric NPs for the colorimetric detection of the dopamine neurotransmitter in blood serum (Fig. 10). As compared with the conventional detection methods, the paper sensors can provide fast and convenient visual on-site analysis without the use of expensive tools or devices.

The system comprised two types of quantum dots with different colour emission: blue carbon quantum dots were embedded in an SiO_2 NP-based inorganic core to maintain a constant fluorescence intensity, while red CdTe quantum dots were incorporated into the imprinted polymer shell and served for recognition of dopamine based on fluorescence quenching upon binding of the molecular template and change in the colour of hybrid emission. Acrylamide and 4-vinylphenylboronic acid served as functional monomers. The proposed test strip clearly revealed the colour differences for dopamine concentrations from 50 to 1200 nM, which attests to relatively low limit of detection of the analyte with the naked eye (80–150 nM). The selectivity of the obtained MIPs was investigated in experiments with structural analogues such as catechol, gallate, levodopa, quinone, noradrenaline and glutamic and γ-aminobutyric acids. It was shown that the fluorescence quenching efficiency was much higher upon binding to dopamine than to analogues. The anti-interference ability of nanocomposites, which is necessary for their practical use, was studied by testing the efficiency of fluorescence quenching in the presence of excess amounts of physiologically common ions, proteins, and saccharides. The results showed no significant interfering effect of these components. When a test strip was used to determine dopamine in a human blood serum sample, the obtained results were similar to the results of high-performance liquid chromatography, which confirms the efficiency and reliability of this approach.

Diagnostic platforms based on molecularly imprinted polymers have attractive physicochemical properties and can serve to detect target molecules at relatively low concentrations in complex samples, which indicates a promise of using the molecular imprinting concept in the design of diagnostic tools. In turn, the relative simplicity and economic feasibility of the synthesis of MIPs make it possible to implement the huge potential of MIPs as accessible and robust analytical devices and to scale up the MIP production. This would enable better and faster detection of various analytes. The diversity of diagnostic systems based on hybrid imprinted materials is demonstrated by examples summarized in Table 5.

Apart from the rapid progress in the development of diagnostic tools based on hybrid MIPs, numerous studies aimed at the preparation and comprehensive investigation of therapeutic platforms using imprinted nanocomposites appeared in the last few years. The interest of researchers in these systems is due to the convenience and ease of handling MIPs, diversity of approaches to MIP production, and the possibility of component optimization and modification for the fabrication of high-performance and multifunctional therapeutic systems. In view of the relevance and intensity of development of this area, the next part of the review is devoted to the use of hybrid MIPs as therapeutic platforms.

3.2. Therapy

As mentioned above, MIP-based hybrid nanomaterials attract considerable attention of researchers owing to effective combination of biomimetic recognition of the imprinted material with unique properties of NPs. The use of such nanocomposites

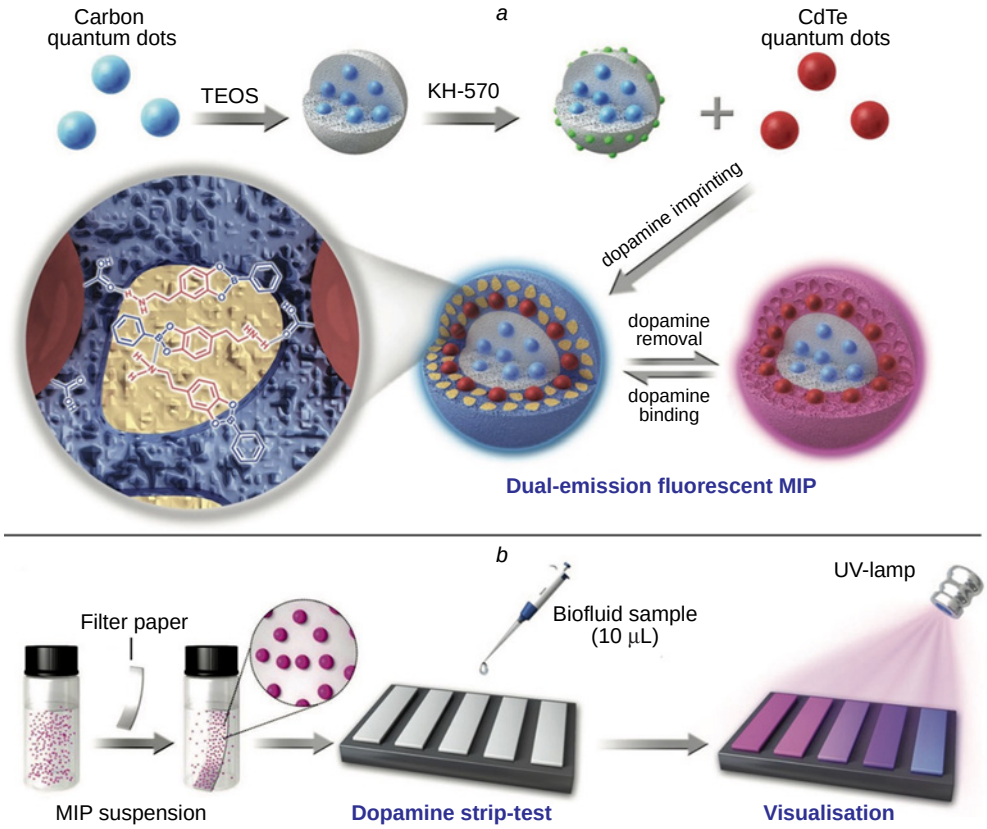

Figure 10. Schematic diagrams of synthesis of MIPs (*a*) and detection of dopamine (*b*) using MIP-based test strips.[177] Copyright 2018, Wiley.

in the therapy requires that a number of important criteria be met, including the ability to bypass the reticuloendothelial system during circulation in blood stream and the possibility of active targeting and/or controlled release of drugs. Fulfilment of these requirements ensures optimization of therapeutic efficacy with minimized side effects.

Currently, the possibilities of application of the molecular imprinting concept in therapy are versatile. The use of medicinal agents as molecular templates makes it possible to use hybrid MIPs as drug carriers. Meanwhile, nanocomposites themselves can act as therapeutic platforms by regulating cell signalling pathways without the use of any medications. Moreover, imprinted materials can integrate quite a few functions in a single system and thus form a potent and versatile tool for synergistic therapy.[212]

3.2.1. Drug delivery

The potential use of MIPs for drug delivery was first reported in 1998.[213] In this study, the imprinted polymer was formed using MAA, while EGDMA served as the cross-linking agent. The resulting MIP could selectively recognize the anti-asthmatic drug theophylline in comparison with the structurally similar caffeine. In addition, the possibility of gradual drug release was described. This study paved the way for *in vivo* application of MIPs and served as a starting point for acknowledging these materials as promising platforms for the delivery of therapeutic agents. Since then, numerous studies appeared describing versatile applications of MIPs, including hybrid ones, in this field.[34,46,170,214,215]

Unlike other nanocarriers the surface of which needs to be modified with targeting ligands, MIPs contain such moieties from the very beginning as sites formed for the specific binding of the target compound. Furthermore, owing to intermolecular interactions such as hydrogen bonds and hydrophobic, dipole–dipole, and ionic interactions between the molecular template and functional groups of the polymer, it is possible to increase the stability or solubility of the drug, as well as regulate the release kinetics.[35]

The nature of the molecularly imprinted template plays the crucial role in the drug release, and the drug release mechanisms can be quite complicated. Here, one can consider ways to regulate the release of the drug from the polymer by using systems with varying swelling ratios. For example, hydrogels with a low degree of cross-linking and a high swelling ratio can be combined with rigid polymer networks that are not prone to swelling.[216] In this type of systems, relaxation of the polymer matrix controls the penetration of physiological fluid into the polymer network, while transport is described by Fick diffusion laws. A possible mechanism consists in the drug release in response to various stimuli (heating, pH change, exposure to electric or magnetic field, or enzymes) that bring changes into the polymer structure or the strength of interactions between functional groups of the polymer matrix and the molecular template. Most often, this mechanism is implemented in hybrid MIPs that use integration with materials that disclose their additional properties.[170,214,217]

3.2.1.1. pH-responsive drug release

The release of therapeutic molecular templates in response to a change in the acidity of the medium is a key method of stimulus-responsive delivery of therapeutic agents. For example, pH-dependent drug release may be appropriate for the treatment of

Table 5. Application of hybrid MIPs in diagnostic systems.

Type of NPs	Functional monomer	Molecular template	Principle of analysis, diagnostic tool	Limit of detection	Test samples	Ref.
CNTs	4-Vinylphenylboronic acid	α-Fetoprotein	Nanosensor for the determination of glycoproteins	1 ng mL^{-1}	Complex samples, including serum	181
Fe_3O_4 NPs	Pentaerythritol tetrakis(3-mercaptopropionate), methacrylic acid (MAA), trimethylolpropane trimethacrylate	Trisaccharide Gal-a-1,3(Fuc-a-1,2)Gal	Optical blood typing based on specific factors rather than whole red blood cells	–	Blood	182
CQDs/SiO_2 NPs	Methylenebisacrylamide, AA, 4-vinylphenylboronic acid	Dopamine	Test strips for colorimetric imaging	$(100–150)\times10^{-9}$ M	Biological fluids	177
Magnetic cluster based on MWCNTs, Fe_2O_3 NPs, and Au NPs	*ortho*-Aminothiophenol	Bilirubin	Electrochemical sensor for detection of neonatal jaundice	1.36 pM	Saliva, blood serum	179
Fe_3O_4 NPs/Au NPs	Tannic acid	Prostate-specific antigen	Surface-enhanced Raman spectroscopy sensor for the detection of cancer biomarkers	0.9 pg mL^{-1}	Blood serum	183
CQD	APTES	Promethazine hydrochloride	Optical sensor	0.5 μmol L^{-1}	Blood serum	178
SiO_2 NPs	AA, MBA, MAA, 2-(вimethyl-amino)ethyl methacrylate	Chicken egg white lysozyme	Recognition material for quality analysis and regulatory control in food matrices	0.5 mg mL^{-1}	Physiological saline solution	184
SiO_2 NPs	MAA	Amlodipine besylate	Biomimetic recognition	4.67 ng mL^{-1}	Aqueous solution	185
SiO_2 NPs	MBA, acrylic acid (AAc), TBAM, NIPAM	Ciprofloxacin	Method for determination of fluoroquinolone antibiotics	0.2 μg mL^{-1}	Urine	186
Fe_3O_4 NPs	1-Vinyl-3-aminoformylmethyl-imidazolium chloride	Lysozyme	Adsorbent for isolation of proteins	–	Aqueous solution	187
CQDs	NIPAM, 4-vinylphenylboronic acid	α-Fetoprotein	Biomimetic fluorescent nanosensor for detection of tumour biomarkers	0.474 ng mL^{-1}	Blood serum	188
Au NPs/graphene	3,4-Ethylenedioxythiophene	Human epidermal growth factor receptor 2 (HER2)	Biomimetic sensor for detecting cancer biomarkers	0.43 ng mL^{-1}	Blood serum	189
Fe_3O_4 NPs	Itaconic acid, allylamine, fluorescein for leukotrienes; ethylene glycol methacrylate phosphate, NIPAM, MBA, allylamine, itaconic acid, fluorescein for insulin	Leukotrienes, insulin	Assay in magnetic microplates	0.73 pM for leukotrienes and 27 pM for insulin	Urine and blood plasma	190
GO	Phenyltriethoxysilane, tetramethoxysilane	Ovalbumin	Biomimetic electrochemical sensor for glycoproteins	0.02 pg mL^{-1}	Chicken and quail eggs	191
Fe_3O_4@SiO_2 NPs	MAA, AA	Pyocyanin	Detector for *Pseudomonas aeruginosa*	–	Sputum	192
Fe_3O_4@SiO_2 NPs	Methyl methacrylate, ethylene glycol dimethacrylate (EGDMA)	Tumour necrosis factor (TNF-α)	Electrochemical sensor for biomarkers of neonatal sepsis	0.01 pM	Phosphate buffer	193
SiO_2 NPs doped with graphene quantum dots	APTES	Metronidazole	Optical nanosensor	0.15 μM	Blood plasma	194
Au NPs	4-Vinylphenylboronic acid	Carcinoembryonic antigen	Surface-enhanced Raman scattering for detection of glycoproteins	0.1 ng mL^{-1}	Blood serum	195

Table 5 (continued).

Type of NPs	Functional monomer	Molecular template	Principle of analysis, diagnostic tool	Limit of detection	Test samples	Ref.
Fe_3O_4 NP/GO/Au NP composite	MAA, MBA	Epinephrine	Electrochemical sensor	5 nM	Urine and blood	196
Fe_3O_4 NP/GO/Ag NP composite	AA	Quercetin	Electrochemical sensor	13 nM	Pharmaceutical samples	197
Fe_3O_4 NPs	4-[(4-Methacryloyloxy)phenyl-azo]benzenesulfonic acid	Paracetamol	Electrochemical sensor	0.43 μmol L^{-1}	Urine	198
Bimetallic nanocluster Ag NPs/Au NPs	*o*-Phenylenediamine	Biomarker of the BRCA1 gene	Aptasensor for detection of the BRCA1 gene	6.4 aM	Blood serum	180
MWCNTs	MAA	Norfloxacin	Electrochemical sensor for pharmaceutical analysis and clinical monitoring	1.58 nM	Pharmaceutical samples, rat plasma	199
MWCNTs functionalized with $CuCo_2O_4$ NPs	Aniline	Metronidazole	Electrochemical sensor	0.48 nM	Blood serum, urine	200
MWCNTs	Aminopropyltrimethoxysilane	Tinidazole	Electrochemical sensor	1.25 pmol L^{-1}	Pharmaceutical samples, blood serum, urine	201
MWCNTs	Cysteine	Ceftizoxime	Electrochenmical sensor	0.1 nmol L^{-1}	Blood serum, urine	202
GO, Au (nanowire)	Aniline	Cefixime	Electrochemical sensor	7.1 nM	Blood serum, urine	203
GO, $ZnFe_2O_4$ NPs	*N*-vinylcaprolactam, MBA	Ciprofloxacin	Electrochemical and optical sensor	0.39 μg L^{-1} for the electrochemical component and 0.40 μg L^{-1} for the optical component	Blood serum, blood	204
Fe_3O_4 NPs/ MWCNT/GO	Methyl acrylate	Prostate-specific antigen, myoglobin	Electrochemical sensor for simultaneous detection of two target analytes	5.4 pg mL^{-1} for the antigen and 0.83 ng mL^{-1} for myoglobin	Blood serum, urine	205
Magnetic nanocluster GO/Ni NPs/Cd NPs	4-Carboxyphenylboronic acid	Cancer markers CA125 and CA15-3	Fluorescent sensor for simultaneous detection of two target analytes and breast cancer screening	50 μU mL^{-1}	Blood serum	206
Au NPs	Dopamine	α-Fetoprotein	Differential pulse voltammetry-based sensor	0.81 pg mL^{-1}	Blood serum	207
Au NPs/GO-based quantum dots	Nicotinamide	Dopamine, chlorpromazine	Electrochemical sensor for simultaneous detection of two target analytes	0.25 – 2.8 nM	Blood serum, urine, and pharmaceutical samples	208
CdTe quantum dots	3-Aminophenylboronic acid	Sialic acid, fucose, mannose	System for multiplexed cancer cell imaging	–	Phosphate buffer	209
CQD	(4-acrylaminophenyl)(amino) methaniminium acetate (AB), methacrylamide	Glucuronic acid	Optical imaging of biomarkers on the surface of cancer cells	–	Phosphate buffer	210
SiO_2 NPs	(4-acrylaminophenyl)(amino) methaniminium acetate (AB), rhodamine, NIPAM	D-glucuronic acid (hyaluronic acid epitope)	Fluorescent nanogel for intracellular location and detection of target molecules	–	Phosphate buffer	211

certain cardiovascular pathologies due to changes in blood serum acidity and for the treatment of cancerous tumours, since almost all tumour tissues are characterized by low pH (5–7). These pH values can be used to cleave acid-labile bonds in an imprinted delivery system formed between a molecular template and a functional monomer or covalent bonds of a cross-linked polymer network. Polymers that respond to a change in pH are polyelectrolytes in which functional groups are protonated or deprotonated upon a change in the acidity, thus inducing a change in the swelling ratio. As a result, the globule conformation is converted to a coil because of the electrostatic repulsion of the generated charges. The sensitivity to the pH value is induced by basic functional groups of the polymer such as amine and morpholine groups and pyridine and piperazine residues (Fig. 11 *a*) or by acidic functional groups including carboxylic, phosphonic, boronic, and sulfonic acid residues (Fig. 11 *b*). Various vinyl monomers containing the above groups are often used to provide for the pH lability of polymers. Thus, the medicinal agent is selectively released from the pH-responsive polymer matrix only around the target site in an acid medium.

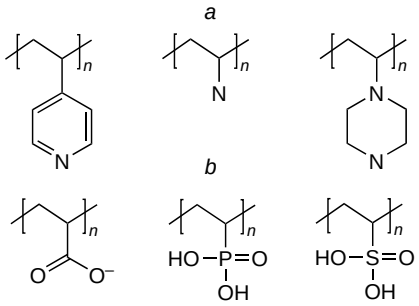

Figure 11. pH-sensitivity of a polymer material is provided by basic (*a*) or acidic (*b*) groups.

Using thermodynamic calculations of the dynamics of interaction between a drug, a monomer, and a solvent, Talavat and Güner[218] predicted the structure of hybrid MIP based on Fe_3O_4 NPs for the delivery and controlled released of the anticancer drug 5-fluorouracil. Relying on the obtained results, the authors chose 4-vinylpyridine (4-VPy) and AAc as the optimal monomers. The results of high-performance liquid chromatography demonstrated that the rate and degree of release of 5-fluorouracil was higher at pH 5.8 than at the biological pH 7.4, which was favourable for the selective drug release in the tumour microenvironment. A comparison of magnetic MIPs containing different functional monomers demonstrated that the release rate was higher for the hybrid material containing 4-VPy than for MIP consisting of acrylamide: in the former case, approximately 90% of the drug was released within 30 days at pH 5.8, while in the latter case, the percentage of release was 80% under the same conditions. Nevertheless, the results obtained in each case illustrate the optimal controlled release of 5-fluorouracil, and the authors also emphasize the biocompatibility of the hybrid materials.

Hassanpour *et al.*[219] proposed a strategy for the delivery and increase in the activity of the anticancer drug azidothymidine using the hybrid molecular imprinting technology (Fig. 12). Methacrylic and itaconic acids were chosen for the comparison as functional monomers, EGDMA and trimethylolpropane triacrylate served as variable cross-linking agents, and Fe_3O_4@SiO_2 NPs were chosen among inorganic materials. The combination of itaconic acid and ethylene glycol dimethacrylate with hybrid NPs proved to be most efficient. The azidothymidine release was studied *in vitro* at pH 5, which corresponds to the intracellular pH for cancer cells, and at pH 7.4, which corresponds to that in healthy cells and plasma. The proposed carrier did not demonstrate a considerable release (the release was approximately 14%) in healthy cells and blood circulatory system, which markedly decreased the dose-dependent side effects. Meanwhile, lower pH resulted in the destruction of hydrogen bonds between the molecular template and the polymer active site, which induced drug release.

The cytotoxicities of free azidothymidine and the obtained delivery system were compared using MCF-10 normal cells and MCF-7 breast cancer cells. It turned out that the cytotoxicity of free azidothymidine did not depend on the cell type, being approximately 11%, while the cytotoxicity of MIPs was much higher in MCF-7 cancer cells (91%), with almost no effect on the normal cell line (MCF-10). These results demonstrate a combination of high efficiency and biocompatibility of the composite.

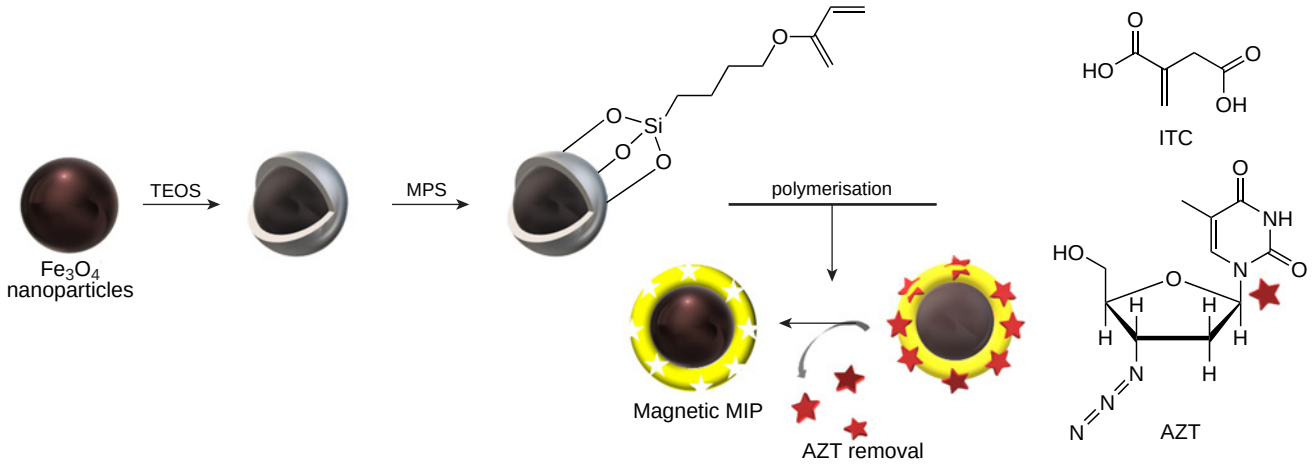

Figure 12. Schematic diagram of the synthesis of hybrid MIPs for the delivery and increase in the therapeutic efficacy of azidothymidine. ITC is itaconic acid, AZT is azidothymidine.[219]

3.2.1.2. Light-responsive drug release

Light-controlled release of a therapeutic agent is another attractive approach for targeting of therapeutic agents. In this type of drug delivery systems based on light-responsive MIPs, the incorporation of azobenzene derivatives into a mixture of functional monomers is used most often. The active groups of this compound can exist in two forms: stable *cis*-isomer and metastable *trans*-isomer. On exposure to ultraviolet radiation (340–380 nm), azobenzene isomerizes, being converted from the *trans*- to the *cis*-form. The reverse conversion can be initiated by visible light or a temperature rise (Fig. 13).[170,220] However, the phototoxicity of ultraviolet radiation limits the use of conventional photosensitive azobenzene-based molecularly imprinted polymers in biomedicine.[221] For biomedical applications, it is more appropriate to use long-wavelength light sources and the near-infrared range; this radiation can penetrate into tissues and provide for light-responsive drug release in the local therapy of tumours. Therefore, researchers develop various approaches that allow the use of alternative wavelengths that have no adverse effect on the body.

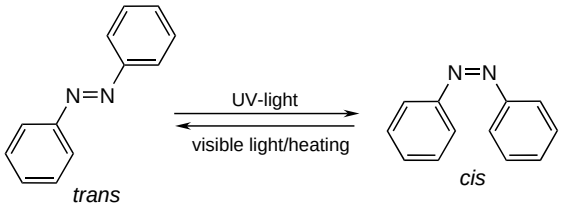

Figure 13. Schematic diagram of light-responsive isomerization of azobenzene.

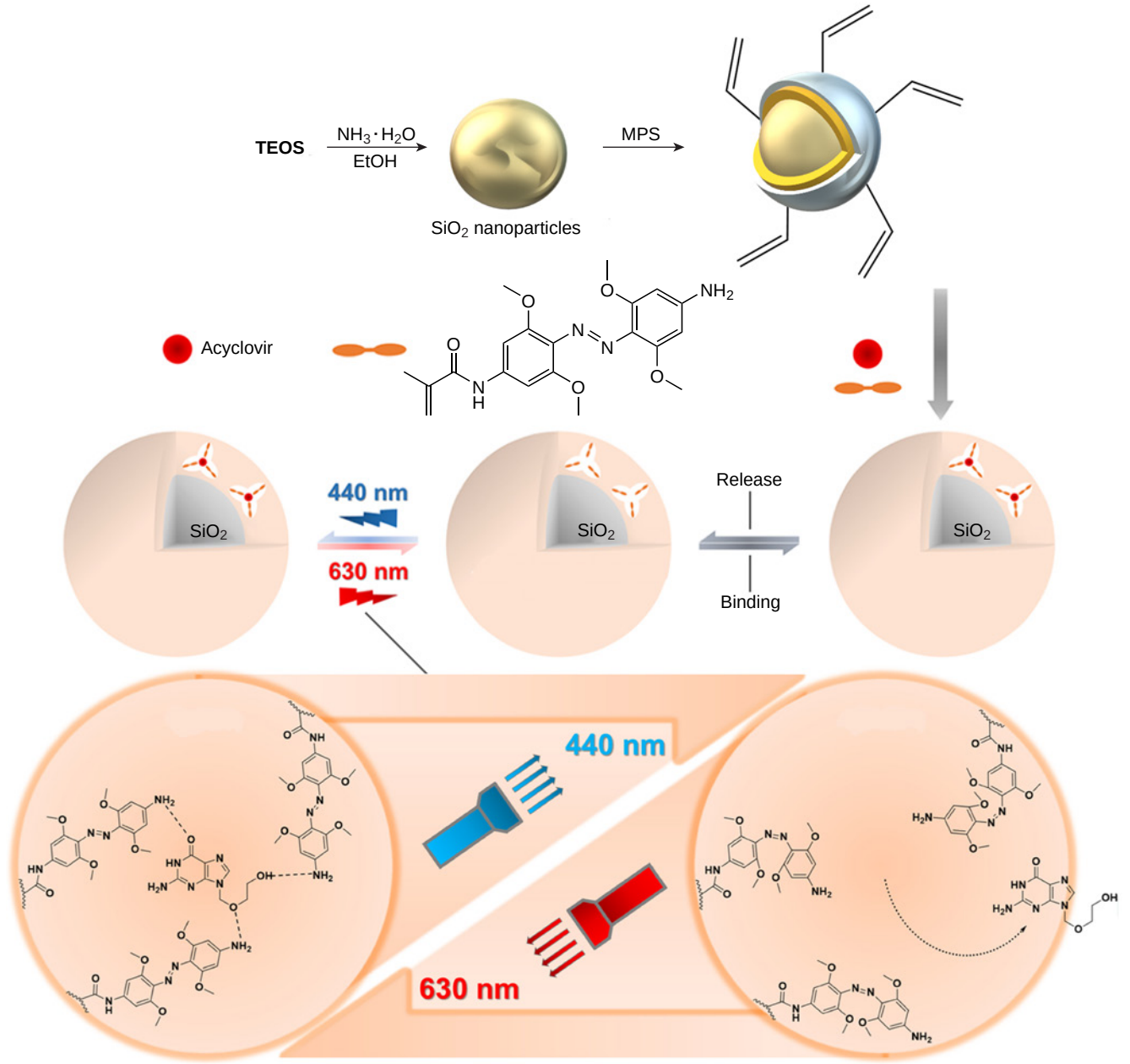

Figure 14. Schematic diagram of the synthesis of hybrid MIP and mechanism of light-induced acyclovir release.[222] Copyright 2018, American Chemical Society.

Liu and co-workers[222] described an approach to the fabrication of a hybrid molecularly imprinted polymer based on SiO_2 NPs and tetra-*ortho*-methoxy-substituted azobenzene derivative for the delivery and controlled release of the drug acyclovir, which is widely used for the treatment of viral diseases (Fig. 14). The functional monomer, *N*-[4-((4-amino-2,6-dimethoxyphenyl)diazenyl)-3,5-dimethoxyphenyl]-methacrylamide, enabled the use of isomerization for the release of the molecular template, owing to photoswitching induced by visible light, which is biocompatible (irradiation at 440 nm for *trans* to *cis* conversion; irradiation at 630 nm for the *cis* to *trans* conversion). The obtained nanocomposite demonstrated high adsorption capacity towards acyclovir (12.65 μmol g^{-1}), which was almost three times higher than this value for the non-imprinted analogue. The selectivity of hybrid MIP to the template was studied in experiments with ganciclovir and triacetyl-ganciclovir as competing drugs. It was found that the most effective binding occurs particularly with acyclovir, that is, the template. Light-induced drug release in deep tissues was evaluated using 1 mm-thick chicken skin, which was located between the light source and the cuvette with the test material. The photoisomerization of the polymer coating under these conditions required more time, but remained effective. This study demonstrates good prospects for the use of red and blue light in combination with molecular imprinting for stimulus-responsive release of medicinal agents.

The limitations related to the use of azobenzene can also be overcome by using hybrid systems based on inorganic NPs owing to certain properties such as pronounced absorption in the infrared region and high efficiency of photothermal conversion. In a recent study, Liu *et al*.[221] proposed an interesting and unconventional approach to the development of a multilayer supramolecular structure of light-responsive hybrid MIPs for the delivery and infrared light-induced release of paracetamol, a widely known analgesic (Fig. 15). Inorganic lanthanide-doped upconversion nanoparticles (UCNPs) that convert infrared radiation (980 nm) to visible light served as the core. An azobenzene derivative sensitive to green light (520–550 nm), 4-[(4-methacryloyloxy)-2,6-dimethylphenylazo]-3,5-dimethylbenzenesulfonic acid, was used as the functional monomer. In the obtained system, the infrared irradiation induced green fluorescence of the inorganic core. This emission was absorbed by azobenzene-containing MIP on the NP surface, which induced *trans*/*cis*-isomerization and release of the medication. In addition, the hybrid material provided light-controlled release of paracetamol into an aqueous solution through pig skin, which demonstrated the potential and efficacy of this system *in vivo*. The synthesized MIP had an imprinting factor of 1.7 and simultaneously demonstrated high specificity to the template in experiments with structural analogues such as antifebrin and phenacetin (the selectivity coefficient was 2–4 depending on the type of analogue). The biocompatibility of MIPs was demonstrated using the CT26 human colon cancer cells; the viability of the studied malignant cells in the presence of MIP did not decrease below 80% even at the concentration of 100 μg mL^{-1}. Thus, the hybrid MIP proposed in this study has a potential for the delivery of therapeutic agents into deep tissues.

3.2.1.3. Temperature-responsive drug release

Another class of materials for stimulus-responsive release of therapeutic agents are thermoresponsive polymer systems. In this case, the mechanism of release of bound molecules upon temperature rise is similar to the mechanism observed for polymers sensitive to the pH change. As a rule, the therapeutic molecules are incorporated into thermoresponsive polymers at minimum temperatures of the solution where the polymer occurs in the hydrophilic state and the imprinted areas are sterically closed and thus hold the useful therapeutic load within the polymer. As the temperature increases to the lower critical

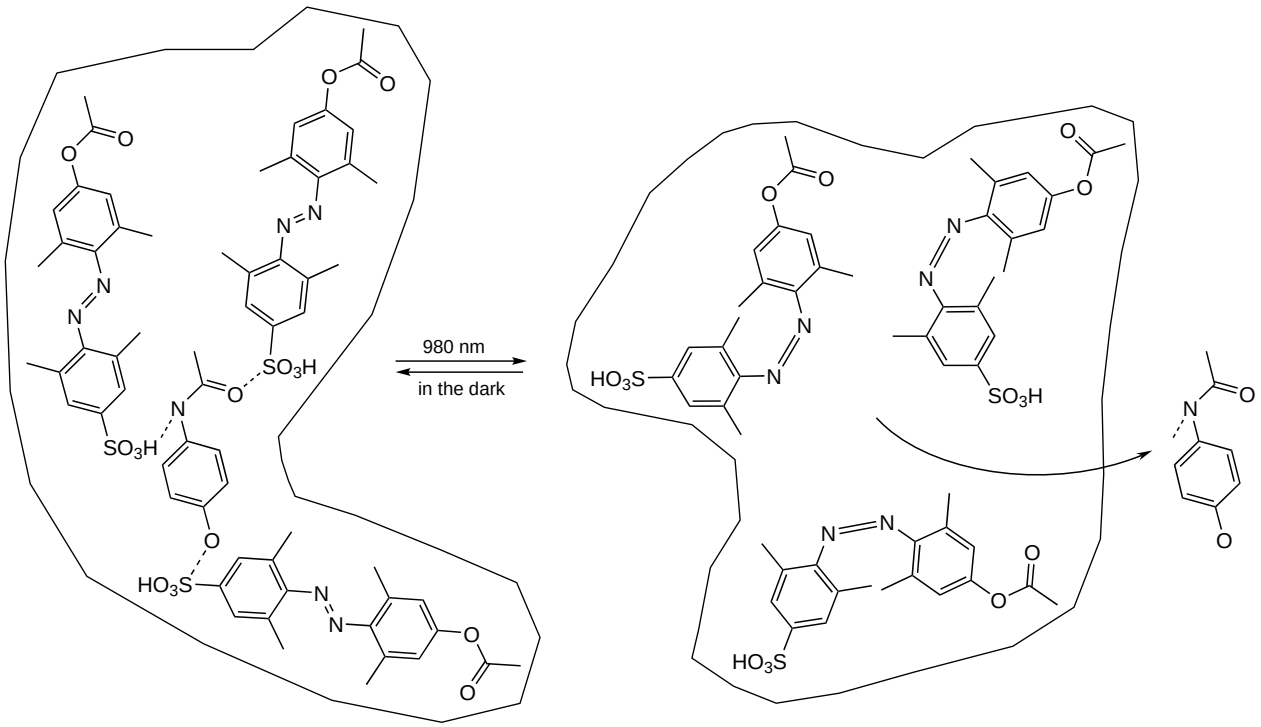

Figure 15. Mechanism of light-induced release of paracetamol from hybrid MIP.[221]

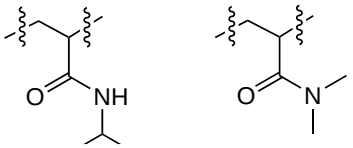

Figure 16. Examples of thermoresponsive functional monomer units.

solution temperature (LCST), a reversible phase transition occurs, the polymer becomes hydrophobic, the binding sites are opened, and the embedded molecules are released to the outside. Thermoresponsive MIPs are usually prepared by incorporation of temperature-dependent functional monomers such as NIPAM or *N*,*N*-dimethylacrylamide (Fig. 16).[170] The former contains a hydrophilic amide and hydrophobic isopropyl group; as a result, it is possible to change the hydrophilic–hydrophobic balance by varying the external temperature. An important concept is the lower critical solution temperature (LCST), below which the mixture components are miscible in any proportions. In the case of NIPAM, this value is approximately 32°C. As a polymer solution is heated above this temperature, a reversible phase transition occurs from a soluble hydrated state, in which the amide group forms hydrogen bonds with water and determines the hydrophilic properties of the polymer, to an insoluble dehydrated state, in which the polymer forms globules and becomes predominantly hydrophobic.[223] Owing to the thermosensitivity, NIPAM-based polymers are capable of releasing the drugs loaded into them at a temperature close to human body temperature and, hence, they can be used as a basis for controlled drug delivery. A combination of thermoresponsive polymers with magnetic NPs in hybrid MIPs allows for targeted delivery of the hybrid system to the target, thus increasing the local therapeutic efficacy.

Sedghi *et al*.[224] presented a new smart molecularly imprinted nanocomposite based on thermoresponsive NIPAM and magnetite NPs for the targeted delivery and controlled release of curcumin, a drug with broad pharmacological action. The hybrid material was supplemented with acryl functionalized cyclodextrin for better covalent binding of the template in the polymer matrix (Fig. 17). The presence of hydrophilic cyclodextrin in the copolymer leads to an increase in the hydrophilic–hydrophobic transition temperature of NIPAM to 34°C. The nanocomposite proved to be selective in experiments with structural analogues such as benzophenone and phthalimide. Examination of the curcumin release profile showed that at room temperature, the major portion of the drug is released from the nanocomposite surface within the first 7 h and, after that, prolonged release of the remaining drug occurs in three days. Temperature rise to 38°C results in a sharp release of approximately 86% of curcumin, which is due to a change in the volume of the temperature-sensitive polymer. These data indicate that increase in the hydrophobicity disrupts the hydrogen bonds between the molecular template and the polymer network, leading to increasing percentage of drug release, while more stable binding sites between cyclodextrin and curcumin ensure prolonged release of the drug remaining in the hybrid MIPs.

The use of magnetic NPs in hybrid MIPs not only allows for the delivery of the targeted system to the desired tissue or organ using an external magnetic field, but also makes it possible to generate heat in a magnetic field of alternating current by weakening of their magnetic moment. Moreover, the amount of released heat can be controlled by modulating the magnetic field strength and the size of NPs.[225]

Cazares–Cortes *et al*.[226] developed and compared two hybrid systems for the delivery and controlled release of doxorubicin under the action of alternating magnetic field. One of the materials represented a magnetic nanogel produced from thermoresponsive and biocompatible polymers based on oligo(ethylene glycol) methyl ether methacrylate, while the second one was a core–shell system with a magnetic core coated with MIP based on acrylic acid and acrylamide (Fig. 18). γ-Fe_2O_3 nanoparticles were used as the magnetic component. The systems behaved in different ways. In the case of magnetic nanogel, only physical capture of the anticancer agent took place. Therefore, doxorubicin was efficiently released both under the action of alternating magnetic field (45%) and without a field (24%). Hybrid MIPs formed hydrogen bonds with the template; as a result, more than half of the drug was released under an external stimulus, whereas passive release was low (10%). Thus, magnetic nanogel can serve as a reservoir for continuous release of doxorubicin, with the maximum release efficiency being observed upon local activation by a magnetic

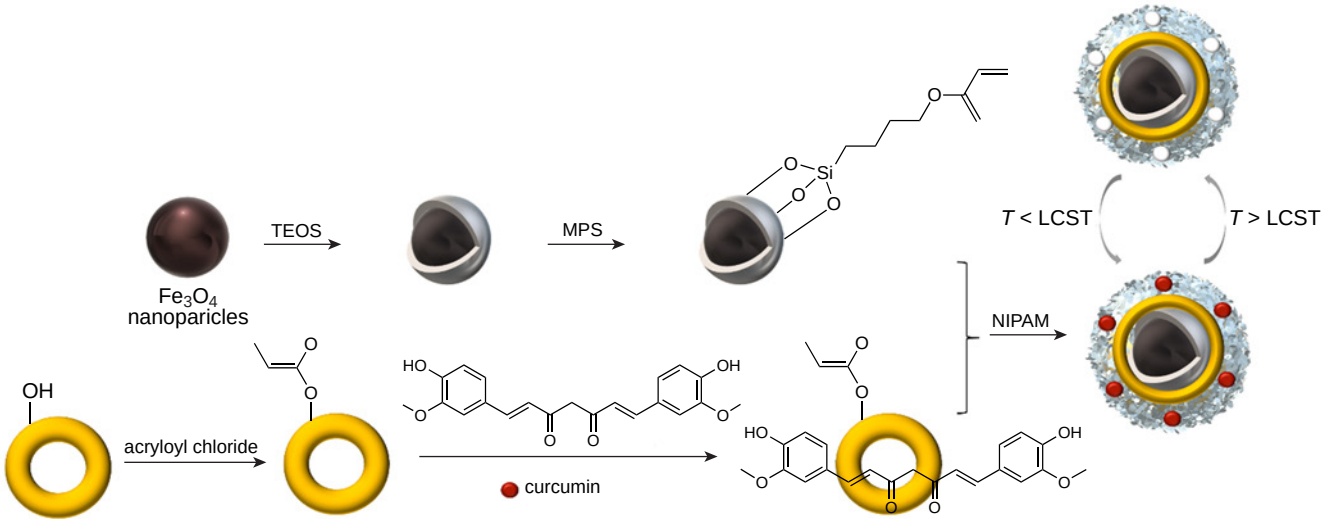

Figure 17. Schematic diagram of the synthesis of hybrid MIPs and mechanism of temperature-induced release of curcumin.[224]

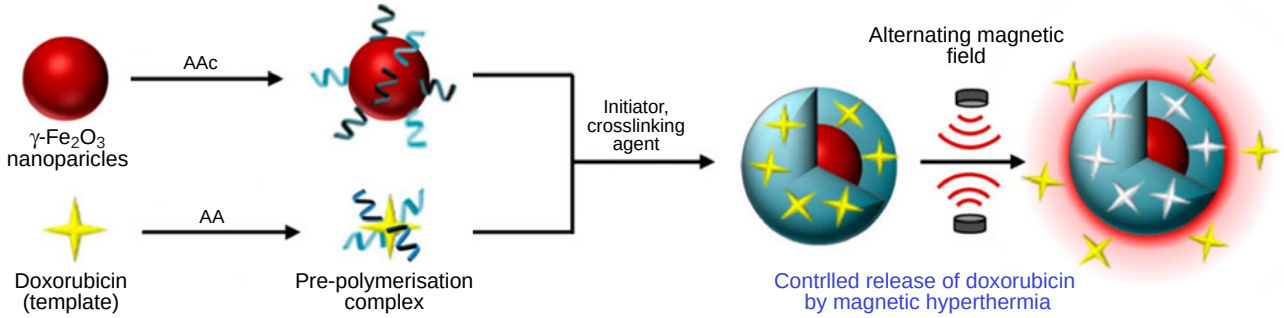

Figure 18. Schematic diagram of the synthesis of hybrid MIPs for the delivery and controlled release of doxorubicin induced by alternating magnetic field.[226] Published under the CC BY license.

field, while MIP can substantially decrease the nonspecific drug release and deliver the drug only under the action of a stimulus. During the release of doxorubicin *in vitro* even when the macroscopic temperature was maintained at 37°C, the temperature inside the polymer matrix was close to 60°C, which was attributable to the local heating of magnetic NPs under the action of alternating magnetic field and resulted in more efficient release of the template and, as a consequence, decreased the viability of cancer cells.

3.2.1.4. Drug release under the action of dual/multiple stimuli

The dual or multiple stimulus sensitivity refers to the response of polymeric material to a set of external stimuli. These systems can include heat/light, heat/pH, magnetic field/light, magnetic field/heat, or other combinations. As compared with MIPs that respond to a single stimulus, the complex composites are characterized by multifunctional and higher-level response; hence, development of hybrid MIPs with multiple stimulus response and multi-parameter targeting is a promising branch in the design of targeted drug delivery systems.[223]

Lin *et al*.[227] reported the synthesis of molecularly imprinted nanospheres with adjustable polymer layer thickness (40–150 nm) and a magnetic core (Fe_3O_4@SiO_2 NPs) for the controlled release of ibuprofen (Fig. 19). 4-Vinylpyridine was used as a functional monomer. The prepared nanospheres were modified with hydrophilic macromolecular chains of poly(*N*-isopropylacrylamide-co-spiropyran acrylate) to obtain a multiresponsive surface. Experiments on binding of the prepared material to structural analogues of ibuprofen such as naproxen and ketoprofen were carried out; this demonstrated the selectivity and specificity of binding to the template (the selectivity coefficient was more than two for both structural analogues). The presence of an inorganic Fe_3O_4 core provided the material with high magnetization and enabled fast separation of the nanospheres from the solution using a magnet. The obtained hybrid MIP possessed multifunctionality, being responsive to both temperature and UV radiation. A study of NIPAM-induced effect of temperature on the drug release dynamics demonstrated that due to the shrinkage of macromolecular chains during the first 5 h, the amount of the released drug was higher at 25°C than at 45°C. However, as the incubation time was increased, the total release coefficient was more than 3.5 times higher at 45°C, which is due to more intense molecular diffusion. The light-responsive behaviour was due to the introduction of spiropyran acrylate units, which provided for the electrostatic interaction between the macromolecular chains as a result of isomerization and affected the drug release dynamics. Upon UV irradiation (λ = 365 nm), the cumulative release of ibuprofen somewhat decreased (from 42 to 38%); however, the process of drug release can be deliberately prolonged in this case. The results clearly attest to the dual response of the proposed hybrid MIP and show the effect of delayed release under the influence of external stimuli.

Abdolyousefi *et al*.[228] proposed a method for the preparation of multifunctional hybrid MIP based on zinc-doped titanium dioxide NPs. The authors used a mixture of two functional monomers: *N*-vinylcaprolactam as a thermoresponsive component and MAA for pH sensitivity. In addition, the introduction of methacrylic acid as a hydrophilic comonomer to *N*-vinylcaprolactam made it possible to increase the LCTS value to optimum for thermoresponsive drug delivery (40°C). In the synthesis of the composite, uracil acted as the 5-fluorouracil pseudo-template molecule; therefore, the selectivity of hybrid MIPs to 5-fluorouracil was evaluated in comparison with its pseudo-template and gemcitabine. Owing to the molecular structural matching of the binding sites, the uracil extraction rate was estimated at approximately 95%, while this value for 5-fluorouracil was calculated as 80% due to the presence of an additional fluorine atom and some changes in the molecular conformation; in the case of gemcitabine, the percentage of binding was only 35% due to pronounced differences in the chemical structure. Thus, the use of pseudo-template instead of the target molecule during the synthesis provided an imprinting factor for 5-fluorouracil of 3.2. The release profiles of the anticancer drug at different pH and temperatures demonstrated effective release in an acidic medium (pH 5.5) and at temperatures exceeding low critical temperature for the copolymer solution (41°C), which ensured selective drug release only in the tumour microenvironment and mitigated toxic side effects. An additional therapeutic effect was also demonstrated for superficial tumours such as melanoma, due to high absorbance of TiO_2 NPs in the visible and infrared regions, resulting in heat release and temperature rise to levels much exceeding the low critical temperature. High biocompatibility (the viability of healthy cells in the presence of drug-free material was more than 80% even at high concentrations) and minor hemolytic activity (less than 5%) of the hybrid MIP even at concentrations of 250 μg mL^{-1} were demonstrated. The results indicate that the proposed system can be used for stimulus-responsive chemotherapy of tumours in combination with additional effects caused by the physicochemical properties of the inorganic component for the treatment of various types of cancer.

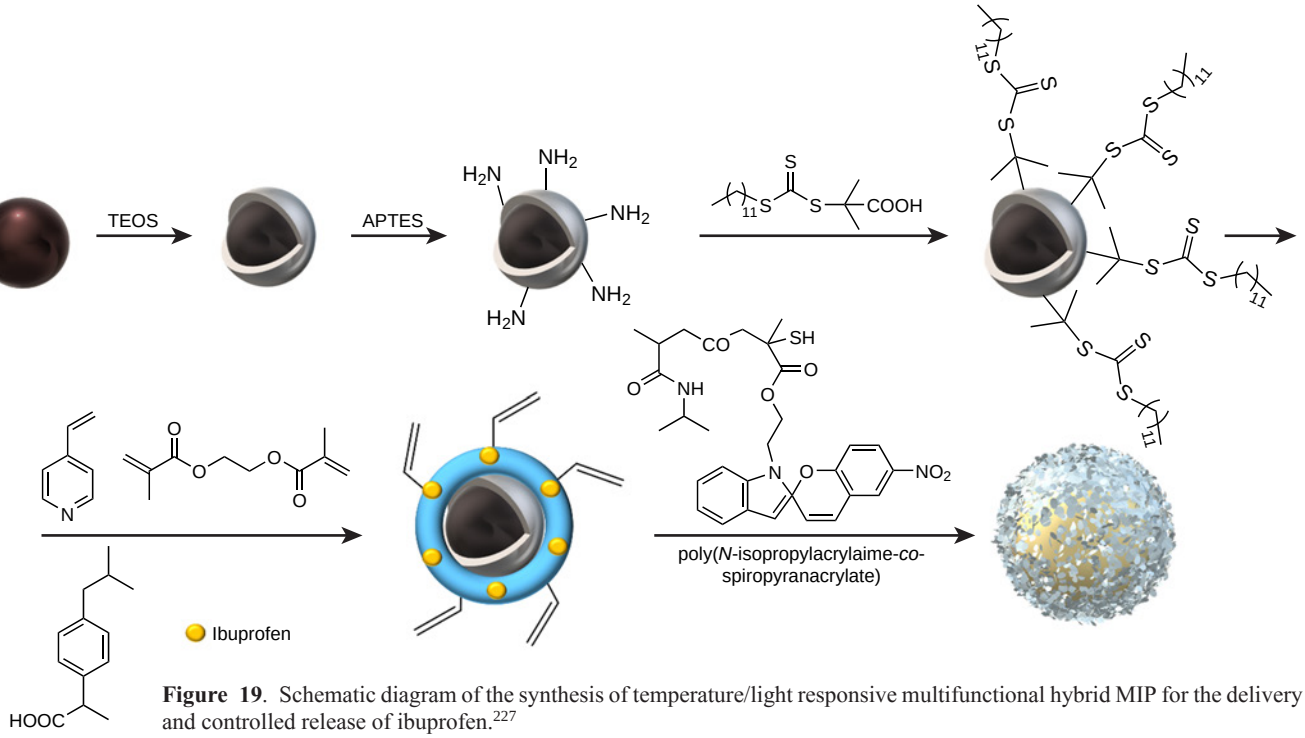

Figure 19. Schematic diagram of the synthesis of temperature/light responsive multifunctional hybrid MIP for the delivery and controlled release of ibuprofen.[227]

3.2.2. Drug-free therapeutic systems

In any type of disease, pathological cells coexist with normal cells, such as fibroblasts, phagocytes, and endothelial cells embedded in a protein-rich extracellular matrix and interstitial fluid, which constitute the complex microenvironment of the tumour. In the administration of nanomedicines into the body, selective targeting to malignant cells is of crucial importance. Biomolecules and biomarkers specifically overexpressed as a result of metabolism of pathological structures or as characteristics of a disease serve as potential candidates for active targeting. In most cases, specific targeting of therapeutic nanostructures is based on biological ligands including antibodies or aptamers. However, screening and preparation of high-quality materials for targeting in this case is an expensive, labour-intensive, and sometimes impossible task. Conversely, MIPs can perform active targeting only owing to the intrinsic specific recognition and do not need additional biological ligands, which are often unstable and immunogenic.[212] In addition, the design of hybrid imprinted materials allows the use of such systems as therapeutic platforms the action of which is based only on the physicochemical properties of the inorganic component.

3.2.2.1. Photothermal therapy

Over the past few years, photothermal therapy (PTT) has become an appealing method for treatment of cancer because it offers a number of advantages over traditional types of treatment such as spatially controlled action, non-invasiveness, and low toxicity. Currently, this approach is used in cancer therapy based on local hyperthermia, which causes apoptosis or necrosis of cancer cells.[229]

Photothermal therapy is based on the use of photothermal agents that generate heat under irradiation at a definite wavelength, thus raising the temperature of cancer tissues and inducing cell death. These agents can be generally divided into four main groups: metal nanostructures possessing plasmon resonance behaviour, carbon-based light-absorbing materials, organic materials, and polymer materials.[230] However, an important drawback of these systems in a pure state is the lack of specificity, which may induce damage of the surrounding healthy tissues. This problem can be solved by conjugation of nanomaterials with components capable of specific recognition, in particular such as MIPs.

Wang *et al.*[231] reported a molecularly imprinted hybrid material based on SiO_2 NPs doped with lanthanides and functionalized with boronic acid for active targeting of tumours and for microinvasive PTT. Dopamine and *m*-aminophenylboronic acid were used as functional monomers, while sialic acid served as the molecular template for the generation of imprinted cavities targeting tumour cells, with the imprinting factor being 4.11 under optimal conditions. Since the expression of monosaccharides on the membrane of tumour cells is heterogeneous, the selectivity of the nanocomposite to sialic acid was assessed in comparison with fucose, galactose, mannose, and glucose; this demonstrated high binding affinity for the molecular template, while binding of non-specific templates did not exceed 7.3%. The highest efficiency of the repeated binding of hybrid MIPs to the template occurred at pH 6.5, which may be used for *in vivo* interactions with sialic acid on the surface of cancer cells in the weakly acidic medium of the tumour. The active pathological cell targeting by the obtained material was studied *in vitro* using two cancer cell lines (HepG2 and MCF-7) and two normal cell lines (L02 and MCF-10A). It was shown that only tumour cells exhibited bright fluorescence after the introduction of the hybrid system. The specificity was additionally assessed using more complex tissue models, hepatocarcinoma and normal liver tissue; fluorescence was observed only for the pathological tissue. These results attest to active selective binding of hybrid MIPs to target monosaccharides on the surface of cancer cells. Cytotoxicity assay *in vitro* showed biocompatibility and biosafety of the composite, since even at high concentrations (0.5 mg mL^{-1}) the

viability of normal cells reached 89%. Infrared thermal imaging was used to evaluate *in vitro* availability of induced infrared PTT. After introduction of the hybrid material and laser treatment at 980 nm, a noticeable death of cancer cells took place (the cell viability was up to 15%), whereas the mortality rate of normal cells was much lower under similar conditions (cell viability above 80%). The *in vivo* assays in HepG2 tumour-bearing mice demonstrated that hybrid MIP can be an effective photothermal agent (the tumour temperature increased to 60°C within 7 s), inhibiting tumour proliferation and finally causing complete destruction of the tumour. The presented system appears promising for cancer therapy.

Wen *et al.*[232] presented a magnetic molecularly imprinted material for cancer therapy. As the molecular template, the authors used a segment of the amino acid sequence of human vascular endothelial growth factor (hVEGF), which is an important factor in the angiogenesis of pathological tissues. The resulting nanocomposite was meant to reduce the amount of hVEGF in the tumour microenvironment by binding to imprinted sites in the polymer matrix and thus to inhibit angiogenesis (Fig. 20). Meanwhile, magnetite present in the hybrid material was an agent for PTT. γ-Methacryloxypropyltrimethoxysilane was chosen as the functional monomer for the formation of molecular imprinted polymer layer. The adsorption capacity of MIP with respect to the molecular template was found to be 72.5 mg g^{-1} with an imprinting factor of 3.1. Experiments *in vitro* using various cell lines proved the specificity and selectivity of the proposed nanocomposite, as it demonstrated selective binding of hVEGH in complex samples and selectively recognized hVEGH among similar factors of a different origin. Cytotoxicity assays showed biocompatibility and effective antitumour activity of hybrid MIPs against several cancer cell lines compared to normal cells upon irradiation with infrared light at 808 nm with a power density of 2.0 W cm^{-2}. Moreover, the synergistic therapeutic effect of angiogenesis and PTT was shown to surpass the effect of monotherapy. The simple strategy for the fabrication of a hybrid multimodal platform proposed in this study has a great potential as an effective tool for cancer therapy.

3.2.2.2. Photodynamic therapy

Photodynamic therapy (PDT) is one more potent strategy for the therapy of cancer, which has attracted attention of researchers for many years owing to its numerous benefits such as non-invasiveness, selective local irradiation, and minor side effects.[229]

The principle of operation of this method is based on three main constituents: light irradiation, photosensitizer, and oxygen. Under particular irradiation conditions, the photosensitizer is activated, being excited from the singlet ground state to a triplet excited state, and then undergoes various photochemical reactions, which are subdivided into two main types, to give highly toxic reactive oxygen species. The mechanism of type I reactions includes electron or hydrogen atom transfer directly from the phorosensitizer to biomolecules to give free radicals and radical ions, which react with molecular oxygen to give reactive oxygen species including hydrogen peroxide, superoxide anions, and hydroxyl radicals. Type II reactions include direct energy transfer from the photosensitizer in the

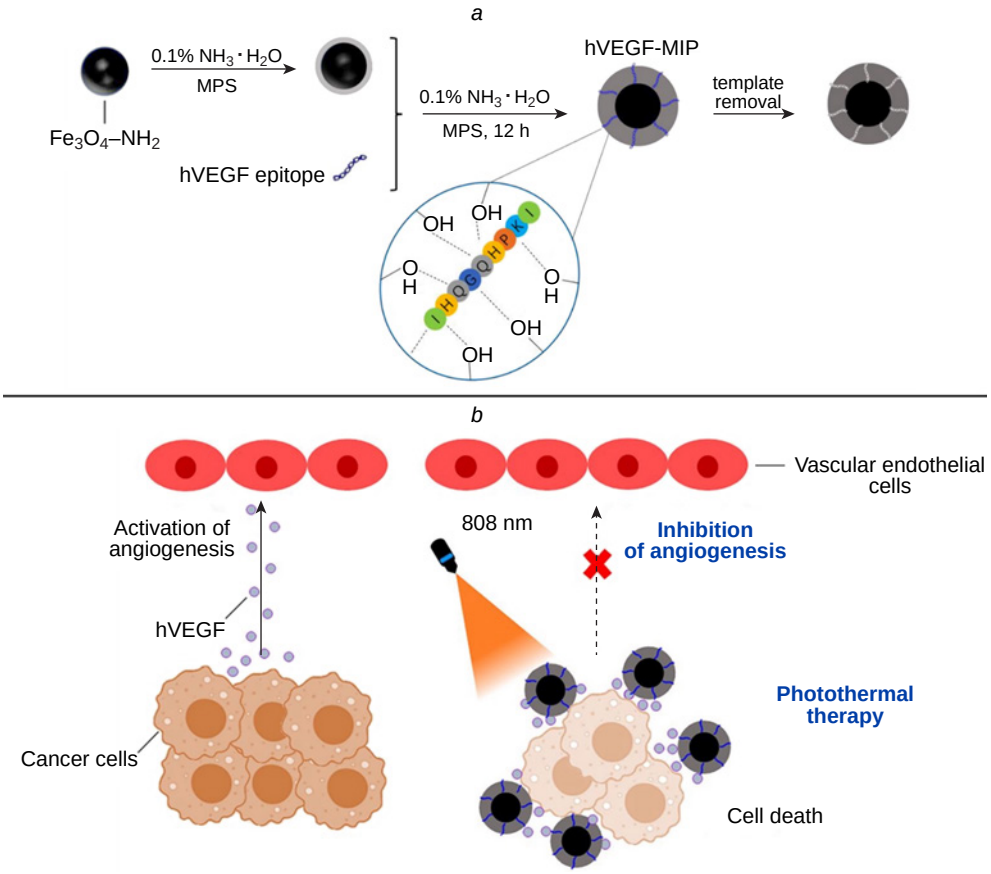

Figure 20. Synthesis of the hybrid MIP for binding to hVEGF (*a*) and diagram of the anticancer photothermal therapy (*b*).[232] Copyright 2023, Royal Society of Chemistry.

Scheme 1

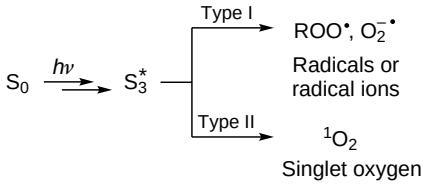

triplet state to molecular oxygen, giving rise to reactive electrophilic singlet oxygen (Scheme 1).[233]

Currently, effective PDT requires overcoming certain limitations related to specific features of the used photosensitizers. Due to their hydrophobic nature, easy aggregation, and low payloads, photosensitizers have poor accumulation and tumour targeting capability, resulting in unsatisfactory therapeutic effects. These problems can be addressed by physically loading photosensitizers into nanocarriers or by chemically conjugating them with nanocarriers.[229] Among various systems used for this purpose, MIPs have attracted attention of researchers due to their high specificity and easy modification.

Lin *et al.*[21] proposed a complex core–shell system based on magnetic NPs doped with the photosensitizer merocyanine 540 with a molecular imprinted poly(ethylene-co-vinyl) alcohol layer for targeting tumour cells followed by PDT (Fig. 21). The effective excitation of the photosensitizer was achieved by using UCNPs, that is lanthanide-doped yttrium lithium tetrafluoride NPs, as the inorganic core to enhance green luminescence upon irradiation in the IR range (the NP emission at a wavelength of 520 nm was thus enhanced by more than 80%). One peptide sequence from the programmed cell death protein (PD-L1) served as the molecular template for imprinting, which facilitated active targeting of tumour cells. The adsorption capacity of hybrid MIPs towards the template was estimated as 28.7 mg g^{-1}, which is approximately 1.8 times higher than that for non-imprinted analogue. The authors measured the viability of HepG2 human liver carcinoma cells upon incubation with the prepared nanocomposites; it was shown that the material was biocompatible, as the cell viability exceeded 90% of this value in the control set. Comparison of the effect of imprinted and non-imprinted materials on tumour cells on exposure to infrared radiation showed that non-imprinted composites had virtually no cytotoxic effect, while imprinted hybrids induced a statistically significant decrease in the viability of tumour cells due to specific binding to the cells. As the system was exposed to infrared light at a wavelength of 980 nm for 5 min, MIP in a concentration of 1.0 mg mL^{-1} induced apoptosis in approximately a half of cancer cells. This result can be attributed to the transfer of luminescence energy from inorganic NPs and excitation of merocyanine 540, which catalyzes the generation of cytotoxic reactive oxygen species. The results presented in the paper show that this hybrid system may be promising for effective PDT.

Gu *et al.*[141] presented a developed strategy for the preparation of a hybrid molecularly imprinted material for PDT of mutated types of cancer that cannot be treated with the classic approach based on the use of antibodies. This is associated with increased proliferation and the emergence of resistance of cancer cells to therapeutic antibodies due to mutations. The new nanocomposite comprised an inorganic core made of UCNPs and a thin polymer shell with a molecular imprint for the specific recognition of the truncated human epidermal growth factor receptor HER2 (P95HER2) (Fig. 22). The formation of this receptor form is a major mechanism of emergence of resistance, since truncated HER2 lacks the extracellular domain that binds to antibodies. The N-terminal epitope of P95HER2 consisting of nine amino acids was used as the molecular template. Considering the amino acid properties of epitopes, 3-ureidopropyltriethoxysilane, APTES, isobutyltriethoxysilane, and benzyltriethoxysilane were chosen as functional monomers to create an imprinted polymer shell. The photodynamic effect in the nanocomposite was achieved by introducing chlorin e6 as the photosensitizer into the polymer matrix. It was shown that the imprinted material specifically binds to P95HER at the peptide level and exhibits selectivity in binding to the truncated receptor on the cell surface

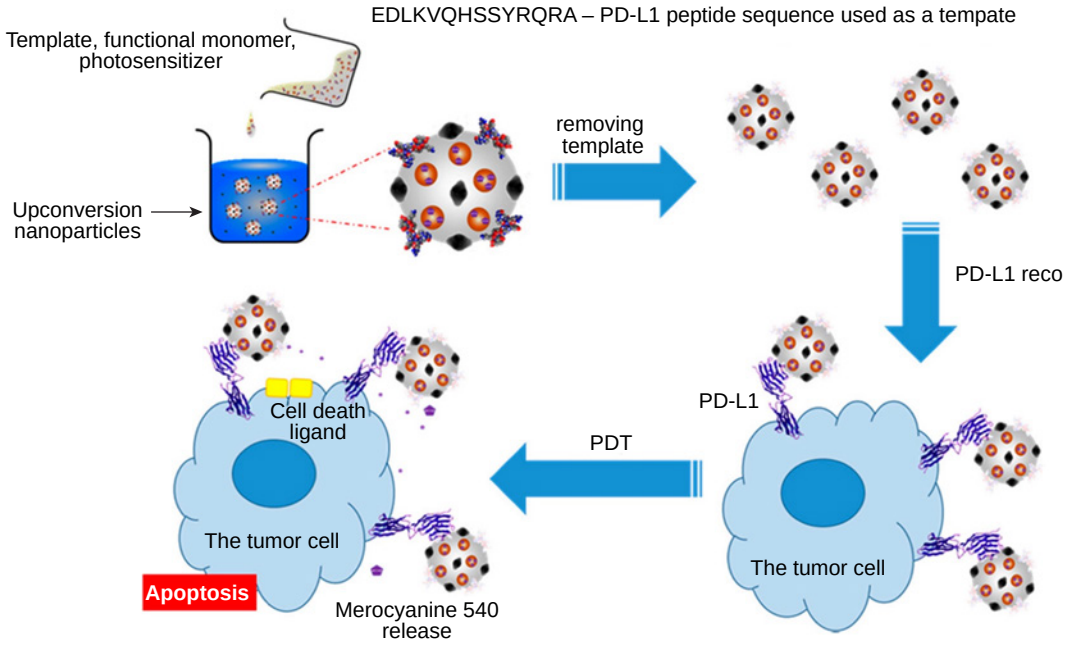

Figure 21. Schematic diagram of the synthesis of hybrid MIP and PDT under the action of merocyanine 540.[21] Published under the CC BY license.

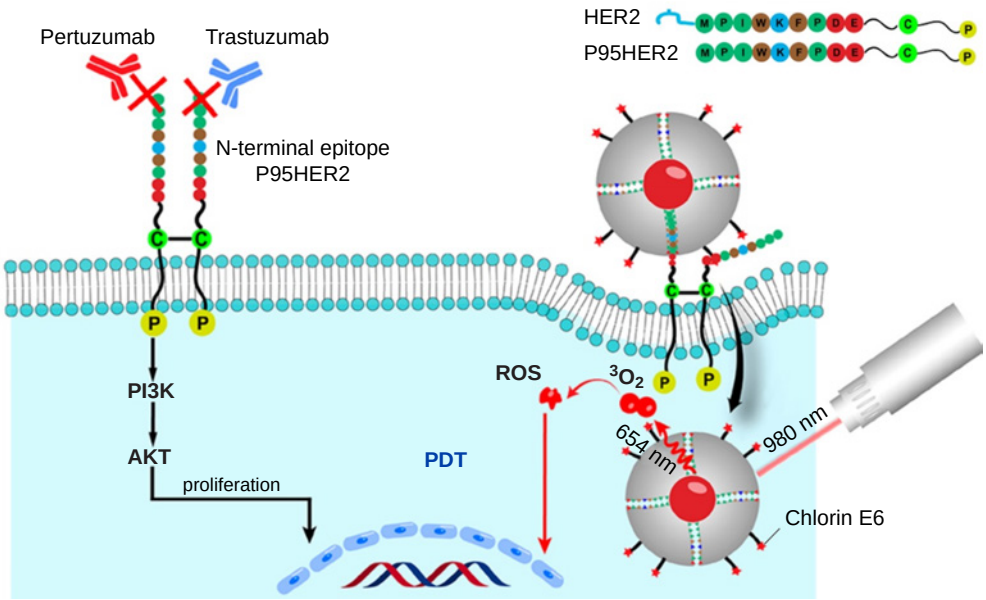

Figure 22. Schematic diagram of specific delivery of hybrid MIP and mechanism of PDT induced by chlorin e6, ROS are reactive oxygen species, PI3K is phosphoinositide 3-kinase, AKT is protein kinase B.[141] Copyright 2023, American Chemical Society.

compared to the normal form at the cellular level. Studies of the photodynamic properties demonstrated that hybrid MIP can effectively generate reactive oxygen species under infrared irradiation (980 nm) and be specifically accumulated in pathological cells and inhibit the growth of tumour tissue *in vivo* by 87%. The presented strategy has great prospects for effective treatment of antibody-resistant cancer.

Over time, scientific progress leads to the appearance of increasingly complex systems that possess multifunctionality owing to the combination of active targeting with drug delivery or several types of therapeutic approaches. In view of the substantial interest of researchers in synergistic methods, examples of such methods are presented in the following Section.

3.2.3. Integrated therapeutic systems

Platforms that simultaneously incorporate a targeting component and a drug are used most widely. This effect can be achieved either by using double imprinting, resulting in the formation of MIPs that possess affinity to several molecular templates and thus providing more effective interaction, or by incorporating an inorganic material possessing an additional function into hybrid MIP.

3.2.3.1. Therapeutic systems sensitive to redox processes

Drug delivery systems that are activated by redox processes are used to treat cancer, cardiovascular, neurological, and other diseases that require the delivery of active substances in a changed redox environments. These systems are activated in pathological tissues such as tumours and ischemic zones. Hence, the drug is released directly in the affected sites, thus increasing the efficiency of the therapy and decreasing side effects. Polymer materials that respond to redox processes are attractive research objects in the field of drug delivery systems, since disruption of the number of molecules that regulate redox reactions is associated with the progression of various diseases. The most frequently encountered biologically active redox molecules are reactive oxygen species and glutathione (Fig. 23 *a*). For MIPs to be responsive to these compounds, appropriate reactive groups should be incorporated into the polymer structure. For example, thioketals and arylboronic ether are widely used in the polymer materials that respond to reactive oxygen species, while disulfide structures are used in glutathione-responsive systems. Diselenides, which are sensitive to both oxidative and reductive conditions, are also used; this enables the design of multifunctional polymer materials (Fig. 23 *b*).[234]

Lu *et al*.[20] developed redox-responsive hybrid MIPs based on biodegradable SiO_2 NPs and boronic acid designed for targeted delivery of a therapeutic protein for the cancer therapy. Cytotoxic ribonuclease A was encapsulated into a matrix of disulfide-hybridized inorganic NPs, while sialic acid serving for targeting cancer cells was used as the molecular template for imprinting (Fig. 24). Study of the composite material under redox conditions

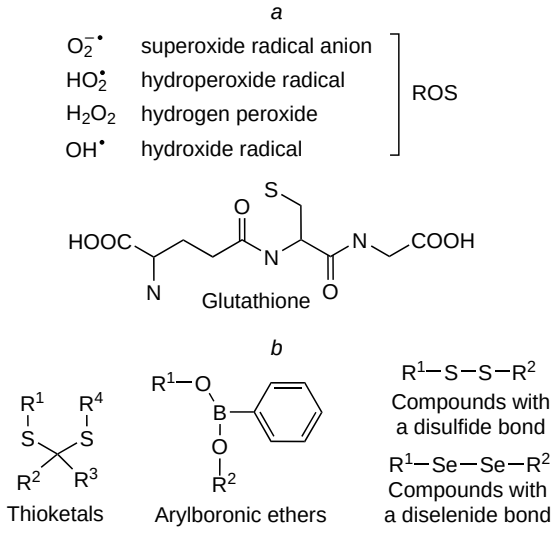

Figure 23. Examples of biologically active redox molecules, ions, and radicals (*a*) and groups sensitive to redox processes (*b*).

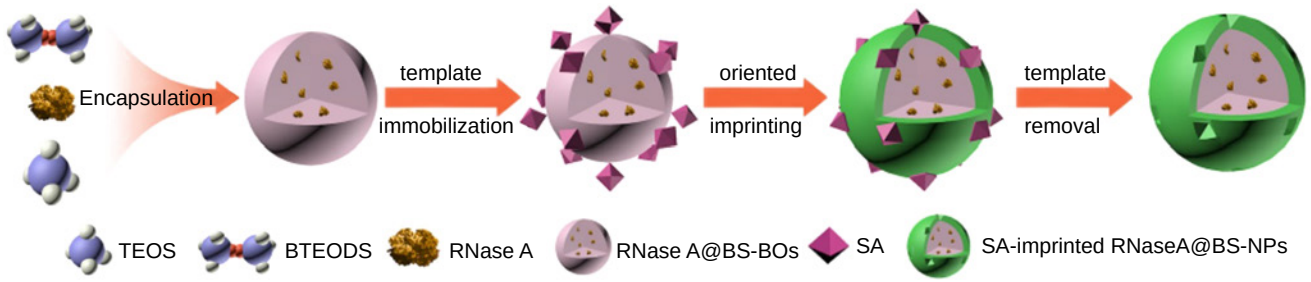

Figure 24. Schematic diagram of the synthesis of hybrid MIP degraded by treatment with glutathione for the targeted delivery of ribonuclease A.[20] Copyright 2021, American Chemical Society.

(10 mM glutathione, 48 h) showed effective degradation of hybrid MIPs with the release of up to 78% of ribonuclease A, with the catalytic activity of the enzyme being retained. The biocompatibility of the hybrid system was assessed using human fetal hepatocyte cells (L02) and human breast epithelial cells (MCF-10A), which showed high cell viability (more than 90%) after 48-h incubation with various MIP concentrations. Also, it was demonstrated that the obtained composite material can be selectively targeted to HepG2 human liver carcinoma cells, which overexpress sialic acid, taken up by the cells *via* endocytosis, and then cleaved by intracellular glutathione to release ribonuclease A, which provides cytotoxicity. The *in vivo* studies in mice demonstrated that this MIP has a specific tumour targeting and high therapeutic efficacy. The *in vivo* biocompatibility was evaluated by administration of elevated doses of the composite (up to 20 mg kg^{-1}) to healthy mice; the subsequent histological analysis did not detect any inflammatory reactions or noticeable tissue damage in main organs; the key blood parameters also did not change. Hybrid MIPs presented in this study can serve as a potent platform for the targeted intracellular delivery of therapeutic proteins in the treatment of cancer.

Liu *et al*.[235] proposed a biodegradable drug delivery system based on dendritic organosilicon materials, sialic acid, and transferrin for the targeted cancer therapy. The dendritic mesoporous disulfide-bridged organosilicon nanoparticles provided a high specific surface area for the molecularly imprinted shell. The imprinted polymer shell was fabricated using 2-amino-*N*-(3,4-dihydroxyphenethyl)-3-mercaptopropanamide and 4-mercaptophenylboronic acid as functional monomers, which promoted stimulus-responsive release of therapeutic agents as a result of degradation in acidic and highly reducing (due to high glutathione concentration) medium around the tumour (Fig. 25). Sialic acid and transferrin acted as molecular templates for specific targeting of the nanocomposite. Mesoporous SiO_2 NPs were modified with disulfide bridges, which enhanced the reductive degradation of nanocarriers. The introduction of chlorin e6 and doxorubicin into the dendrite core enhanced the appearance of chemical and photodynamic synergistic antitumour effect. The obtained hybrid MIP was shown to have a high adsorption capacity for molecular templates compared to competing compounds and structural analogues such as beta-hydroxybutyrate, CA-125 glycoprotein, immunoglobulin A, and fulvic acid, which can be present in the tumour microenvironment and body fluids. The ability of the composite to selectively capture transferrin was assessed using mouse blood samples. The biodegradation and drug release efficiency were evaluated at different pH values and glutathione contents in the medium: the optimal degradation took place in the phosphate buffer containing 10 mM of glutathione at pH 5.5; as a result, the particle diameter decreased from 130 to 15 nm after incubation for 150 h, which promoted easy renal excretion of the material *in vivo*. In a model tumour microenvironment, the hybrid MIPs demonstrated extended release of therapeutic drugs owing to cleavage of disulfide and amide bonds in the polymer layer, which not only prevented premature release of molecular templates, but also contributed to maintaining drug concentrations at a level needed for therapeutic effect. The biocompatibility of the materials was assessed *in vitro* using normal MCF-10A cells and 4T1 and MCF-7 breast cancer cells upon laser irradiation at 655 nm. Throughout the experiment, the activity of MCF-10A cells remained above 90%, while in the case of cancer cells, pronounced cytotoxicity was observed (the cancer cell mortality reached 88%) due to specific binding and enhanced uptake of nanocomposites. In *in vivo* assay of anticancer effects in mice, it was shown that hybrid MIP was mainly accumulated in the tumour environment, while causing no adverse changes in healthy tissues and organs. This indicates the presence of specific recognition of pathological cells. In addition, the authors noted a synergistic therapeutic effect, which was manifested as suppression of the tumour growth, high efficiency of MIP degradation, and fast excretion from the body.

The proposed approach has a considerable potential for translational medicine.

3.2.3.2. Combined PTT and PDT systems

Platforms for PTT and PDT can be used in combination with other therapeutic approaches to increase the sensitivity of cancer cells. Compared to treatments based on a single method, the integration of these approaches with chemotherapy increases the efficacy of treatment and reduces the repeated growth of residual tumour tissue by increasing therapeutic coverage.

Shi *et al*.[236] used an approach to the manufacture of an integrated hybrid system based on magnetic NPs for the targeted synergistic treatment of breast cancer (Fig. 26). In this study, the researchers focused attention on the selection of effective photosensitizer, as it should ensure the formation of a sufficient amount of reactive oxygen species in a physiological medium under light irradiation. As mentioned in Section 3.2.2.2, the molecules of traditional photosensitizers often have a planar hydrophobic structure, form aggregates under these conditions, which results in a critical decrease in the level of generated oxygen radicals. This problem can be solved by using photosensitizers, the emission of which is induced by aggregation. In this study, for the fabrication of an imprinted therapeutic nanoplatform, a photosensitizer and a cell-penetrating peptide incorporated for active tumour cell targeting of the hybrid system were covalently conjugated on the MIP

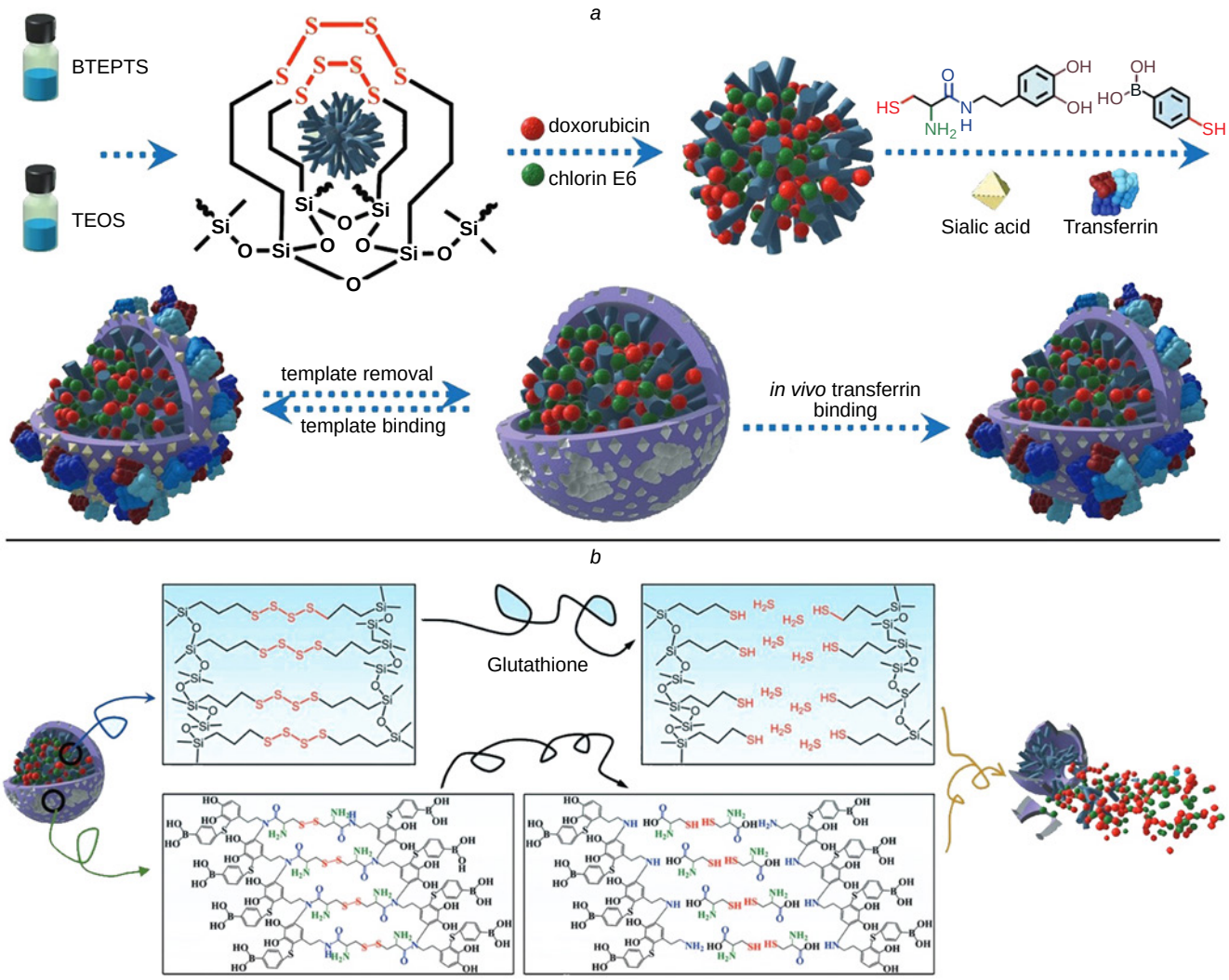

Figure 25. Schematic diagram of the synthesis of hybrid MIP for the targeted delivery of doxorubicin and chlorin e6 (*a*) and glutathione-induced biodegradation of MIP (*b*). BTEPTS is bis(triethoxysilyl)propyl tetrasulfide.[235] Copyright 2023, Wiley.

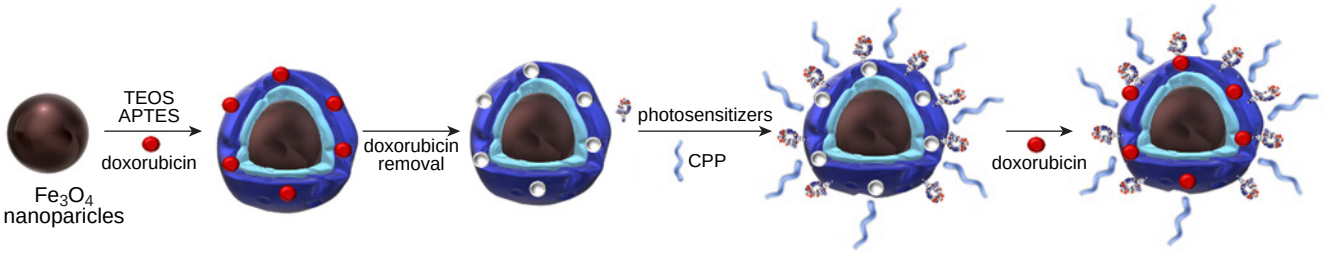

Figure 26. Schematic diagram of the synthesis of hybrid MIP for synergistic chemotherapy/photodynamic therapy and active tumour cell targeting.[236] CPP is cell-penetrating peptide.

surface. The anticancer drug doxorubicin served as the molecular template, while TEOS and APTES were the functional monomers. The experiments demonstrated that the covalent binding of the photosensitizer to the polymer surface did not lead to the loss of photodynamic properties. A study of the adsorption properties of conventional MIP compared to covalently conjugated MIP revealed no influence on the adsorption capacity (58.9 and 58.8 mg g^{-1}, respectively). Meanwhile, in the case of non-imprinted material, this value was much lower (14.0 mg g^{-1}), which attests to high efficiency of imprinting (the imprinting factor was 4.2). The proposed system exhibited prolonged pH-dependent release of doxorubicin (17.1% at pH 5.5 after 48 h); this is beneficial for long-term maintenance of high concentration of the drug in the tumour environment. *In vitro* experiments showed enhanced cellular uptake of the hybrid system and effective release of doxorubicin, which is attributable to the presence of cell-penetrating peptide. The biocompatibility of conventional nanocomposites was demonstrated on 4T1 breast cancer cell line. The covalently conjugated MIPs exhibited a greater cytotoxicity due to enhanced penetration and the presence of a photosensitizer. It is noteworthy that irradiation with white light resulted in sharp enhancement of toxic effects with increasing concentration of the therapeutic platform because of high photodynamic effect.

Histological analysis of tumour tissues after *in vivo* study on mice with 4T1 tumour demonstrated specific and prolonged accumulation of the multifunctional system in the tumour and synergistic efficacy of chemotherapy and photodynamic therapy. This study proved the possibility of creating a promising model based on hybrid MIP by integrating different therapeutic approaches to achieve optimized results.

Ma *et al.*[237] reported a hybrid imprinted system based on Fe_3O_4 NPs directed towards an increase in the efficiency of PTT and decrease in the elimination of magnetic NPs by the reticuloendothelial system (Fig. 27). Serum albumin, which is the main transport protein in the human body, was used as a molecular template. This made it possible to achieve immune stealth owing to the formation of protein corona and targeted accumulation of nanocomposite in the tumour tissue as a result of albumin binding to the receptors overexpressed in cancer cells such as SPARC. The imprinted polymer layer was prepared by oxidative polymerization of dopamine as a functional monomer. The adsorption capacity of the imprinted hybrid material was calculated to be 180 mg g^{-1}, which was almost 3.5 times higher than that of the non-imprinted analogue. Evaluation of the MIP selectivity in experiments with proteins such as bovine haemoglobin, immunoglobulin G, and fibrinogen showed the predominant binding to particularly the molecular template (selectivity coefficient of 3.46). According to the study of photothermal properties of the nanocomposite, the polydopamine layer increased the efficiency of photothermal conversion, while the hybrid material itself remained stable upon repeated laser irradiation. The formation of the albumin corona on the MIP surface markedly reduced internalization by macrophages, which was mentioned in Section 2.3 as a key aspect for *in vivo* use of a system. The biocompatibility of conventional nanocomposites was demonstrated using 4T1 breast cancer cell line without laser irradiation; under laser irradiation at 808 nm, high anticancer activity was observed. *In vivo* biodistribution studies on mice with 4T1 tumour demonstrated accumulation of MIP in pathological tissues, which was facilitated by the enhanced permeability and retention effects, transmembrane transport, and the interaction of albumin with SPARC receptors. An unusual approach in this study was the use of PD-L1 antibodies, which promote the immune activity by tuning the relationship between tumour cells and the immune system of the body, to prevent breast cancer metastasis. The synergistic therapy proved to be much more effective than monotherapy protocols, in which PTT did not make it possible to prevent lung metastasis, while PD-L1 antibodies alone did not suppress the progression of cancer at all, which may be attributable to the absence of an activated immune system. In the integrated approach, hybrid MIP improved the penetration of T-cells into the tumour *via* PTT; this activated the immune system towards the action of therapeutic antibodies, resulting in the prevention of cancer cell development and elimination of metastasis. The proposed strategy demonstrates the great potential of synergistic therapy and reflects the advantages of using molecularly imprinted materials *in vivo*.

The information on the studies considered in Section 3.2 and additional examples of therapeutic systems based on hybrid MIPs are summarized in Table 6.

As can be seen from the examples, therapeutic platforms based on hybrid MIPs have enormous potential for clinical use to treat various diseases. A reasonable combination of an imprinted polymer matrix with inorganic NPs gives rise to materials in which each component possesses a particular function, for example, a combination of active targeting and hyperthermia, or in which the properties are combined to enable functioning of the whole system, *e.g.*, thermosensitive polymers in combination with heat-generating inorganic nanomaterials. In addition, hybrid MIPs can act as therapeutic agents in drug-loaded or drug-free states, depending on the goal set by researchers. The diversity of compatible components and their properties makes hybrid MIPs really versatile systems.

3.3. Theranostics

A rapidly developing trend in modern biomedicine is theranostics, an area that combines the capabilities of diagnostics and therapy. As shown in previous parts of the review, the applications of MIPs as separate platforms directed towards screening, delivery of therapeutic agents, and targeted therapy have been extensively investigated and are actively utilized. In turn, the interest in using an integrated approach has emerged quite recently; therefore, there is a modest number of effective

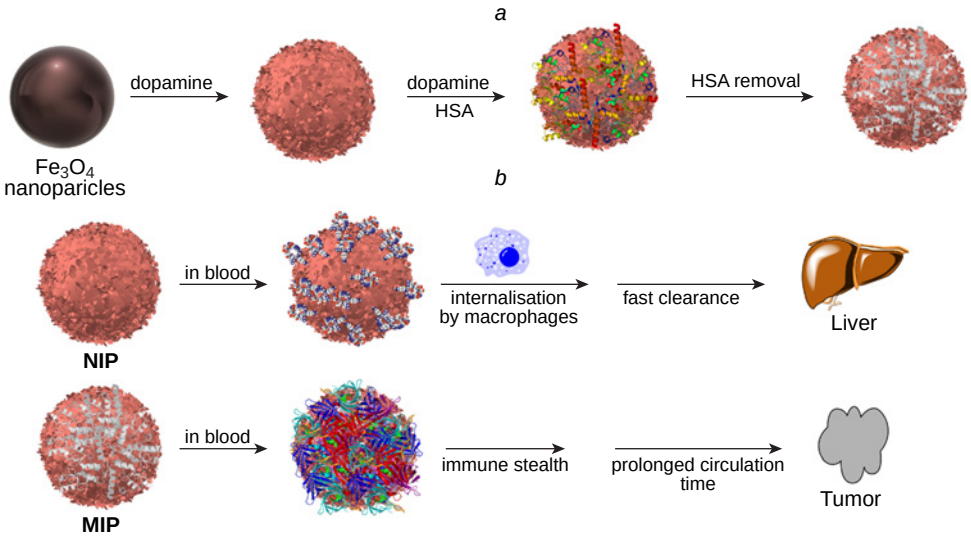

Figure 27. Schematic diagram of the synthesis of hybrid MIP for PTT and immune stealth (*a*) and differences between the circulation mechanisms of MIP and non-imprinted polymer (NIP) (*b*).[237] HSA is human serum albumin.

Table 6. Application of hybrid MIPs in therapeutic systems.

NP type	Functional monomer	Molecular template	Release trigger	Note	Ref.
Fe_3O_4	4-VPy, AAc	5-Fluorouracil	pH	pH-responsive release of 5-fluorouracil	218
Fe_3O_4@SiO_2	MAA, itaconic acid	Azidothymidine	pH	pH-responsive release of azidothymidine	219
SiO_2	*N*-{4-[(4-amino-2,6-dimethoxyphenyl)diazenyl]-3,5-dimethoxyphenyl}methacrylamide	Acyclovir	Irradiation (440 nm for the *trans* to *cis*-conversion and 630 nm for *cis*- to *trans*-conversion)	Light-responsive release of acyclovir	222
Graphene quantum dots	Methyl methacrylate	Doxorubicin	Heating induced by IR irradiation (808 nm)	Thermoresponsive release of doxorubicin, PTT	238
SiO_2 doped with lanthanides (Yb, Er)	4-[(4-methacrylotloxy)-2,6-dimethylphenylazo]-3,5-dimethylbenzenesulfonic acid	Paracetamol	Irradiation in the near-IR range (980 nm, 5 W cm^{-2})	Light-induced release of paracetamol	221
Fe_3O_4	NIPAM	Curcumin	Temperature	Thermoresponsive release of curcumin	224
Fe_3O_4	MAA	Methotrexate	Heating induced by alternating magnetic field	Release of methotrexate induced by magnetic hyperthermia	225
γ-Fe_2O_3 coated with an acrylic acid polymer layer	AAc, AA	Doxorubicin	Heating induced by alternating magnetic field	Release of doxorubicin induced by magnetic hyperthermia	226
Modified biodegradable SiO_2-based NPs	4-formylphenylboronic acid	Sialic acid	Reduction of the S–S bond	Release of ribonuclease A induced by redox processes	20
Modified biodegradable SiO_2-based NPs	2-amino-*N*-(3,4-dihydroxyphenethyl)-3-mercapropropanamide, 4-mercaptophenylboronic acid	Sialic acid, transferrin	Reduction of the S–S bond	Release of doxorubicin and chlorin e6 induced by redox processes, PDT, targeting tumour cells	235
Fe_3O_4@SiO_2	4-VPy	Ibuprofen	Temperature, UV irradiation (365 nm)	Temperature-/light-responsive release of ibuprofen	227
Fe_3O_4 and GO composite	Dopamine, boronic acid	Carcinoembryonic antigen CA125	pH	pH-responsive release of doxorubicin with magnetic targeting, tumour cell targeting	239
Fe_3O_4 coated by acrylamide polymer layer	Methacrylamide	Doxorubicin	pH	pH-responsive release of doxorubicin	240
TiO_2	MAA	Mitoxantrone	X-ray radiation	PDT	241
Zinc-doped TiO_2	*N*-Vinylcaprolactam, MAA	5-Fluorouracil	pH, temperature	pH/temperature-responsive release of 5-fluorouracil, PTT and PDT	228
MOF doped with ethylenediamine-functionalized CQDs	2-Aminoterephthalic acid	Doxorubicin	pH	pH-sensitive release of doxorubicin	242
Fe_3O_4	Dopamine	Human serum albumin	Heating induced by IR irradiation (808 nm)	Enhancement of PTT efficiency, achieving immune stealth	237
SiO_2	Dopamine, *m*-aminophenylboronic acid	Sialic acid	Irradiation in near-IR region (980 nm, 4.0 W cm^{-2})	PTT, tumour cell targeting	231
Gd- and SiO_2-based quantum dots doped with a photosensitizer (chlorin e6)	NIPAM, TBAM, AA	Doxorubicin, CD59 protein epitope	pH	pH-sensitive release of doxorubicin; PDT induced by chlorin e6; fluorescence imaging, tumour cell targeting	171

Table 6 (continued).

NP type	Functional monomer	Molecular template	Release trigger	Note	Ref.
SiO_2 doped with a fluorescence dye (FITC, NIR797)	4-formylphenylboronic acid	HER2 glycans	None	Blocking the HER2 signalдing pathway in cancer cells	173
CNTs	MAA	Aminoglutethimide	None	Controlled release of aminoglutethimide	243
γ-Fe_2O_3	Diethylaminoethyl methacrylate	Pemetrexed	Heating induced by alternating magnetic field	Thermoresponsive pemetrexed release	244
Fe_3O_4 doped with 1,6-diaminohexane	γ-Methacryloxypropyltrimethoxysilane	Segment of the amino acid sequence of human vascular endothelial growth factor hVEGF	Heating induced by IR irradiation	Inhibition of angiogenesis, PTT	232
Fe_3O_4@SiO_2 enriched with upconversion $NaYF_4$ particles (Er^{3+}, Ho^{3+}, Yb^{3+})	Poly(ethylene-*co*-vinyl) alcohol	Peptide sequence from the programmed cell death protein	Heating induced by IR irradiation	Tumour cell targeting, PDT under the action of merocyanine 540	21
SiO_2-based NPs enriched with upconversion $NaYF_4$ particles (Er^{3+}, Yb^{3+})	3-Ureidopropyltriethoxysilane, APTES, isobutyltriethoxy-silane, benzyltriethoxysilane	N-terminal epitope of the truncated human epidermal growth factor receptor P95HER	Irradiation in the near-IR range (980 nm, 1.5 W cm^{-2})	Mutated tumour cell targeting, PDT induced by chlorin E6	141
Mesoporous SiO_2 NPs	3-(Trimethoxysilyl)propyl methacrylate	Sialic acid	pH	pH-responsive release of doxorubicin, tumour cell targeting	245
Fe_3O_4@SiO_2	APTES, TEOS	Doxorubicin	pH	pH-responsive release of doxorubicin, PDT, cell penetration due to the presence of a cell-penetrating peptide	236
CNTs	MAA, EGDMA, 4-methyl-phenyldicyclohexylethylene	Levofloxacin	None	Liquid-crystalline material for controlled release of levofloxacin	246

systems combining diagnosis and therapy that have been developed and comprehensively studied to date. However, the rapid development of this area brings every year new results worthy of attention.[35]

Using hybrid molecularly imprinted materials, it is possible to design systems with various combinations of the performed functions. Thus, combining the capabilities of platforms for imaging and drug delivery allows for simultaneous precise detection of the affected area and controlled release of the therapeutic agent. For example, Wang *et al.*[247] described a bifunctional system based on fluorescent SiO_2 NPs and a molecularly imprinted polymer for imaging and targeted therapy. As molecular templates, the authors used a linear peptide of the extracellular domain of human epidermal growth factor (HER2), which is overexpressed on the surface of pathological cells, for the specific detection of breast cancer cells, and the anticancer drug doxorubicin. Zinc acrylate and AA served as functional monomers. The two-colour fluorescence of the hybrid material (blue fluorescence from the inorganic component and red fluorescence from doxorubicin) provided imaging of cancer cells and real-time monitoring of drug distribution. The prepared nanocomposite showed high adsorption capacity towards each molecular template: 55.2 mg g^{-1} for the peptide and 110.5 mg g^{-1} for doxorubicin. The proposed hybrid system exhibited pH-dependent release of doxorubicin reaching a maximum at pH 5.5, which amounted to 17.5% after incubation for 23 h. Experiments using various HER2-positive and HER2-negative cell lines demonstrated high MIP biocompatibility and specific pathological cell targeting, which ensured the therapeutic effect. This proves the prospects of using the proposed approach as a promising biomedical nanoplatform.

Examples of hybrid systems that could potentially be used for therapeutic purposes are given in Table 7. As can be seen from the publications covered in this review, the most recent achievements in the field of hybrid MIPs include platforms for diagnosis, therapy, drug delivery, and bioimaging and integrated systems combining a few functions. The vast number of approaches to the preparation of nanocomposites, as well as cost-effectiveness and simplicity of synthesis, expand the range of biomedical applications and enable scaling-up of the methods.[252]

4. Conclusion

The integration of MIPs with inorganic nanoparticles provides the fabrication of complex materials that combine targeting, imaging, and drug delivery functions, and in some cases, therapeutic action, owing to the ability of NPs to respond to external physicochemical stimuli. Hybrid MIPs exhibit high specificity of molecular template binding and chemical and mechanical stability, which makes them promising therapeutic and diagnostic tools. MIPs can be used as specific drug carriers, providing gradual and controlled drug release in the body, and the properties of the inorganic material present in the hybrid system allow for the use of photothermal and photodynamic therapy approaches, which increases the efficiency of therapy and reduces the side effects.

The drawbacks of MIPs include the necessity of selecting the conditions of synthesis for each molecular template, potential toxicity, and low biocompatibility and biodegradability. It is necessary to thoroughly select monomers and synthesis conditions to avoid the formation of toxic residues that can cause undesirable reactions in the body. In addition, the low biodegradability of MIPs limits their use in long-term implants and requires the development of new biocompatible materials.

In view of the high interest of the scientific community in imprinted materials, the appearance of new and improved methods for the production and application of hybrid molecularly imprinted polymers should be expected in the next few years with the goal of solving biomedical problems such as targeted drug delivery, biosensor design, development of artificial organs and tissues, and separation and purification of biological molecules.

New synthetic strategies towards the development of hybrid molecularly imprinted polymers will focus on improving synthetic methods, expanding the scope of functions of the materials by invoking new monomers and additives, developing smart polymers that respond to external stimuli, and designing multifunctional theranostic platforms based on non-toxic and biocompatible hybrid molecularly imprinted materials. The progress in this area would provide for the substantial expansion of the range of therapeutic and diagnostic tools and for the transition from scientific research to production and practical application of MIPs in various fields of biomedicine.

Table 7. Application of hybrid MIPs in theranostic systems.

Type of NPs	Functional monomer	Molecular template	Notes	Ref.
Fe_3O_4@SiO_2	Dopamine	Catalase	Inhibition of the catalytic activity of catalase; reaction of Fe with excess H_2O_2 giving reactive hydroxyl radicals, resulting in apoptosis; PTT; magnetic targeting	248
Fe_3O_4 and GO cluster	Dopamine	Carcinoembryonic antigen CA125	Chemotherapy by doxorubicin; magnetic targeting; active targeting owing to biomarkers on the cancer cell surface; possible magnetic resonance imaging	239
Fe_3O_4	Poly(ethylene-*co*-vinylene alcohol)	Programmed cell death protein ligand 1 (PD-L1)	Merocyanine-induced PDT; active targeting and immunotherapy owing to receptors on the surface of cancer cells; possible magnetic resonance imaging	249
SiO_2	Copper arylate	Cell surface glycoprotein CD47	Haemodynamic therapy; active targeting owing to receptors on the cancer cell surface; fluorescent diagnosis owing to the presence of fluorescent calcium peroxide	250
Au	Pyrrolidyl acrylate	Human serum albumin	Low-dose X-ray radiation therapy; passive targeting due to increased permeability and retention effect; protein corona formation *in vivo* for stealth masking; possible magnetic resonance imaging	251

This review was prepared within the State Assignment of the Institute of Chemical Biology and Fundamental Medicine, Siberian Branch, Russian Academy of Sciences, No. 125012300656-5.

5. List of abbreviations and symbols

AA — acrylamide,
AAc — acrylic acid,
APTES — 3-aminopropyltriethoxysilane,
CQD — carbon quantum dot,
CNT — carbon nanotube,
DNA — deoxyribonucleic acid,
dsDNA — double-stranded deoxyribonucleic acid,
ssDNA — single-strand deoxyribonucleic acid,
EGDMA — ethylene glycol dimethacrylate,
GO — graphene oxide,
MIPs — molecular imprinted polymers,
MRI — magnetic resonance imaging,
MMA — methacrylic acid,
MBA — *N*,*N*′-methylene-bis(acrylamide),
MPS — 3-methacryloxypropyltrimethoxysilane,
MWCNT — multi-walled carbon nanotube,
NA — nucleic acid,
NP — nanoparticle,
NIPAM — *N*-isopropylacrylamide,
PDT — photodynamic therapy,
PTT — photothermal therapy,
RNA — ribonucleic acid,
TBAM — *N*-*tert*-butylacrylamide,
TEOS — tetraethoxysilane,
UCNP — upconversion nanoparticle,
4-VPy — 4-vinylpyridine.

6. References

1. Y.Shen, P.Miao, S.Liu, J.Gao, X.Han, Y.Zhao, T.Chen. *Polymers*, **15**, 2344 (2023); https://doi.org/10.3390/polym15102344
2. D.Kong, N.Qiao, N.Wang, Z.Wang, Q.Wang, Z.Zhou, Z.Ren. *Phys. Chem. Chem. Phys.*, **20**, 12870 (2018); https://doi.org/10.1039/c8cp01163j
3. H.Wang, Y.Lin, Y.Li, A.Dolgormaa, H.Fang, L.Guo, J.Huang, J.Yang. *J. Inorg. Organomet. Polym. Mater.*, **29**, 1874 (2019); https://doi.org/10.1007/s10904-019-01148-6
4. Z.Zhou, X.Liu, M.Zhang, J.Jiao, H.Zhang, J.Du, B.Zhang, Z.Ren. *Sci. Total Environ.*, **699**, 134334 (2020); https://doi.org/10.1016/j.scitotenv.2019.134334
5. F.Yin, H.Yang, K.Huo, X.Liu, M.Yuan, H.Cao, T.Ye, X.Sun, F.Xu. *New J. Chem.*, **46**, 15460 (2022); https://doi.org/10.1039/d2nj02075k
6. Z.Zhou, D.Kong, H.Zhu, N.Wang, Z.Wang, Q.Wang, W.Liu, Q.Li, W.Zhang, Z.Ren. *J. Hazard. Mater.*, **341**, 355 (2018); https://doi.org/10.1016/j.jhazmat.2017.06.010
7. Q.Wang, X.Liu, M.Zhang, Z.Wang, Z.Zhou, Z.Ren. *Ind. Eng. Chem. Res.*, **58**, 6670 (2019); https://doi.org/10.1021/acs.iecr.8b06396
8. E.Y.Bivián-Castro, A.Zepeda-Navarro, J.L.Guzmán-Mar, M.Flores-Alamo, B.Mata-Ortega. *Polymers*, **15**, 1186 (2023); https://doi.org/10.3390/polym15051186
9. T.Tadić, B.Marković, J.Radulović, J.Lukić, L.Suručić, A.Nastasović, A.Onjia. *Sustainability*, **14**, 9222 (2022); https://doi.org/10.3390/su14159222
10. M.Caldara, J.W.Lowdon, J.Royakkers, M.Peeters, T.J.Cleij, H.Diliën, K.Eersels, B.van Grinsven. *Foods*, **11**, 2906 (2022); https://doi.org/10.3390/foods11182906
11. T.Zhou, Z.Deng, Q.Wang, H.Li, S.Li, X.Xu, Y.Zhou, S.Sun, C.Xuan, Q.Tian, L.Lun. *Molecules*, **27**, 6084 (2022); https://doi.org/10.3390/molecules27186084
12. P.Sun, Y.Wang, S.Yang, X.Sun, B.Peng, L.Pan, Y.Jia, X.Zhang, C.Nie. *Molecules*, **28**, 2052 (2023); https://doi.org/10.3390/molecules28052052
13. E.Lafuente-González, M.Guadaño-Sánchez, I.Urriza-Arsuaga, J.L.Urraca. *Int. J. Mol. Sci.*, **24**, 3453 (2023); https://doi.org/10.3390/ijms24043453
14. X.Ma, S.Li, J.Qiu, Z.Liu, S.Liu, Z.Huang, Y.Yong, Y.Li, Z.Yu, X.Liu, H.Lin, X.Ju, A.M.Abd El-Aty. *Polymers*, **15**, 1187 (2023); https://doi.org/10.3390/polym15051187
15. S.S.Piletsky, E.Piletska, M.Poblocka, S.Macip, D.J.L.Jones, M.Braga, T.H.Cao, R.Singh, A.C.Spivey, E.O.Aboagye, S.A.Piletsky. *Nano Today*, **41**, 101304 (2021); https://doi.org/10.1016/j.nantod.2021.101304
16. J.P.Fan, W.Y.Dong, X.H.Zhang, J.X.Yu, C.B.Huang, L.J.Deng, H.P.Chen, H.L.Peng. *Molecules*, **27**, 7304 (2022); https://doi.org/10.3390/molecules27217304
17. H.Fan, J.Wang, Q.Meng, X.Xu, T.Fan, Z.Jin. *Molecules*, **22**, 288 (2017); https://doi.org/10.3390/molecules22020288
18. J.W.Byeon, J.C.Yang, C.H.Cho, S.J.Lim, J.P.Park, J.Park. *Chemosensors*, **11**, 189 (2023); https://doi.org/10.3390/chemosensors11030189
19. R.Liu, Q.Cui, C.Wang, X.Wang, Y.Yang, L.Li. *ACS Appl. Mater. Interfaces*, **9**, 3006 (2017); https://doi.org/10.1021/acsami.6b14320
20. H.Lu, S.Xu, Z.Guo, M.Zhao, Z.Liu. *ACS Nano*, **15**, 18214 (2021); https://doi.org/10.1021/acsnano.1c07166
21. C.C.Lin, H.Y.Lin, J.L.Thomas, J.X.Yu, C.Y.Lin, Y.H.Chang, M.H.Lee, T.L.Wang. *Biomedicines*, **9**, 1923 (2021); https://doi.org/10.3390/biomedicines9121923
22. Y.Han, J.Tao, N.Ali, A.Khan, S.Malik, H.Khan, C.Yu, Y.Yang, M.Bilal, A.A.Mohamed. *Eur. Polym. J.*, **179**, 111582 (2022); https://doi.org/10.1016/J.EURPOLYMJ.2022.111582
23. S.He, L.Zhang, S.Bai, H.Yang, Z.Cui, X.Zhang, Y.Li. *Eur. Polym. J.*, **143**, 110179 (2021); https://doi.org/10.1016/j.eurpolymj.2020.110179
24. T.Sajini, B.Mathew. *Talanta Open*, **4**, 100072 (2021); https://doi.org/10.1016/j.talo.2021.100072
25. E.V.Dmitrienko, I.A.Pyshnaya, O.N.Martyanov, D.V.Pyshnyi. *Russ. Chem. Rev.*, **85**, 513 (2016); https://doi.org/10.1070/rcr4542
26. B.Fresco-Cala, A.D.Batista, S.Cárdenas. *Molecules*, **25**, 1 (2020); https://doi.org/10.3390/molecules25204740
27. N.A.Ramin, M.R.Ramachandran, N.M.Saleh, Z.M.Mat Ali, S.Asman. *Curr. Nanosci.*, **19**, 372 (2022); https://doi.org/10.2174/1573413718666220727111319
28. M.Polyakov. *Zh. Fiz. Khim.*, **2**, 799 (1931)
29. C.Alexander, H.S.Andersson, L.I.Andersson, R.J.Ansell, N.Kirsch, I.A.Nicholls, J.O'Mahony, M.J.Whitcombe. *J. Mol. Recognit.*, **19**, 106 (2006); https://doi.org/10.1002/jmr.760
30. G.Wulff, A.Sarhan, K.Zabrocki. *Tetrahedron Lett.*, **14**, 4329 (1973); https://doi.org/10.1016/S0040-4039(01)87213-0
31. L.Andersson, B.Sellergren, K.Mosbach. *Tetrahedron Lett.*, **25**, 5211 (1984); https://doi.org/10.1016/S0040-4039(01)81566-5
32. G.Wulff, D.Oberkobusch, M.Minárik. *React. Polym. Ion Exch. Sorbents*, **3**, 261 (1985); https://doi.org/10.1016/0167-6989(85)90017-0
33. G.Vasapollo, R.Del Sole, L.Mergola, M.R.Lazzoi, A.Scardino, S.Scorrano, G.Mele. *Int. J. Mol. Sci.*, **12**, 5908 (2011); https://doi.org/10.3390/ijms12095908
34. Z.El-Schich, Y.Zhang, M.Feith, S.Beyer, L.Sternbæk, L.Ohlsson, M.Stollenwerk, A.G.Wingren. *Biotechniques*, **69**, 407 (2020); https://doi.org/10.2144/btn-2020-0091
35. O.I.Parisi, F.Francomano, M.Dattilo, F.Patitucci, S.Prete, F.Amone, F.Puoci. *J. Funct. Biomater.*, **13** (1) (2022); https://doi.org/10.3390/jfb13010012
36. G.Wulff, R.Grobe-Einsler, W.Vesper, A.Sarhan. *Makromol. Chem.*, **178**, 2817 (1977); https://doi.org/10.1002/macp.1977.021781005

37. H.Yan, H.R.Kyung. *Int. J. Mol. Sci.*, **7**, 155 (2006); https://doi.org/10.3390/i7050155
38. L.Chen, S.Xu, J.Li. *Chem. Soc. Rev.*, **40**, 2922 (2011); https://doi.org/10.1039/c0cs00084a
39. L.Wang, Y.Liu, W.Li, X.Jiang, Y.Ji, X.Wu, L.Xu, Y.Qiu, K.Zhao, T.Wei, Y.Li, Y.Zhao, C.Chen. *Nano Lett.*, **11**, 772 (2011); https://doi.org/10.1021/nl103992v
40. G.Vlatakis, L.I.Andersson, R.Müller, K.Mosbach. *Nature*, **361**, 645 (1993); https://doi.org/10.1038/361645a0
41. J.Zhou, X.He, Y.Li. *Anal. Commun.*, **36**, 243 (1999); https://doi.org/10.1039/a902025j
42. T.Takagishi, A.Hayashi, N.Kuroki. *J. Polym. Sci. A-1*, **20**, 1533 (1982); https://doi.org/10.1002/pol.1982.170200614
43. K.Sreenivasan. *Talanta*, **44**, 1137 (1997); https://doi.org/10.1016/S0039-9140(96)02204-7
44. B.Sellergren. *TrAC – Trends Anal. Chem.*, **16**, 310 (1997); https://doi.org/10.1016/S0165-9936(97)00027-7
45. M.J.Whitcombe, M.E.Rodriguez, P.Villar, E.N.Vulfson. *J. Am. Chem. Soc.*, **117**, 7105 (1995); https://doi.org/10.1021/ja00132a010
46. B.Sellergren, C.J.Allender. *Adv. Drug Deliv. Rev.*, **57**, 1733 (2005); https://doi.org/10.1016/j.addr.2005.07.010
47. L.Wang, K.Zhi, Y.Zhang, Y.Liu, L.Zhang, A.Yasin, Q.Lin. *Polymers*, **11**, 602 (2019); https://doi.org/10.3390/polym11040602
48. A.N.Hasanah, N.Safitri, A.Zulfa, N.Neli, D.Rahayu. *Molecules*, **26**, 5612 (2021); https://doi.org/10.3390/molecules26185612
49. Z.Zhou, Y.Hu, Z.Wang, H.Zhang, B.Zhang, Z.Ren. *New J. Chem.*, **45**, 9582 (2021); https://doi.org/10.1039/d1nj00568e
50. Y.Hu, S.Feng, F.Gao, E.C.Y.Li-Chan, E.Grant, X.Lu. *Food Chem.*, **176**, 123 (2015); https://doi.org/10.1016/j.foodchem.2014.12.051
51. Y.Zhang, G.Zhao, K.Han, D.Sun, N.Zhou, Z.Song, H.Liu, J.Li, G.Li. *Molecules*, **28**, 301 (2023); https://doi.org/10.3390/molecules28010301
52. X.Zhang, M.Wang, Y.Zhang, P.Zhao, J.Cai, Y.Yao, J.Liang. *Molecules*, **28**, 3646 (2023); https://doi.org/10.3390/molecules28093646
53. R.Song, X.Yu, M.Liu, X.Hu, S.Zhu. *Polymers*, **14**, 2011 (2022); https://doi.org/10.3390/polym14102011
54. J.Li, X.Zhou, Y.Yan, D.Shen, D.Lu, Y.Guo, L.Xie, B.Deng. *Polymers*, **14**, 175 (2022); https://doi.org/10.3390/polym14010175
55. I.Polyakova, L.Borovikova, A.Osipenko, E.Vlasova, B.Volchek, O.Pisarev. *React. Funct. Polym.*, **109**, 88 (2016); https://doi.org/10.1016/j.reactfunctpolym.2016.10.010
56. N.A.Burmistrova, P.S.Pidenko, S.A.Pidenko, A.M.Zacharevich, Y.S.Skibina, N.V Beloglazova, I.Yu. *Talanta*, **208** (120445) (2020); https://doi.org/10.1016/j.talanta.2019.120445
57. A.Rachkov, N.Minoura. *Biochim. Biophys. Acta*, **1544**, 255 (2001); https://doi.org/10.1016/S0167-4838(00)00226-0
58. A.Afzal, A.Mujahid, R.Schirhagl, S.Z.Bajwa, U.Latif, S.Feroz. *Chemosensors*, **5**, 7 (2017); https://doi.org/10.3390/chemosensors5010007
59. Y.Zhang, C.Deng, S.Liu, J.Wu, Z.Chen, C.Li, W.Lu. *Angew. Chem., Int. Ed.*, **54**, 5157 (2015); https://doi.org/10.1002/anie.201412114
60. C.Y.Chou, C.Y.Lin, C.H.Wu, D.F.Tai. *Sensors*, **20**, 3592 (2020); https://doi.org/10.3390/s20123592
61. S.Liu, Q.Bi, Y.Long, Z.Li, S.Bhattacharyya, C.Li. *Nanoscale*, **9**, 5394 (2017); https://doi.org/10.1039/c6nr09449j
62. A.G.Ayankojo, R.Boroznjak, J.Reut, A.Öpik, V.Syritski. *Sens. Actuators B: Chem.*, **353**, 131160 (2022); https://doi.org/10.1016/j.snb.2021.131160
63. Y.Zhang, S.Li, X.T.Ma, X.W.He, W.Y.Li, Y.K.Zhang. *Microchim. Acta*, **187**, 228 (2020); https://doi.org/10.1007/s00604-020-4198-7
64. P.Zahedi, M.Ziaee, M.Abdouss, A.Farazin, B.Mizaikoff. *Polym. Adv. Technol.*, **27**, 1124 (2016); https://doi.org/10.1002/pat.3754
65. S.Ding, Z.Lyu, X.Niu, Y.Zhou, D.Liu, M.Falahati, D.Du, Y.Lin. *Biosens. Bioelectron.*, **149**, 111830 (2020); https://doi.org/10.1016/j.bios.2019.111830
66. L.Ye, P.A.G.Cormack, K.Mosbach. *Anal. Commun.*, **36**, 35 (1999); https://doi.org/10.1039/a809014i
67. D.Refaat, M.G.Aggour, A.A.Farghali, R.Mahajan, J.G.Wiklander, I.A.Nicholls, S.A.Piletsky. *Int. J. Mol. Sci.*, **20**, 6304 (2019); https://doi.org/10.3390/ijms20246304
68. L.Chen, X.Wang, W.Lu, X.Wu, J.Li. *Chem. Soc. Rev.*, **45**, 2137 (2016); https://doi.org/10.1039/c6cs00061d
69. K.Haupt, P.X.Medina Rangel, B.T.S.Bui. *Chem. Rev.*, **120**, 9554 (2020); https://doi.org/10.1021/acs.chemrev.0c00428
70. D.Vaihinger, K.Landfester, I.Kräuter, H.Brunner, G.E.M.Tovar. *Macromol. Chem. Phys.*, **203**, 1965 (2002); https://doi.org/10.1002/1521-3935(200209)203:13<1965::AID-MACP1965>3.0.CO;2-C
71. G.Zhao, J.Liu, M.Liu, X.Han, Y.Peng, X.Tian, J.Liu, S.Zhang. *Appl. Sci.*, **10**, 2868 (2020); https://doi.org/10.3390/APP10082868
72. S.Shinde, Z.El-Schich, A.Malakpour, W.Wan, N.Dizeyi, R.Mohammadi, K.Rurack, A.Gjörloff Wingren, B.Sellergren. *J. Am. Chem. Soc.*, **137**, 13908 (2015); https://doi.org/10.1021/jacs.5b08482
73. L.Wan, Z.Chen, C.Huang, X.Shen. *TrAC – Trends Anal. Chem.*, **95**, 110 (2017); https://doi.org/10.1016/j.trac.2017.08.010
74. F.Canfarotta, A.Cecchini, S.Piletsky. *RSC Polym. Chem. Ser.*, 1 (2018); https://doi.org/10.1039/9781788010474-00001
75. E.V.Dmitrienko, R.D.Bulushev, K.Haupt, S.S.Kosolobov, A.V.Latyshev, I.A.Pyshnaya, D.V.Pyshnyi. *J. Mol. Recognit.*, **26**, 368 (2013); https://doi.org/10.1002/jmr.2281
76. A.Sedelnikova, Y.Poletaeva, V.Golyshev, A.Chubarov, E.Dmitrienko. *Magnetochemistry*, **9**, 196 (2023); https://doi.org/10.3390/magnetochemistry9080196
77. P.Colas, B.Cohen, T.Jessen, I.Grishina, J.McCoy, R.Brent. *Nature*, **380**, 548 (1996); https://doi.org/10.1038/380548a0
78. J.Xu, H.Miao, J.Wang, G.Pan. *Small*, **16**, 1906644 (2020); https://doi.org/10.1002/smll.201906644
79. C.K.Dixit, S.Bhakta, K.K.Reza, A.Kaushik. *Hybrid Adv.*, **1**, 100001 (2022); https://doi.org/10.1016/j.hybadv.2022.100001
80. M.Naseri, M.Mohammadniaei, Y.Sun, J.Ashley. *Chemosensors*, **8**, 32 (2020); https://doi.org/10.3390/CHEMOSENSORS8020032
81. K.Smolinska-Kempisty, A.Guerreiro, F.Canfarotta, C.Cáceres, M.J.Whitcombe, S.Piletsky. *Sci. Rep.*, **6**, 37638 (2016); https://doi.org/10.1038/srep37638
82. J.Pang, P.Li, H.He, S.Xu, Z.Liu. *Chem. Sci.*, **13**, 4589 (2022); https://doi.org/10.1039/d2sc01093c
83. M.Garnier, M.Sabbah, C.Ménager, N.Griffete. *Nanomaterials*, **11**, 3091 (2021); https://doi.org/10.3390/nano11113091
84. S.Orbay, O.Kocaturk, R.Sanyal, A.Sanyal. *Micromachines*, **13**, 1464 (2022); https://doi.org/10.3390/mi13091464
85. A.Alayli, H.Nadaroğlu, A.Alayli Güngör, S.İnce. *Int. J. Innov. Res. Rev.*, **1**, 6 (2017)
86. X.Bai, Y.Wang, Z.Song, Y.Feng, Y.Chen, D.Zhang, L.Feng. *Int. J. Mol. Sci.*, **21**, 2480 (2020); https://doi.org/10.3390/ijms21072480
87. L.Jauffred, A.Samadi, H.Klingberg, P.M.Bendix, L.B.Oddershede. *Chem. Rev.*, **119**, 8087 (2019); https://doi.org/10.1021/acs.chemrev.8b00738
88. J.L.Li, M.Gu. *Biomaterials*, **31**, 9492 (2010); https://doi.org/10.1016/j.biomaterials.2010.08.068
89. G.Haran, L.Chuntonov. *Chem. Rev.*, **118**, 5539 (2018); https://doi.org/10.1021/acs.chemrev.7b00647
90. X.Huang, M.A.El-Sayed. *Alexandria J. Med.*, **47**, 1 (2011); https://doi.org/10.1016/j.ajme.2011.01.001
91. M.R.K.Ali, Y.Wu, M.A.El-Sayed. *J. Phys. Chem. C*, **123**, 15375 (2019); https://doi.org/10.1021/acs.jpcc.9b01961
92. P.Vijayaraghavan, C.-H.Liu, R.Vankayala, C.-S.Chiang, K.C.Hwang. *Adv. Mater.*, **26**, 6688 (2014); https://doi.org/10.1002/adma.201470268

93. Q.Chen, J.Chen, Z.Yang, L.Zhang, Z.Dong, Z.Liu. *Nano Res.*, **11**, 5657 (2018); https://doi.org/10.1007/s12274-017-1917-4
94. S.Ramanathan, S.C.B.Gopinath, M.K.M.Arshad, P.Poopalan, P.Anbu. *Microchim. Acta*, **186**, 546 (2019); https://doi.org/10.1007/s00604-019-3696-y
95. E.Assah, W.Goh, X.T.Zheng, T.X.Lim, J.Li, D.Lane, F.Ghadessy, Y.N.Tan. *Colloids. Surf. B: Biointerfaces*, **169**, 214 (2018); https://doi.org/10.1016/j.colsurfb.2018.05.007
96. J.Huang, Y.L.Liou, Y.N.Kang, Z.R.Tan, M.J.Peng, H.H.Zhou. *Int. J. Nanomedicine*, **11**, 5335 (2016); https://doi.org/10.2147/IJN.S116288
97. M.Moskovits. *Rev. Mod. Phys.*, **57**, 783 (1985); https://doi.org/10.1103/RevModPhys.57.783
98. X.Qian, S.Nie, P.M.Champion, L.D.Ziegler. *AIP Conf. Proc*., **1267**, 81 (2010); https://doi.org/10.1063/1.3482831
99. M.K.Hossain, H.Y.Cho, J.W.Choi. *J. Nanosci. Nanotechnol.*, **16**, 6299 (2016); https://doi.org/10.1166/jnn.2016.12122
100. M.Shiota, M.Naya, T.Yamamoto, T.Hishiki, T.Tani, H.Takahashi, A.Kubo, D.Koike, M.Itoh, M.Ohmura, Y.Kabe, Y.Sugiura, N.Hiraoka, T.Morikawa, K.Takubo, K.Suina, H.Nagashima, O.Sampetrean, O.Nagano, H.Saya, S.Yamazoe, H.Watanabe, M.Suematsu. *Nat. Commun.*, **9**, 1561 (2018); https://doi.org/10.1038/s41467-018-03899-1
101. D.Lin, S.Feng, J.Pan, Y.Chen, J.Lin, G.Chen, S.Xie, H.Zeng, R.Chen. *Opt. Express*, **19**, 13565 (2011); https://doi.org/10.1364/oe.19.013565
102. L.A.Lane, X.Qian, S.Nie. *Chem. Rev.*, **115**, 10489 (2015); https://doi.org/10.1021/acs.chemrev.5b00265
103. H.Shi, X.Ye, X.He, K.Wang, W.Cui, D.He, D.Li, X.Jia. *Nanoscale*, **6**, 8754 (2014); https://doi.org/10.1039/c4nr01927j
104. Y.Fu, J.Zhang, J.R.Lakowicz. *J. Am. Chem. Soc.*, **132**, 5540 (2010); https://doi.org/10.1021/ja9096237
105. D.E.Berning, K.V.Katti, W.A.Volkert, C.J.Higginbotham, A.R.Ketring. *Nucl. Med. Biol.*, **25**, 577 (1998); https://doi.org/10.1016/S0969-8051(98)00023-7
106. C.S.Cutler, H.M.Hennkens, N.Sisay, S.Huclier-Markai, S.S.Jurisson. *Chem. Rev.*, **113**, 858 (2013); https://doi.org/10.1021/cr3003104
107. N.Chanda, P.Kan, L.D.Watkinson, R.Shukla, A.Zambre, T.L.Carmack, H.Engelbrecht, J.R.Lever, K.Katti, G.M.Fent, S.W.Casteel, C.J.Smith, W.H.Miller, S.Jurisson, E.Boote, J.D.Robertson, C.Cutler, M.Dobrovolskaia, R.Kannan, K.V.Katti. *Nanomed. Nanotechnol., Biol. Med.*, **6**, 201 (2010); https://doi.org/10.1016/j.nano.2009.11.001
108. C.H.Chen, F.S.Lin, W.N.Liao, S.L.Liang, M.H.Chen, Y.W.Chen, W.Y.Lin, M.H.Hsu, M.Y.Wang, J.J.Peir, F.I.Chou, C.Y.Chen, S.Y.Chen, S.C.Huang, M.H.Yang, D.Y.Hueng, Y.Hwu, C.S.Yang, J.K.Chen. *Anal. Chem.*, **87**, 601 (2015); https://doi.org/10.1021/ac503260f
109. Y.Wang, Y.Liu, H.Luehmann, X.Xiaohu, Y.Xia. *Nano Lett.*, **13**, 581 (2014); https://doi.org/10.1021/nl304111v
110. Y.Guo, T.Aweda, K.C.L.Black, Y.Liu. *Curr. Top. Med. Chem.*, **13**, 470 (2013); https://doi.org/10.2174/1568026611313040007
111. Y.Fazaeli, O.Akhavan, R.Rahighi, M.R.Aboudzadeh, E.Karimi, H.Afarideh. *Mater. Sci. Eng. C*, **45**, 196 (2014); https://doi.org/10.1016/j.msec.2014.09.019
112. S.Payton. *Nat. Rev. Urol.*, **9**, 544 (2012); https://doi.org/10.1038/nrurol.2012.156
113. S.Her, D.A.Jaffray, C.Allen. *Adv. Drug Deliv. Rev.*, **109**, 84 (2017); https://doi.org/10.1016/j.addr.2015.12.012
114. E.Brun, L.Sanche, C.Sicard-Roselli. *Colloids Surf. B: Biointerfaces*, **72**, 128 (2009); https://doi.org/10.1016/j.colsurfb.2009.03.025
115. S.H.Cho, B.L.Jones, S.Krishnan. *Phys. Med. Biol.*, **54**, 4889 (2009); https://doi.org/10.1088/0031-9155/54/16/004
116. E.Lechtman, N.Chattopadhyay, Z.Cai, S.Mashouf, R.Reilly, J.P.Pignol. *Phys. Med. Biol.*, **56**, 4631 (2011); https://doi.org/10.1088/0031-9155/56/15/001
117. M.Alqathami, A.Blencowe, U.J.Yeo, S.J.Doran, G.Qiao, M.Geso. *Int. J. Radiat. Oncol. Biol. Phys.*, **84**, 549 (2012); https://doi.org/10.1016/j.ijrobp.2012.05.029
118. S.Khademi, S.Sarkar, A.Shakeri-Zadeh, N.Attaran, S.Kharrazi, M.R.Ay, H.Azimian, H.Ghadiri. *Int. J. Biochem. Cell Biol.*, **114**, 105554 (2019); https://doi.org/10.1016/j.biocel.2019.06.002
119. H.Jans, Q.Huo. *Chem. Soc. Rev.*, **41**, 2849 (2012); https://doi.org/10.1039/c1cs15280g
120. Y.Lin, J.Ren, X.Qu. *Adv. Mater.*, **26**, 4200 (2014); https://doi.org/10.1002/adma.201400238
121. Y.Jv, B.Li, R.Cao. *Chem. Commun.*, **46**, 8017 (2010); https://doi.org/10.1039/c0cc02698k
122. A.Zhang, S.Pan, Y.Zhang, J.Chang, J.Cheng, Z.Huang, T.Li, C.Zhang, J.M.De La Fuentea, Q.Zhang, D.Cui. *Theranostics*, **9**, 3443 (2019); https://doi.org/10.7150/thno.33266
123. J.Feng, P.Huang, S.Shi, K.Y.Deng, F.Y.Wu. *Anal. Chim. Acta*, **967**, 64 (2017); https://doi.org/10.1016/j.aca.2017.02.025
124. S.Gao, H.Lin, H.Zhang, H.Yao, Y.Chen, J.Shi. *Adv. Sci.*, **6**, 1801733 (2019); https://doi.org/10.1002/advs.201801733
125. P.Mukherjee, R.Bhattacharya, P.Wang, L.Wang, S.Basu, J.A.Nagy, A.Atala, D.Mukhopadhyay, S.Soker. *Clin. Cancer Res.*, **11**, 3530 (2005); https://doi.org/10.1158/1078-0432.CCR-04-2482
126. R.Bhattacharya, C.R.Patra, R.Verma, S.Kumar, P.R.Greipp, P.Mukherjee. *Adv. Mater.*, **19**, 711 (2007); https://doi.org/10.1002/adma.200602098
127. A.I.Demenshin, V.Solovyeva. *Russ. Chem. Rev.*, **94** (6), RCR5169 (2025); https://doi.org/10.59761/RCR5169
128. A.Akbarzadeh, M.Samiei, S.Davaran. *Nanoscale Res. Lett.*, **7**, 144 (2012); https://doi.org/10.1186/1556-276X-7-144
129. L.Wang, J.Bai, Y.Li, Y.Huang. *Angew. Chem., Int. Ed.*, **47**, 2439 (2008); https://doi.org/10.1002/anie.200800014
130. U.Jeong, X.Teng, Y.Wang, H.Yang, Y.Xia. *Adv. Mater.*, **19**, 33 (2007); https://doi.org/10.1002/adma.200600674
131. E.Y.Sun, L.Josephson, R.Weissleder. *Mol. Imaging*, **5** (2006); https://doi.org/10.2310/7290.2006.00013
132. K.Wu, D.Su, J.Liu, R.Saha, J.P.Wang. *Nanotechnology*, **30**, 502003 (2019); https://doi.org/10.1088/1361-6528/ab4241
133. M.Jeon, M.V.Halbert, Z.R.Stephen, M.Zhang. *Adv. Mater.*, **33**, 1906539 (2021); https://doi.org/10.1002/adma.201906539
134. T.I.Shabatina, O.I.Vernaya, V.P.Shabatin, M.Y.Melnikov. *Magnetochemistry*, **6**, 30 (2020); https://doi.org/10.3390/magnetochemistry6030030
135. E.Alsberg, E.Feinstein, M.P.Joy, M.Prentiss, D.E.Ingber. *Tissue Eng.*, **12** 3247 (2006); https://doi.org/10.1089/ten.2006.12.3247
136. C.Wilhelm, L.Bal, P.Smirnov, I.Galy-Fauroux, O.Clément, F.Gazeau, J.Emmerich. *Biomaterials*, **28**, 3797 (2007); https://doi.org/10.1016/j.biomaterials.2007.04.047
137. I.A.Rahman, P.Vejayakumaran, C.S.Sipaut, J.Ismail, C.K.Chee. *Mater. Chem. Phys.*, **114**, 328 (2009); https://doi.org/10.1016/j.matchemphys.2008.09.068
138. M.Qhobosheane, S.Santra, P.Zhang, W.Tan. *Analyst*, **126**, 1274 (2001); https://doi.org/10.1039/b101489g
139. Y.Zheng, C.D.Fahrenholtz, C.L.Hackett, S.Ding, C.S.Day, R.Dhall, G.S.Marrs, M.D.Gross, R.Singh, U.Bierbach. *Chem. – A Eur. J.*, **23**, 3386 (2017); https://doi.org/10.1002/chem.201604868
140. K.Shin, J.W.Choi, G.Ko, S.Baik, D.Kim, O.K.Park, K.Lee, H.R.Cho, S.I.Han, S.H.Lee, D.J.Lee, N.Lee, H.C.Kim, T.Hyeon. *Nat. Commun.*, **8**, 15807 (2017); https://doi.org/10.1038/ncomms15807
141. Z.Gu, Z.Guo, S.Gao, L.Huang, Z.Liu. *ACS Nano*, **17**, 10152 (2023); https://doi.org/10.1021/acsnano.3c00148
142. R.N.Amirkhanov, V.F.Zarytova, M.A.Zenkova. *Russ. Chem. Rev.*, **86** (2), 113 (2017); https://doi.org/10.1070/rcr4604
143. A.Liberman, N.Mendez, W.C.Trogler, A.C.Kummel. *Surf. Sci. Rep.*, **69**, 132 (2014); https://doi.org/10.1016/j.surfrep.2014.07.001

144. Y.Wang, Q.Zhao, N.Han, L.Bai, J.Li, J.Liu, E.Che, L.Hu, Q.Zhang, T.Jiang, S.Wang. *Nanomed. Nanotechnol., Biol. Med.*, **11**, 313 (2015); https://doi.org/10.1016/j.nano.2014.09.014
145. Y.Zhang, J.Wang, X.Bai, T.Jiang, Q.Zhang, S.Wang. *Mol. Pharm.*, **9**, 505 (2012); https://doi.org/10.1021/mp200287c
146. R.P.Bagwe, L.R.Hilliard, W.Tan. *Langmuir*, **22**, 4357 (2006); https://doi.org/10.1021/la052797j
147. Y.P.Sun, B.Zhou, Y.Lin, W.Wang, K.A.S.Fernando, P.Pathak, M.J.Meziani, B.A.Harruff, X.Wang, H.Wang, P.G.Luo, H.Yang, M.E.Kose, B.Chen, L.M.Veca, S.Y.Xie. *J. Am. Chem. Soc.*, **128**, 7756 (2006); https://doi.org/10.1021/ja062677d
148. S.C.Ray, A.Saha, N.R.Jana, R.Sarkar. *J. Phys. Chem. C*, **113**, 18546 (2009); https://doi.org/10.1021/jp905912n
149. S.L.Hu, K.Y.Niu, J.Sun, J.Yang, N.Q.Zhao, X.W.Du. *J. Mater. Chem.*, **19**, 484 (2009); https://doi.org/10.1039/b812943f
150. D.Pan, J.Zhang, Z.Li, M.Wu. *Adv. Mater.*, **22**, 734 (2010); https://doi.org/10.1002/adma.200902825
151. X.T.Zheng, A.Ananthanarayanan, K.Q.Luo, P.Chen. *Small*, **11**, 1620 (2015); https://doi.org/10.1002/smll.201402648
152. X.Li, Y.Shimizu, A.Pyatenko, H.Wang, N.Koshizaki. *J. Mater. Chem.*, **21**, 14406 (2011); https://doi.org/10.1039/c1jm12696b
153. S.Zhu, J.Zhang, C.Qiao, S.Tang, Y.Li, W.Yuan, B.Li, L.Tian, F.Liu, R.Hu, H.Gao, H.Wei, H.Zhang, H.Sun, B.Yang. *Chem. Commun.*, **47**, 6858 (2011); https://doi.org/10.1039/c1cc11122a
154. M.A.Sk, A.Ananthanarayanan, L.Huang, K.H.Lim, P.Chen. *J. Mater. Chem. C*, **2**, 6954 (2014); https://doi.org/10.1039/c4tc01191k
155. L.Cao, M.J.Meziani, S.Sahu, Y.P.Sun. *Acc. Chem. Res.*, **46**, 171 (2013); https://doi.org/10.1021/ar300128j
156. H.Li, Z.Kang, Y.Liu, S.T.Lee. *J. Mater. Chem.*, **22**, 24230 (2012); https://doi.org/10.1039/c2jm34690g
157. T.N.Pashirova, A.V Nemtarev, E.B.Souto, V.F.Mironov. *Russ. Chem. Rev.*, **92** (10) RCR5095 (2023); https://doi.org/10.59761/RCR5095
158. B.Yin, J.Deng, X.Peng, Q.Long, J.Zhao, Q.Lu, Q.Chen, H.Li, H.Tang, Y.Zhang, S.Yao. *Analyst*, **138**, 6551 (2013); https://doi.org/10.1039/c3an01003a
159. L.Cao, X.Wang, M.J.Meziani, F.Lu, H.Wang, P.G.Luo, Y.Lin, B.A.Harruff, L.M.Veca, D.Murray, S.Y.Xie, Y.P.Sun. *J. Am. Chem. Soc.*, **129**, 11318 (2007); https://doi.org/10.1021/ja0735271
160. Q.Liu, B.Guo, Z.Rao, B.Zhang, J.R.Gong. *Nano Lett.*, **13**, 2436 (2013); https://doi.org/10.1021/nl400368v
161. E.Lee, J.Ryu, J.Jang. *Chem. Commun.*, **49**, 9995 (2013); https://doi.org/10.1039/c3cc45588b
162. S.Zhu, J.Zhang, X.Liu, B.Li, X.Wang, S.Tang, Q.Meng, Y.Li, C.Shi, R.Hu, B.Yang. *RSC Adv.*, **2**, 2717 (2012); https://doi.org/10.1039/c2ra20182h
163. L.Zheng, Y.Chi, Y.Dong, J.Lin, B.Wang. *J. Am. Chem. Soc.*, **131**, 4564 (2009); https://doi.org/10.1021/ja809073f
164. L.L.Li, J.Ji, R.Fei, C.Z.Wang, Q.Lu, J.R.Zhang, L.P.Jiang, J.J.Zhu. *Adv. Funct. Mater.*, **22**, 2971 (2012); https://doi.org/10.1002/adfm.201200166
165. J.Lu, M.Yan, L.Ge, S.Ge, S.Wang, J.Yan, J.Yu. *Biosens. Bioelectron.*, **47**, 271 (2013); https://doi.org/10.1016/j.bios.2013.03.039
166. I.Khan, K.Saeed, I.Zekker, B.Zhang, A.H.Hendi, A.Ahmad, S.Ahmad, N.Zada, H.Ahmad, L.A.Shah, T.Shah, I.Khan. *Water*, **14** (2) (2022); https://doi.org/10.3390/w14020242
167. O.Afzal, A.S.A.Altamimi, M.S.Nadeem, S.I.Alzarea, W.H.Almalki, A.Tariq, B.Mubeen, B.N.Murtaza, S.Iftikhar, N.Riaz, I.Kazmi. *Nanomaterials*, **12**, 4494 (2022); https://doi.org/10.3390/nano12244494
168. M.I.Anik, M.K.Hossain, I.Hossain, A.M.U.B.Mahfuz, M.T.Rahman, I.Ahmed. *Nano Select*, **2**, 1146 (2021); https://doi.org/10.1002/nano.202000162
169. J.Dolai, K.Mandal, N.R.Jana. *ACS Appl. Nano Mater.*, **4**, 6471 (2021); https://doi.org/10.1021/acsanm.1c00987
170. K.G.Shevchenko, I.S.Garkushina, F.Canfarotta, S.A.Piletsky, N.A.Barlev. *RSC Adv.*, **12**, 3957 (2022); https://doi.org/10.1039/d1ra08385f
171. H.Peng, Y.T.Qin, X.W.He, W.Y.Li, Y.K.Zhang. *ACS Appl. Mater. Interfaces*, **12**, 13360 (2020); https://doi.org/10.1021/acsami.0c00468
172. C.Boitard, A.Curcio, A.L.Rollet, C.Wilhelm, C.Ménager, N.Griffete. *ACS Appl. Mater. Interfaces*, **11**, 35556 (2019); https://doi.org/10.1021/acsami.9b11717
173. Y.Dong, W.Li, Z.Gu, R.Xing, Y.Ma, Q.Zhang, Z.Liu. *Angew. Chem., Int. Ed.*, **58**, 10621 (2019); https://doi.org/10.1002/anie.201904860
174. Q.Y.Ang, S.C.Low. *Sens. Rev.*, **39**, 862 (2019); https://doi.org/10.1108/SR-08-2018-0211
175. T.Sergeyeva, O.Piletska, S.Piletsky. *BBA Adv.*, **3**, 100070 (2023); https://doi.org/10.1016/j.bbadva.2022.100070
176. O.S.Ahmad, T.S.Bedwell, C.Esen, A.Garcia-Cruz, S.A.Piletsky. *Trends Biotechnol.*, **37**, 294 (2019); https://doi.org/10.1016/j.tibtech.2018.08.009
177. J.Wang, J.Dai, Y.Xu, X.Dai, Y.Zhang, W.Shi, B.Sellergren, G.Pan. *Small*, **15**, 1803913 (2019); https://doi.org/10.1002/smll.201803913
178. A.A.Ensafi, P.Nasr-Esfahani, B.Rezaei. *Sens. Actuators B: Chem.*, **257**, 889 (2018); https://doi.org/10.1016/J.SNB.2017.11.050
179. F.Parnianchi, S.Kashanian, M.Nazari, M.Peacock, K.Omidfar, K.Varmira. *Microchem. J.*, **179**, 107474 (2022); https://doi.org/10.1016/J.MICROC.2022.107474
180. S.M.Majd, F.Mirzapour, M.Shamsipur, I.Manouchehri, E.Babaee, A.Pashabadi, R.Moradian. *Talanta*, **257**, 124394 (2023); https://doi.org/10.1016/j.talanta.2023.124394
181. J.Ouyang, Z.Liu, Y.Han, K.Zeng, J.Sheng, L.Deng, Y.N.Liu. *ACS Appl. Mater. Interfaces*, **8**, 35004 (2016); https://doi.org/10.1021/acsami.6b12010
182. S.S.Piletsky, S.Rabinowicz, Z.Yang, C.Zagar, E.V.Piletska, A.Guerreiro, S.A.Piletsky. *Chem. Commun.*, **53**, 1793 (2017); https://doi.org/10.1039/c6cc08716g
183. E.Turan, A.Zengin, Z.Suludere, N.Ö. Kalkan, U.Tamer. *Talanta*, **237**, 122926 (2022); https://doi.org/10.1016/J.TALANTA.2021.122926
184. A.Kotyrba, M.Dinc, B.Mizaikoff. *Nanomaterials*, **11**, 3287 (2021); https://doi.org/10.3390/nano11123287
185. S.Roshan, A.Mujahid, A.Afzal, I.Nisar, M.N.Ahmad, T.Hussain, S.Z.Bajwa. *Adv. Polym. Technol.*, **2019**, 9432412 (2019); https://doi.org/10.1155/2019/9432412
186. M.Chiarello, L.Anfossi, S.Cavalera, F.Di Nardo, T.Serra, C.Baggiani. *Separations*, **8**, 226 (2021); https://doi.org/10.3390/separations8110226
187. X.Wei, Y.Wang, J.Chen, R.Ni, J.Meng, Z.Liu, F.Xu, Y.Zhou. *Anal. Chim. Acta*, **1081**, 81 (2019); https://doi.org/10.1016/J.ACA.2019.07.025
188. C.Sun, L.Pan, L.Zhang, J.Huang, D.Yao, C.Z.Wang, Y.Zhang, N.Jiang, L.Chen, C.S.Yuan. *Analyst*, **144**, 6760 (2019); https://doi.org/10.1039/c9an01065c
189. A.A.Lahcen, S.Rauf, A.Aljedaibi, J.I.de Oliveira Filho, T.Beduk, V.Mani, H.N.Alshareef, K.N.Salama. *Sens. Actuators B: Chem.*, **347**, 130556 (2021); https://doi.org/10.1016/J.SNB.2021.130556
190. A.Garcia-Cruz, T.Cowen, A.Voorhaar, E.Piletska, S.A.Piletsky. *Analyst*, **145**, 4224 (2020); https://doi.org/10.1039/d0an00419g
191. J.Huang, Y.Wu, J.Cong, J.Luo, X.Liu. *Sens. Actuators B: Chem.*, **259**, 1 (2018); https://doi.org/10.1016/J.SNB.2017.12.049
192. S.Rajpal, S.Bhakta, P.Mishra. *J. Mater. Chem. B*, **9**, 2436 (2021); https://doi.org/10.1039/d0tb02842h
193. S.Balayan, N.Chauhan, P.Kumar, R.Chandra, U.Jain. *3 Biotech*., **12**, 37 (2022); https://doi.org/10.1007/s13205-021-03083-1

194. M.Mehrzad-Samarin, F.Faridbod, A.S.Dezfuli, M.R.Ganjali. *Biosens. Bioelectron.*, **92**, 618 (2017); https://doi.org/10.1016/J.BIOS.2016.10.047
195. J.Feng, X.Li, H.Cheng, W.Huang, H.Kong, Y.Li, L.Li. *Microchim. Acta*, **186**, 774 (2019); https://doi.org/10.1007/s00604-019-3972-x
196. L.Mardani, M.T.Vardini, M.Es'Haghi, E.Ghorbani-Kalhor. *Anal. Sci.*, **35**, 1173 (2019); https://doi.org/10.2116/analsci.19P107
197. Z.Yao, X.Yang, X.Liu, Y.Yang, Y.Hu, Z.Zhao. *Microchim. Acta*, **185**, 1 (2018); https://doi.org/10.1007/s00604-017-2613-5
198. Y.Wei, Q.Zeng, S.Bai, M.Wang, L.Wang. *ACS Appl. Mater. Interfaces*, **9**, 44114 (2017); https://doi.org/10.1021/acsami.7b14772
199. Z.Liu, M.Jin, H.Lu, J.Yao, X.Wang, G.Zhou, L.Shui. *Sens. Actuators B: Chem.*, **288**, 363 (2019); https://doi.org/10.1016/J.SNB.2019.02.097
200. Y.Wang, L.Yao, X.Liu, J.Cheng, W.Liu, T.Liu, M.Sun, L.Zhao, F.Ding, Z.Lu, P.Zou, X.Wang, Q.Zhao, H.Rao. *Biosens. Bioelectron.*, **142**, 111483 (2019); https://doi.org/10.1016/J.BIOS.2019.111483
201. H.Wang, D.Qian, X.Xiao, C.Deng, L.Liao, J.Deng, Y.W.Lin. *Bioelectrochemistry*, **121**, 115 (2018); https://doi.org/10.1016/J.BIOELECHEM.2018.01.006
202. M.R.Ali, M.S.Bacchu, M.R.Al-Mamun, M.M.Rahman, M.S.Ahommed, M.A.S.Aly, M.Z.H.Khan. *J. Mater. Sci.*, **56**, 12803 (2021); https://doi.org/10.1007/s10853-021-06115-6
203. M.Dehghani, N.Nasirizadeh, M.E.Yazdanshenas. *Mater. Sci. Eng. C*, **96**, 654 (2019); https://doi.org/10.1016/J.MSEC.2018.12.002
204. S.Kumar, P.Karfa, K.C.Majhi, R.Madhuri. *Mater. Sci. Eng. C*, **111**, 110777 (2020); https://doi.org/10.1016/J.MSEC.2020.110777
205. P.Karami, H.Bagheri, M.Johari-Ahar, H.Khoshsafar, F.Arduini, A.Afkhami. *Talanta*, **202**, 111 (2019); https://doi.org/10.1016/J.TALANTA.2019.04.061
206. D.Bahari, B.Babamiri, A.Salimi. *Anal. Bioanal. Chem.*, **413**, 4049 (2021); https://doi.org/10.1007/s00216-021-03362-z
207. Y.Lai, C.Zhang, Y.Deng, G.Yang, S.Li, C.Tang, N.He. *Chinese Chem. Lett.*, **30**, 160 (2019); https://doi.org/10.1016/J.CCLET.2018.07.011
208. Z.Lu, Y.Li, T.Liu, G.Wang, M.Sun, Y.Jiang, H.He, Y.Wang, P.Zou, X.Wang, Q.Zhao, H.Rao. *Chem. Eng. J.*, **389**, 124417 (2020); https://doi.org/10.1016/J.CEJ.2020.124417
209. S.Wang, Y.Wen, Y.Wang, Y.Ma, Z.Liu. *Anal. Chem.*, **89**, 5646 (2017); https://doi.org/10.1021/acs.analchem.7b00965
210. B.Demir, M.M.Lemberger, M.Panagiotopoulou, P.X.Medina Rangel, S.Timur, T.Hirsch, B.Tse Sum Bui, J.Wegener, K.Haupt. *ACS Appl. Mater. Interfaces*, **10**, 3305 (2018); https://doi.org/10.1021/acsami.7b16225
211. P.X.Medina Rangel, S.Laclef, J.Xu, M.Panagiotopoulou, J.Kovensky, B.Tse Sum Bui, K.Haupt. *Sci. Rep.*, **9**, 1 (2019); https://doi.org/10.1038/s41598-019-40348-5
212. S.Xu, L.Wang, Z.Liu. *Angew. Chem., Int. Ed.*, **60**, 3858 (2021); https://doi.org/10.1002/anie.202005309
213. M.C.Norell, H.S.Andersson, I.A.Nicholls. *J. Mol. Recognit.*, **11**, 98 (1998); https://doi.org/10.1002/(SICI)1099-1352(199812)11:1/6<98::AID-JMR399>3.0.CO;2-Y
214. E.Balcer, M.Sobiech, P.Luliński. *Pharmaceutics*, **15**, 1647 (2023); https://doi.org/10.3390/pharmaceutics15061647
215. J.R.Choi, K.W.Yong, J.Y.Choi, A.C.Cowie. *Comb. Chem. High Throughput Screen*, **22**, 78 (2019); https://doi.org/10.2174/1386207322666190325115526
216. O.V.Arzhakova, M.S.Arzhakov, E.R.Badamshina, E.B.Bryuzgina, E.V.Bryuzgin, A.V.Bystrova, G.V.Vaganov, V.V.Vasilevskaya, A.Yu.Vdovichenko, M.O.Gallyamov, R.A.Gumerov, A.L.Didenko, V.V.Zefirov, S.V.Karpov, P.V.Komarov, V.G.Kulichikhin, S.A.Kurochkin, S.V.Larin, A.Ya. Malkin,S.A.Milenin, A.M.Muzafarov, V.S.Molchanov, A.V.Navrotskiy, I.A.Novakov,E.F.Panarin, I.G.Panova, I.I.Potemkin, V.M.Svetlichny, N.G.Sedush, O.A.Serenko,S.A.Uspenskii, O.E.Philippova, A.R.Khokhlov, S.N.Chvalun, S.S.Sheiko, A.V.Shibaev, I.V.Elmanovich, V.E.Yudin, A.V.Yakimansky, A.A.Yaroslavov. *Russ.Chem. Rev*., **91** (12), RCR5062 (2022); https://doi.org/10.57634/RCR5062
217. N.Sanadgol, J.Wackerlig. *Pharmaceutics*, **12**, 831 (2020); https://doi.org/10.3390/pharmaceutics12090831
218. L.Talavat, A.Güner. *Inorg. Chem. Commun.*, **103**, 119 (2019); https://doi.org/10.1016/j.inoche.2019.02.009
219. A.Hassanpour, M.Irandoust, E.Soleimani, H.Zhaleh. *Mater. Sci. Eng. C*, **103**, 109771 (2019); https://doi.org/10.1016/j.msec.2019.109771
220. C.Gong, M.H.W.Lam, H.Yu. *Adv. Funct. Mater.*, **16**, 1759 (2006); https://doi.org/10.1002/adfm.200500907
221. L.tao Liu, M.jun Chen, H.lin Yang, Z.jie Huang, Q.Tang, C.fai Chow, C.bin Gong, M.hang Zu, B.Xiao. *Mater. Sci. Eng. C*, **106**, 110253 (2020); https://doi.org/10.1016/j.msec.2019.110253
222. L.Liu, N.Li, M.Chen, H.Yang, Q.Tang, C.Gong. *ACS Appl. Bio Mater.*, **1**, 845 (2018); https://doi.org/10.1021/acsabm.8b00275
223. Y.Zhang, Q.Wang, X.Zhao, Y.Ma, H.Zhang, G.Pan. *Molecules*, **28**, 918 (2023); https://doi.org/10.3390/molecules28030918
224. R.Sedghi, M.Yassari, B.Heidari. *Colloids Surf. B: Biointerfaces*, **162**, 154 (2018); https://doi.org/10.1016/j.colsurfb.2017.11.053
225. T.Kubo, K.Tachibana, T.Naito, S.Mukai, K.Akiyoshi, J.Balachandran, K.Otsuka. *ACS Biomater. Sci. Eng.*, **5**, 759 (2019); https://doi.org/10.1021/acsbiomaterials.8b01401
226. E.Cazares-Cortes, M.Nerantzaki, J.Fresnais, C.Wilhelm, N.Griffete, C.Ménager. *Nanomaterials*, **8**, 850 (2018); https://doi.org/10.3390/nano8100850
227. F.Lin, J.Chen, M.Lee, B.Lin, J.Wang. *ACS Appl. Nano Mater.*, **3**, 1147 (2020); https://doi.org/10.1021/acsanm.9b01669
228. L.M.Abdolyousefi, G.Yousefi, A.M.Tamaddon, Z.Sobhani. *Colloids Surf. A: Physicochem. Eng. Asp.*, **680**, 132690 (2024); https://doi.org/10.1016/j.colsurfa.2023.132690
229. M.S.Kang, E.Cho, H.E.Choi, C.Amri, J.H.Lee, K.S.Kim. *Biomater. Res.*, **27** (1), 47 (2023); https://doi.org/10.1186/s40824-023-00388-5
230. J.Chen, C.Ning, Z.Zhou, P.Yu, Y.Zhu, G.Tan, C.Mao. *Prog. Mater. Sci.*, **99**, 1 (2019); https://doi.org/10.1016/j.pmatsci.2018.07.005
231. S.Wang, Y.Ding, H.Wang, W.Li, W.Xu, P.Sun, W.Huang, Y.Chen, J.Gu, P.Lin, L.Ma, Z.Liu, Q.Ling, Q.Zhang, H.Chen, T.Yan. *J. Mater. Sci.*, **57**, 5177 (2022); https://doi.org/10.1007/s10853-022-06965-8
232. M.Wen, H.Shi, Y.Wan, J.Wu, X.Tian, Q.Chen, M.Y.Wu, S.Feng. *Chem. Commun.*, **59**, 4229 (2023); https://doi.org/10.1039/d3cc00088e
233. Q.Liu, L.Z.Wu. *Natl. Sci. Rev.*, **4**, 359 (2017); https://doi.org/10.1093/nsr/nwx039
234. P.H.Hsu, A.Almutairi. *J. Mater. Chem. B*, **9**, 2179 (2021); https://doi.org/10.1039/d0tb02190c
235. S.Liu, S.Han, Y.Song, R.Sun, L.Zhao, C.Yan. *Adv. Healthcare Mater.*, **12**, 2300184 (2023); https://doi.org/10.1002/adhm.202300184
236. H.Shi, Y.Wan, X.Tian, L.Wang, L.Shan, C.Zhang, M.Y.Wu, S.Feng. *ACS Appl. Mater. Interfaces*, **14**, 56585 (2022); https://doi.org/10.1021/acsami.2c17731
237. J.Ma, Y.Zhang, H.Sun, P.Ding, D.Chen. *J.Mater. Chem. B*, **10**, 4226 (2022); https://doi.org/10.1039/d2tb00396a
238. Y.Xu, X.Hu, P.Guan, C.Du, Y.Tian, S.Ding, Z.Li, C.Yan. *J. Mater. Sci.*, **54**, 9124 (2019); https://doi.org/10.1007/s10853-019-03500-0
239. S.Han, F.Teng, Y.Wang, L.Su, Q.Leng, H.Jiang. *RSC Adv.*, **10**, 10980 (2020); https://doi.org/10.1039/d0ra00574f

240. A.Saboury, R.Mohammadi, S.Javanbakht, M.Ghorbani. *J. Drug Deliv. Sci. Technol.*, **79**, 103998 (2023); https://doi.org/10.1016/J.JDDST.2022.103998
241. M.Bakhshizadeh, S.A.Mohajeri, H.Esmaily, S.A.Aledavood, F.Varshoei Tabrizi, M.Seifi, F.Hadizadeh, A.Sazgarnia. *Photodiagnosis Photodyn. Ther.*, **25**, 472 (2019); https://doi.org/10.1016/J.PDPDT.2019.02.006
242. Y.Shi, Y.Wang, J.Zhu, W.Liu, M.Z.H.Khan, X.Liu. *Nanomaterials*, **10**, 1 (2020); https://doi.org/10.3390/nano10091655
243. L.Zhao, M.H.Chai, H.F.Yao, Y.P.Huang, Z.S.Liu. *Pharm. Res.*, **37**, 193 (2020); https://doi.org/10.1007/s11095-020-02902-z
244. T.Kubo, M.Shimonaka, Y.Watabe, K.Akiyoshi, J.Balachandran, K.Otsuka. *Nanocomposites*, **7**, 215 (2021); https://doi.org/10.1080/20550324.2021.2008206
245. Y.Yin, L.Guan, Y.Wang, Y.Ma, J.Pan, Y.Peng, G.Pan. *Colloids Interface Sci. Commun.*, **42**, 100421 (2021); https://doi.org/10.1016/j.colcom.2021.100421
246. L.P.Zhang, X.X.Tan, Y.P.Huang, Z.S.Liu. *Eur. J. Pharm. Biopharm.*, **127**, 150 (2018); https://doi.org/10.1016/J.EJPB.2018.02.012
247. H.Y.Wang, P.P.Cao, Z.Y.He, X.W.He, W.Y.Li, Y.H.Li, Y.K.Zhang. *Nanoscale*, **11**, 17018 (2019); https://doi.org/10.1039/c9nr04655k
248. J.Chen, S.Lei, K.Zeng, M.Wang, A.Asif, X.Ge. *Nano Res.*, **10**, 2351 (2017); https://doi.org/10.1007/s12274-017-1431-8
249. M.H.Lee, J.L.Thomas, J.A.Li, J.R.Chen, T.L.Wang, H.Y.Lin. *Pharmaceuticals*, **14**, 1 (2021); https://doi.org/10.3390/ph14060508
250. H.Y.Wang, Z.C.Su, X.W.He, W.Y.Li, Y.K.Zhang. *Nanoscale*, **13**, 12553 (2021); https://doi.org/10.1039/d1nr02524d
251. Y.Kitayama, T.Yamada, K.Kiguchi, A.Yoshida, S.Hayashi, H.Akasaka, K.Igarashi, Y.Nishimura, Y.Matsumoto, R.Sasaki, E.Takano, H.Sunayama, T.Takeuchi. *J. Mater. Chem. B*, **10**, 6784 (2022); https://doi.org/10.1039/d2tb00481j
252. S.Garg, P.Singla, S.Kaur, F.Canfarotta, E.Velliou, J.A.Dawson, N.Kapur, N.J.Warren, S.Amarnath, M.Peeters. *Macromolecules*, **58**, 1157 (2025); https://doi.org/10.1021/acs.macromol.4c01621